

**SYNTHESIS AND CHARACTERIZATION OF PHOSPHONATE
SUBSTITUTED NOVEL PORPHYRAZINES**

Nürüfe KEMİKLİ

M.S. Thesis In Chemistry

January 2008

by

Nürüfe KEMİKLİ

January 2008

**SYNTHESIS AND CHARACTERIZATION OF PHOSPHONATE
SUBSTITUTED NOVEL PORPHYRAZINES**

by

Nürüfe KEMİKLİ

January 2008

**SYNTHESIS AND CHARACTERIZATION OF PHOSPHONATE
SUBSTITUTED NOVEL PORPHYRAZINES**

by

Nürüfe KEMİKLİ

A thesis submitted to

the Graduate Institute of Sciences and Engineering

of

Fatih University

in partial fulfillment of the requirements for the degree of

Master of Science

in

Chemistry

January 2008
Istanbul, Turkey

APPROVAL PAGE

I certify that this thesis satisfies all the requirements as a thesis for the degree of Master of Science.

Assist. Prof. Dr. Metin TÖLÜ
Head of Department

This is to certify that I have read this thesis and that in my opinion it is fully adequate, in scope and quality, as a thesis for the degree of Master of Science.

Assist. Prof. Dr. Ramazan ÖZTÜRK
Supervisor

Examining Committee Members

Prof. Dr. Ahmet GÜL

Assist. Prof. Dr. Ramazan ÖZTÜRK

Assist. Prof. Dr. Burak ESAT

It is approved that this thesis has been written in compliance with the formatting rules laid down by the Graduate Institute of Sciences and Engineering.

Assist. Prof. Dr. Nurullah ARSLAN
Director

SYNTHESIS AND CHARACTERIZATION OF PHOSPHONATE SUBSTITUTED NOVEL PORPHYRAZINES

By Nürüfe KEMİKLİ

M.Sc. Thesis in Chemistry
January 2008

Supervisor: Assist. Prof. Dr. Ramazan ÖZTÜRK

ABSTRACT

The porphyrazines are class of porphyrin derivatives being studied for their properties with peripherally ionic groups and also they are interesting area of supramolecular chemistry due to having macrocyclic, stable and planar structures, containing functional groups on the peripheral positions. Water soluble ionic groups provide binding of porphyrazines to some macromolecules such as DNA, RNA and proteins according their charge and also they can be synthesized with multinuclear centered via donor groups on them.

In this study; the synthesis of peripherally phosphonate substituted porphyrazine, its complexes and phosphonic acid substituted porphyrazine were studied.

Firstly phosphonate substituted maleonitrile was synthesized from the dithiomaleonitrile disodium salt and 2-bromoethyldiethylphosphonate. Then, phosphonate substituted porphyrazine were prepared by the template of freshly prepared $Mg(OPr)_2$ and 1,2-bis{2-(diethylphosphonate)ethylthio}maleonitrile. Metal free porphyrazine was obtained by the treatment of TFA acid and following the NH_3 neutralization. The phosphonic acid substituted porphyrazine was obtained by the cleavage of phosphonate esters to phosphonic acid via the TMSBr. Phosphonic acid groups were treated with 0.5 M NaOH solution and following $CaCl_2$ solution, and water insoluble calcium salt of porphyrazine was obtained. All products were characterized with the spectrophotometric methods (UV, FTIR, H-NMR, C-NMR, P-NMR).

Keywords: Porphyrazine, phosphonic acid, supramolecule, TMSBr.

FOSFONAT İÇEREN YENİ PORFİRAZİNLERİN SENTEZİ VE KARAKTERİZASYONU

Nürüfe KEMİKLİ

Yüksel Lisans Tezi-Kimya Bölümü
Ocak 2008

Tez Yöneticisi: Yrd. Doç. Dr. Ramazan ÖZTÜRK

ÖZ

Makrosiklik yapıdaki tetrapirollerden olan porfirazinler kararlı düzlemsel yapıları ve periferik konumlarında değişik fonksiyonel gruplar ihtiva etmesi bakımından supramoleküler kimyanın ilgi çeken konuları arasındadır. Suda çözünür katyonik yapılarının biyolojik makromoleküllerle (DNA, RNA ve proteinler) etkileşimlerinin yanı sıra ihtiva ettikleri donör gruplar üzerinden de multinükleer yapıların sentezlenmesine imkan vermektedirler. Termal ve asidik kararlılıklarının yanı sıra sentezlenmesinin kolaylığı ile de benzer moleküller olan ftalosiyanın ve porfirin kimyasına alternatif olarak düşünülmektedir.

Bu çalışmada periferik konumda sekiz tane fosfonat grubu ihtiva eden porfirazin sentezlenmesi ve bu porfirazinlerin fosfonat uçlarından supramoleküler etkileşimlerle değişik metal komplekslerinin hazırlanması hedeflenmiştir.

Porfirazin sentezinde; önce ditiyo maleonitrildisodyum tuzu bilinen yöntemle sentezlenip 2-bromoetilfosfonat ile reaksiyona sokularak 1,2-bis{2-(diethylfosfonat) etiltiyo}-maleonitril ligandı elde edildi. Daha sonra 1,2-bis{2-(diethylfosfonat) etiltiyo}-maleonitril ligantının magnezyum propionat varlığında tetramerizasyonu sonucunda fosfonat içeren porfirazin sentezlendi. Fosfonat içeren porfirazin TFA ile muamele edildikten sonra, NH₃ nötralizasyonu yapılarak metallsiz porfirazin elde edildi. Fosfonat uçlarının TMSBr yardımı ile hirolizlendirilmesi sonucu periferik konumlarda fosfonik asit oluşumu gerçekleştirildi. Sentezlenen porfirazin molekülünün periferik konumlarındaki fosfonik asit grupları 0.5 M NaOH ile muale edildi ve elde edilen çözeltiye CaCl₂ çözeltisi eklenerek suda çözünmeyen, kalsiyum fosfonat ihtiva eden porfirazin elde edildi. Bütün ürünler bilinen spektroskopik metodlarla karakterize edildi (UV, FTIR, H-NMR, C-NMR, P-NMR).

Anahtar Kelimeler: Porfirazin, fosfonik asit, supramolekül, TMSBr.

ACKNOWLEDGEMENT

I express sincere appreciation to Assist. Prof. Dr. Ramazan ÖZTÜRK for his guidance and insight throughout the research.

I express my thanks and appreciation to my family for their understanding, motivation and patience. Lastly, but in no sense the least, I am thankful to all colleagues and friends who made my stay at the university a memorable and valuable express.

TABLE OF CONTENTS

ABSTRACT.....	iii
ÖZ	iv
ACKNOWLEDGEMENT	v
TABLE OF CONTENTS.....	vi
LIST OF TABLES.....	x
LIST OF FIGURES	xi
ABBREVIATIONS	xv
CHAPTER 1 INTRODUCTION.....	1
1.1 GENERAL INFORMATION ABOUT PORPHYRAZINES	1
CHAPTER 2 SYNTHESIS METHODS OF AZAPORPHYRINS.....	8
2.1 GENERAL SYNTHESIS METHODS.....	8
2.2 TRANSITION METAL COMPLEXES OF PORPHYRAZINES	12
2.3 RECENT PROGRESS FOR PORPHYRAZINE SYNTHESIS.....	15
CHAPTER 3 PROPERTIES OF PORPHYRAZINES.....	17
3.1 STRUCTURAL AND SPECTRAL PROPERTIES OF PORPHYRINIC MOLECULES	17
3.1.1 Reaction Center of Porphyrinic Molecules.....	19
3.1.2. The Influence of Benzo and Aza substitution.....	21
3.1.3 The Location of the NH Hydrogen Atoms and the State of the N-H Bonds	23
3.1.3.1 Quantum- Chemical Investigations	26
3.1.3.2 Nuclear Magnetic Resonance Spectroscopy.....	28
3.2 ACID-BASE PROPERTIES OF AZAPORPHYRINS	33
3.2.1 Acid Ionization of Azaporphyrins	35
3.2.2 Spectral Picture of the Acid Ionization.....	36
3.2.3 Methods of the Quantitative Estimation of Acidity.....	39
3.2.4 Acidity of Common Porphyrins.....	40
3.2.5 Azaporphyrins.....	41

3.2.6	N-base Adducts of Tetraazaporphyrins	43
3.2.7	Basic Properties of Azaporphyrins	44
CHAPTER 4	APPLICATIONS	46
4.1	BIOMEDICAL APPLICATIONS OF SOME WATER SOLUBLE PORPHYRINIC MOLECULES	46
4.1.1	Developing a Structure–function Relationship for Anionic Porphyrazines Exhibiting Selective Anti-tumor Activity	46
4.1.2	Studies on Photodynamic Activity of New Water-soluble Azaphthalocyanines	48
4.1.3	Super-Charged Porphyrazines: Octacationic Tetraazaporphyrins and Investigation Binding Properties of Octa-plus Porphyrazines to DNA ..	50
4.1.4	Generation of Singlet Oxygen with Anionic Aluminum Phthalocyanines in Water	54
4.1.5	Photodynamic Activity of Some Tetraazoporphyrin Derivatives	56
4.1.6	Tetracationic Phthalocyanines	57
4.1.7	Nonanuclear Supramolecular Structures from Simple Modular Units ..	59
4.1.8	Porphyrazines with Tertiary or Quaternized Aminoethyl Substituents ..	61
4.2	PRINCIPLES OF PHOTO DYNAMIC THERAPY	62
4.2.1	Photochemotherapy	62
4.2.2	How to Perform PDT	65
4.2.3	Photosensitisers amphiphilicity in PDT	66
4.2.4	Singlet Oxygen Yields	68
4.2.5	Development of Photosensitisers	68
4.2.6	Porphyrin, porphyrazine and Phthalocyanines as Photosynthesizers	69
CHAPTER 5	EXPERIMENTAL PART	72
5.1	CHEMICALS AND APPARATUS	72
5.2	INSTRUMENTATIONS	72
5.3	SYNTHESIS OF PORPHYRAZINE	73
5.3.1	Synthesis of Dithiomaleonitrile Disodium salt (1)	73
5.3.2	Synthesis of 1,2-Bis {2-(diethyl phosphonate) ethylthio} Maleonitrile (2)	74
5.3.3	Synthesis of Magnesium Octakis(2-(diethylphosphonate)ethylthio(3a) or Magnesium Octakis(2-(dipropylphosphonate)ethylthio (3b) Porphyrazines	75

5.3.4	Synthesis of Metal Free Octakis(2-(dipropylphosphonate)ethylthio Porphyrazine (4)	76
5.3.5	Dealkylation of Phosphonate Esters of MgPz with TMSBr (5)	77
5.3.6	Synthesis of Metal Complexes of Octakis(2- (diethylphosphonate)ethylthio Porphyrazines	78
5.3.6.1	Synthesis of Co II) Porphyrazine.....	78
5.3.6.2	Synthesis of Cu (II) Porphyrazine	79
5.3.6.3	Synthesis of (VO) ²⁺ Porphyrazine	80
5.3.7	Na and Ca salts of Phosphonate Substituted Porphyrazines.....	80
CHAPTER 6	RESULTS AND DISCUSSION.....	82
6.1	DITHIOMALEONITRILE SALT	82
6.1	1,2-BIS{2-DIETHYLPHOSPHONATE}ETHYLDITHIO}MALEONITRILE	82
6.3	MAGNESIUM OCTAKIS(2-(DIETHYLPHOSPHONATE) ETHYLTHIO PORPHYRAZINES.....	83
6.4	METAL FREE PORPHYRAZINES	85
6.5	PHOSPHONIC ACID SUBSTITUTD PORPHYRAZINES	87
6.6	METALATION OF METAL FREE PORPHYRAZINES.....	88
6.7	SODIUM AND CALCIUM SALT OF PORPHYRAZINES.....	88
CHAPTER 7	CONCLUSION	90
REEERENCES	91
APPENDIX A	FT-IRSPECTRUM OF DISODIUM DITHIOMALEONITRILE 1.	102
APPENDIX B	FT-IR SPECTRUM OF of 1,2-BIS{2-(DIETHYLPHOSPHONATE) ETHYLTHIO} MALEONITRILE LIGAND 2	103
APPENDIX C	¹ H NMR of 1,2-BIS{2-(DIETHYLPHOSPHONATE) ETHYLTHIO} MALEONITRILE LIGAND 2	105
APPENDIX D	¹³ C NMR of 1,2-BIS{2-(DIETHYLPHOSPHONATE) ETHYLTHIO} MALEONITRILE LIGAND 2	106
APPENDIX E	³¹ P NMR OF 1,2-BIS{2-(DIETHYLPHOSPHONATE) ETHYLTHIO} MALEONITRILE LIGAND 2	106
APPENDIX F	FAB-MS SPECTRUM of 1,2-BIS{2-(DIETHYL PHOSPHONATE) ETHYLTHIO}MALEONITRILE LIGAND 2.....	107
APPENDIX G	UV-VISIBLE SPECTRUM OF(a) ETHYL 3a AND (b) PROPYL 3b PHOSPHONATE ESTERS OF Pzs	108

APPENDIX H	FT-IR SPECTRUM of MgPz 3b.....	109
APPENDIX I	^1H NMR OF MgPz 3b	110
APPENDIX J	^{13}C and ^{31}P NMR OF MgPz 3b	111
APPENDIX K	EXPANDED ^{13}C NMR OF MgPz 3b	112
APPENDIX L	FT-IR SPECTRUM OF Pz 3a	113
APPENDIX M	FAB-MS SPECTRUM OF MgPz (ETHYL) 3a.....	114
APPENDIX N	FAB-MS SPECTRUM of MgPz (PROPYL) 3b.....	115
APPENDIX O	UV-VISIBLE SPECTRUM OF H_2Pz	116
APPENDIX P	FT-IR SPECTRUM OF H_2Pz	117
APPENDIX Q	^1H NMR OF H_2Pz	118
APPENDIX R	^{13}C NMR H_2Pz	119
APPENDIX S	UV-VISIBLE SPECTRUM OF MgPz-P(O)(OH)_2	120
APPENDIX T	FT-IR SPECTRUM OF MgPz-P(O)(OH)_2	121
APPENDIX U	^1H NMR OF (MgPz-P(O)(OH)_2)	122
APPENDIX V	EXPANDED ^1H NMR OF (MgPz-P(O)(OH)_2)	123
APPENDIX W	^{13}C NMR OF (MgPz-P(O)(OH)_2)	124
APPENDIX X	UV-VISIBLE SPECTRUM OF Co-Pz AND Cu-Pz	125
APPENDIX Y	FT-IR SPECTRA OF Co-Pz, AND Cu-Pz	126
APPENDIX Z	UV-VISIBLE AND FTIR SPECTRA OF VO-Pz.....	127
APPENDIX A1	UV-VISIBLE SPECTRUM OF Ca_8MgPz	128
APPENDIX B1	FT-IR SPECTRUM OF Ca_8MgPz	129

LIST OF TABLES

TABLES

2.1 Preparation of substituted porphyrazines by treatment of maleonitrile derivatives with $Zn(OAc)_2$ and HMDS in DMF	16
3.1 UV-visible spectra of H_2Pz : Experimental and calculated parameters	28
3.2 Thermodynamic parameters of the acid ionization of porphyrins and azaporphyrins.....	39
4.1 Quantum yields of singlet oxygen generation by phthalocyanines IV-VI in aqueous solutions.....	55

LIST OF FIGURES

FIGURES

1.1	Tetrapyrrole-macrocycles	2
1.2	UV-visible spectrum of a porphyrin	4
1.3	Electronic absorption spectrum of (H ₂ Pz)	5
1.4	Electronic absorption spectrum of	5
1.5	Electronic transitions in the visible and close UV regions of metalated and non-metalated porphyrazines	6
2.1	An example of porphyrazine synthesis	8
2.2	Synthesis of porphyrazine molecules from two different precursor	9
2.3	Synthesis of metal free porphyrazine directly from succinoimidine	10
2.4	Synthesis of metal free porphyrazine by acid treatment	10
2.5	Synthesis of <i>trans</i> -substituted porphyrazine	11
2.6	Synthesis of unsymmetrical porphyrazine	12
2.7	Metal complex formation of porphyrazine	13
2.8	The synthesis of metal complex of porphyrazine with Ni (central) and Pd (peripherally) metals	14
2.9	Synthesis of metalloporphyrazine with HMDS method	15
3.1	General structure of porphyrazine molecules	18
3.2	Some substituted porphyrinic molecules	19
3.3	The skeleton of A, pyrrole type B, pyrrolenine-type rings	20
3.4	Changes in the geometry of the CN skeleton produced by tetrabenzo substitution (left side) in porphyrins (Δ) and tetraazaporphyrins (δ) and by tetraaza substitution (right side) in porphyrins (Δ) and tetrabenzoporphyrins (δ). The angles are in degrees and the bond lengths in 10 ⁴	22
3.5	The possible structures of the N ₄ H ₂ reaction center in porphyrin-type ligands, where X = CH in porphyrins, X = N in azaporphyrins: LS, localized (bonded) structure; US, unlocalized (shared or bridged structure); HS, hydrogen-bonded structure; IS, intraionized structure	24

3.6 Interpretation of the ^{15}N NMR spectra of solid H_2P and H_2Pc . Values of the chemical shifts are from for H_2Pc and from for H_2P	30
3.7 The state of NH protons depending on temperature	32
3.8 Porpphyrazine metal complex	34
3.9 Absorption spectra of the neutral form (I), monoanion (2) and dianion (3) of H_2EP (a), $\text{H}_2(\text{Me})\text{PEt}$, (b), H_2MAEP (c) and H_2TAP (d) in $\text{DMSO-H}_2\text{O-PhMe}(82:10:8)$ (a-c) and in DMSO	36
3.10 Symmetry properties of HOMO (π_1 and π_2) and LUMO (π^* and π_2^*) for the porphyrin type macrocyclic chromophor having $\text{D}_{2\text{h}}$ symmetry	37
3.11 Schematic representation (first order perturbation theory approximation)of the HOMO and LUMO energy changes of H_2TAP during formation of the monoanion HTAP^- , dianion TAP^{2-} and successive substitution of meso-nitrogens with methine bridges in the dianion.....	37
3.12 (a) Absorption spectra of H_2TAPPh_g (1) and its "pyridinium salt" (2); (b) Possible structure of the "pyridinium salt".....	43
4.1 Synthesis of $\text{H}_2[\text{Pz}(\text{A}_n;\text{B}_{4-n})]$, where A is $[\text{S}(\text{CH}_2)_3\text{COOR}]_2$ (R) n-Pr, H) and B is a fused β,β -diisopropoxybenzo group, including the compounds with n - 4 (6), n- 3 (7) and the trans compound with n- 2 (8).....	47
4.2 Synthesis of water soluble AzaPcs	49
4.3 Absorption spectra of 6 in pyridine (A) and in 0.2% aqueous NaHCO_3 (B). Concentration was 12.5×10^{-6} mol/dm ³ in both cases	49
4.4 Degradation of DPBF by singlet oxygen generation	50
4.5 Synthesis octa-methyl-pyridyl porphyrazines	51
4.6 Absorption (—) and emission (— • —) of the octapyridylporphyrazines: (A) $[\text{Mgpz}(\text{pyr})_8]$ in 20% MeOH in CHCl_3 , emission excitation at 378 nm; (B) $[\text{H}_2\text{pz}(\text{pyr})_8]$ in 20% MeOH in CHCl_3 , emission excitation at 367 nm; (C) $[\text{H}_2\text{pz}(\text{H-pyr})_8]^{8+}$ in aqueous HCl (~1.2 M), emission excitation at 607 nm	52
4.7 Electronic absorption spectra of CuPz^{+8} alone (solid line) and in the presence of CT DNA (dashed line). B. Difference absorption spectra in the Q-band region for CuPz^{+8} titrated with CT DNA. C. Electronic absorption spectra for the titration of ZnPz^{+8} with DNA at pH 7.00 in 0.1 M NaCl and 0.01 M phosphate buffer D. Plot of the absorbance at 660 nm of ZnPz^{+8} versus the concentration of CT DNA base pairs	53
4.8 Cartoon of three possible binding modes of tetra-N-methyl pyridyl porphyrins with DNA.....	53

4.9 (A) Phosphonate substituted aluminum phthalocyanines. (B) Electronic absorption spectra of I, II, and III in aqueous buffer solution (pH 7.4) and (4) of III in the same solution with addition of 1 wt % Triton X-100	55
4.10 Synthesis of cyano and cyano free, and metallo porphyrazines ($R_1=CN,H$, $R_2=diethylamino$).....	56
4.11 Synthesis of pcs. (i) K_2CO_3 , DMF, 30 °C; (ii) DBU, 1-hexanol,24 h; (iii) metal salts,24 h	58
4.12 Phthalocyanines 3-5, B: Quaternized Pc 6.....	58
4.13 Electronic absorption spectra of octakis(4- pyridoxyethylthio)porphyrza-zinato magnesium octakis(4- pyridoxyethylthio)porphyrzinato magnesium and $[VO(acac)_2(4-pyCOOCH_2CH_2S)]_8MgPz$	60
4.14 X-band EPR spectra of (a) $VO(acac)_2$ and (b) 3 in powder form at 300 K.....	60
4.15 Octakis(2-dimethylaminoethylthio)porphyrzinatomagnesium (MgPz) and Octakis(2-trimethylammoniumethylthio)porphyrzinato-magnesium] octaiodide (MgPz)	61
4.16 Photosensitizations of oxygen via type II mechanism.....	64
4.17 How PDT works	65
4.18 Schematic representation of membrane layer.....	66
5.1 Synthesis of disodium dithiomaleonitrile salt.....	73
5.2 Synthesis of 1,2-Bis{2-(diethyl phosphonate) ethylthio} maleonitrile ligand 2 ...	74
5.3 Preparation of magnesium propanolates.....	75
5.4 The synthesis of magnesium octakis(2-(diethylphosphonate)ethylthio porphyrzine (MgPzs) R: C_2H_5 (3a), C_3H_7 (3b).....	76
5.5 Synthesis of metal free porphyrzine (H_2Pz) 4, R: C_2H_5 or C_3H_7	77
5.6 Synthesis of phosphonic acid substituted porphyrzine5	78
5.7 Synthesis of Co(II)Pz.....	79
5.8 Synthesis of Cu(II)Pz.....	79
5.9 Synthesis of $(VO)^{2+}Pz$	80
5.10 Synthesis of Ca_8MgPz	81
6.1 The structure of 1,2-Bis{2-(diethyl phosphonate) ethylthio} maleonitrile ligand2	83
6.2 The structure of magnesium octakis(2-(diethylphosphonate)ethylthio) porphyrzine Spectrum of with lines (ethyl) and (propyl) esters of Pzs	84
6.3 UV-visible spectrum of with lines __ 3a (ethyl) and3b (propyl) esters of Pzs in	

chloroform	85
6.4 The structure of metal free octakis(2-(diethylphosphonate)ethylthio) porphyrzine 4	86
6.5 The UV-vis spectrum of metal free octacis(2-(diethylphosphonate)ethylthio) porphyrzine 4	86
6.6 The structure phosphonic acid substituted porphyrzine MgPzOH 5	87
6.7 The structure metalated porphyrzines	88
6.8 The structure Ca_8MgPz	89

LIST OF SYMBOLS AND / OR ABBREVIATIONS

SYMBOLS AND / OR ABBREVIATION

H ₂ AP	Azaporphyrins
H ₂ MAP	Monoazaporphine
H ₂ MATBP	Monoazatetrabenzoporphine
H ₂ P	Porphine
H ₂ TAP	Tetraazaporphine
Pc	Phthalocyanine
H ₂ Pc	Metal Free Phthalocyanine
H ₂ TATBP	Triazatetrabenzoporphine
H ₂ TBP	Tetrabenzoporphine
H ₂ TPP	Meso-tetraphenylporphine
DBU	1,8-Diazabicyclo[5.4.0]undec-7-ene
MAP	Metalloazaporphyrin
NMR	Nucleic Magnetic Resonance
H ₂ Pz	Metal Free Porphyrazine
Nc	Naphthalocyanine
TFAA	Trifluoroacetic acid
HCl	Hydrochloric acid
Zn (OAc ₂)	Zinc(II)Acetate
MnCl ₂	Manganese(II) chloride
DPBF	1,3-diphenylisobenzofuran
HMDS	Hexamethyldisilazane
PTSA	<i>p</i> -toluene sulfonic acid
ΔE(Q)	Energy difference of electronic transitions
TAP or Pz	Tetraazaporphyrin or porphyrazine

CHAPTER 1

INTRODUCTION

1.1 GENERAL INFORMATION ABOUT PORPHYRAZINES

Porphyritic conjugated macrocycles have been a subject of great interest due to various high synthetic possibilities, numerous technological applications, and biological importance in coordination chemistry. The physical properties of these square planar porphyrine-like molecules depend strongly on their chemical and geometric structure, providing an enormous opportunity for molecular design and control of properties by ligand substitution and ring symmetry modification. Porphyrin, phthalocyanine and porphyrazine molecules have also been a theme of considerable theoretical interest due to their high symmetry, planar molecular arrangements, and electronic delocalization. A large number of theoretical works have been devoted to the understanding of the atomic scale structure of these molecules, their building blocks and the mechanisms of charge transport and optical properties [1, 2].

Porphyrazines contain a central conjugated C_8N_8 ring with four pyrrole groups. The analogies between porphyrazines and porphyrins were motivated by their similar chemical structure; they differ only by the presence of four meso-nitrogen atoms (in porphyrazines) as opposed to four methine groups (in porphyrins) in the central ring. The porphyrazine class of molecules is generally understood to include the tetraazaporphyrin (or porphyrazine) (TAP) and its analogues: the phthalocyanine (Pc), naphthalocyanine (Nc) molecules. Those molecules are presented in Figure 1.1. The chemical structure difference between TAP, Pc, and Nc is the number of benzene units in the composition of the molecule, or more precisely, the number of benzene groups fused on each pyrrole unit (0, 1 and 2 respectively). Thus, TAPs are compounds lying structurally in-between normal porphyrins and phthalocyanines [3].

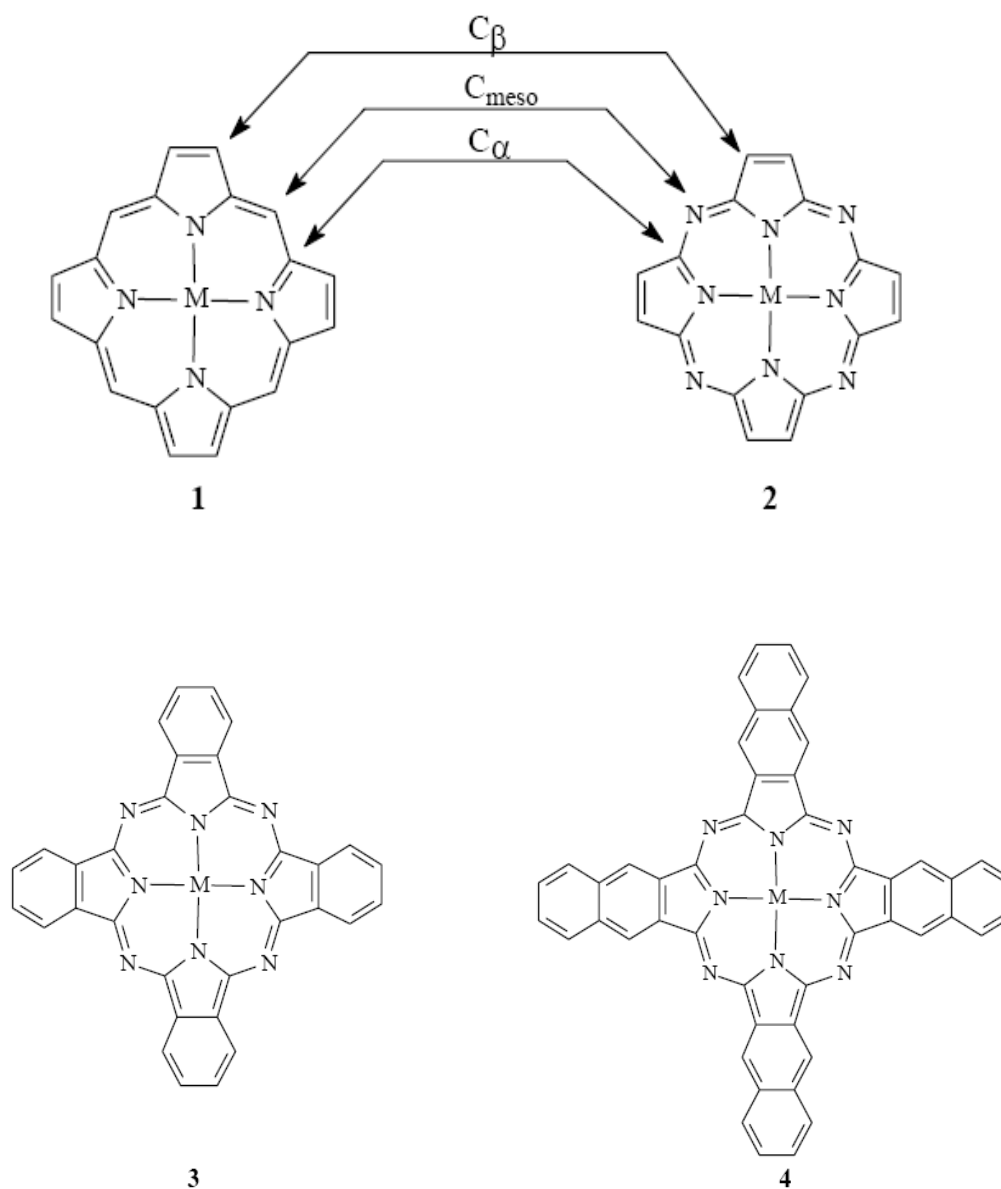


Figure 1.1 Tetrapyrrole-macrocycles (M=Metal or H₂) [4].

1. Porphyrin **2.** Porphyrazine **3.** Phthalocyanine **4.** Naphthalocyanine

Porphyrazines (Figure 1.1) are distinguished from phthalocyanines by the presence of benzo rings fused to the pyrrole rings in the latter. On the other hand, naphthalocyanines (tetranaphthaloporphyrazines) differ from porphyrazines by the presence of naphthalene rings fused to pyrrole rings in the former. All porphyrins, porphyrazines, phthalocyanines and naphthalocyanines share a common macrocyclic substructure which consists of four pyrrolic subunits. Porphyrazines also contain a 22- π electron system present in porphyrins, a feature that is critical for affecting a wide range of extraordinary properties such as the ability to absorb visible light, to mediate the

conversion of absorbed light to other forms of chemical and physical energy, and to enhance thermodynamic and kinetic stability. These conjugated systems assume many resonance forms and can accept substituents at a number of positions.

While phthalocyanines and naphthalocyanines are porphyrine analogs, porphyrins differ from porphyrines only in the meso-positions, wherein porphyrins have methine bridges and porphyrines aza bridges. A porphyrin has twelve positions available for substitution including eight β positions and four meso-positions. On the other hand, porphyrines, phthalocyanines, and naphthalocyanines have 8, 16 and 24 positions available for substitution, respectively.

The chemical versatility of the porphyrine macrocycle offers the opportunity of varying the electronic structure through ligand and metal modifications; this includes substitution, elaboration, and truncation of the macrocycle. Substitutions in a very controlled manner with certain electron-withdrawing or electron-donating groups to the macrocycle were found to change the electronic properties [4, 5].

Understanding of the electronic and structural properties of porphyrin molecules is important to have more insight into biological processes such as photosynthesis or oxygen transport. Phthalocyanines and porphyrins are also studied for their possible application in optoelectronic devices [6, 7].

The porphyrine is isoelectronic with the porphyrin, but because of its nitrogen atoms at the meso positions chemically much closer to the technologically important phthalocyanines. To investigate the electronic properties of the phthalocyanines it is, therefore, necessary to address the influence of those nitrogens on the electronic structure.

In the visible absorption spectra of porphyrins, the highly conjugated aromatic macrocycle shows an intense absorption in the region of about 400 nm which is referred to as the Soret Band (Figure 1.2). Visible spectra of porphyrins also show four weaker bands, the Q bands, at longer wavelengths from about 450-700 nm giving rise to reddish purple color of porphyrins [8].

The effects of meso-tetraaza substitution on the UV-visible absorption bands of porphyrins are to date well documented [4, 14]. Porphyrine complexes exhibit for

instance a significant red shift and an intensification of the lowest energy $\pi \rightarrow \pi^*$ Q band, and a more complicated Soret band region due to additional $\pi \rightarrow \pi^*$ transitions introduced by azamethine groups [9, 10].

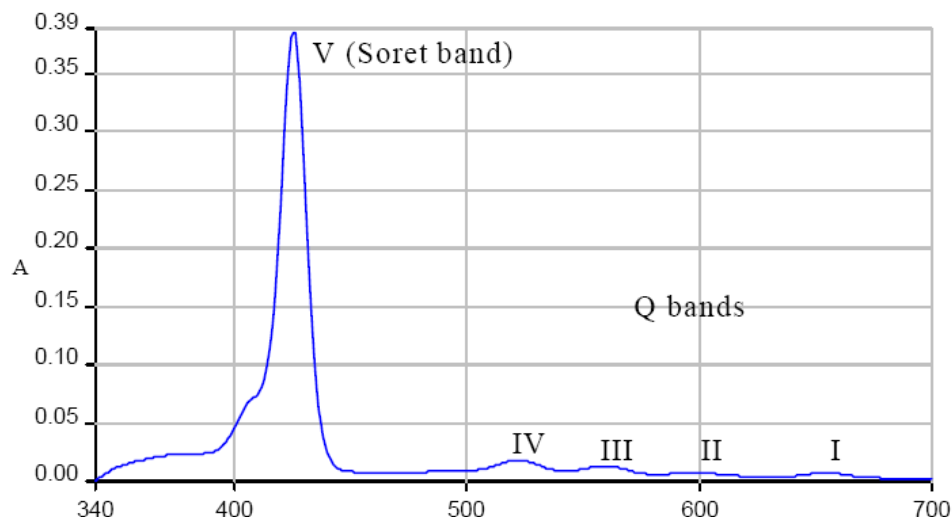


Figure 1.2 UV-visible spectrum of a porphyrin [4, 8].

The UV-visible spectra in porphyrazines are influenced by substituents and the presence or absence of a metal at the centre. Peripheral substitution influences the UV-visible spectra with *cis*- and *trans*- isomers showing different split in LUMOs. *Trans*-isomers show large splitting compared to *cis*-peripherally substituted porphyrazines. In non-metallated porphyrazines with reduced symmetry, reduction in symmetry removes degeneracy of e_g LUMO and gives a split Q-band (Figure 1.3) [11]. In cases where a lone pair of electrons in peripheral ligating atoms (N) becomes bonded to metal ions, the Q-band is split into two sharp bands (Figure 1.3) because their interaction with the porphyrazine ring is suppressed [11].

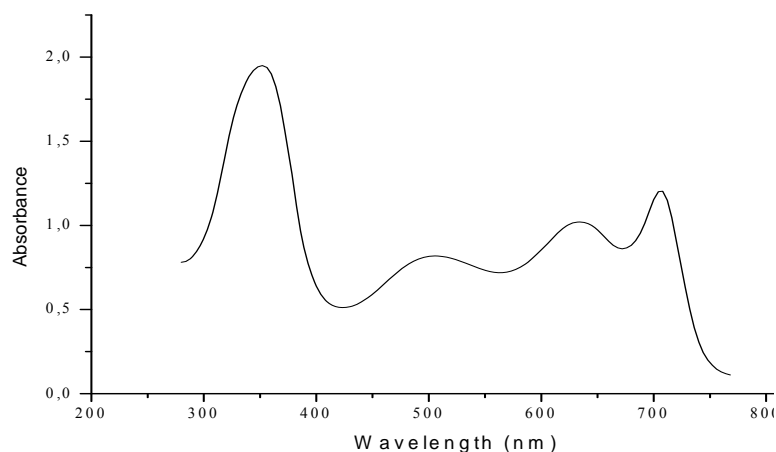


Figure 1.3 Electronic absorption spectrum of (H₂Pz).

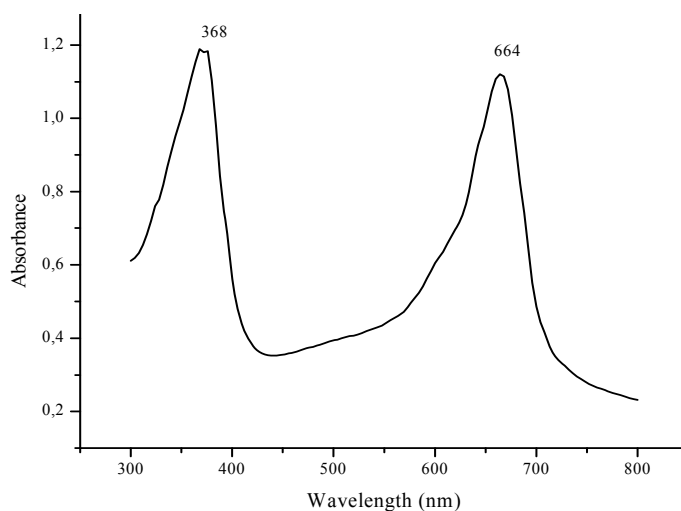


Figure 1.4 Electronic absorption spectrum of MgPz.

For nonmetalated (metal-free) porphyrazines (D_{2h} symmetry), the UV-visible spectra show two lower energy split Q-bands at 550-700 nm and a higher energy Soret (B) band at 300-400 nm, which are assigned to $a_u \rightarrow b_{2g}$ (Qx), $a_u \rightarrow b_{3g}$ (Qy) and $b_{1u} \rightarrow b_{2g}$ (Qx), $b_{1u} \rightarrow b_{3g}$ (By) transitions (Figure 1.5). These transition bands are assigned to excitations from the two highest-occupied molecular orbitals (HOMO) (a_{1u} and a_{2u}) into lowest unoccupied molecular orbitals (LUMO, e_g) [11-14]. The lower energy peak which could be found at 400- 500 nm is assigned to $n-\pi^*$ transitions from the lone-pair electrons in external meso-nitrogen atoms into a π^* ring system.

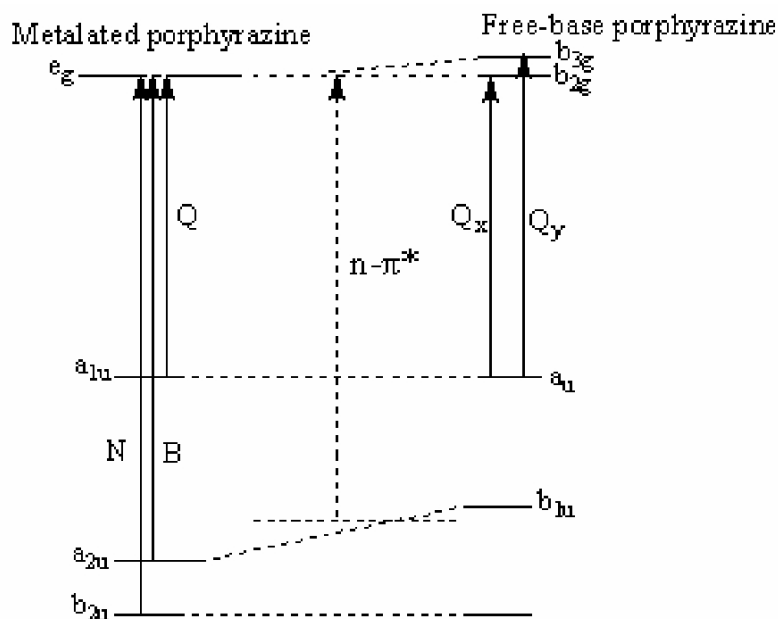


Figure 1.5 Electronic transitions in the visible and close UV regions of metalated and non-metalated porphyrazines [4].

Metalated porphyrazines exhibit two intense $\pi \rightarrow \pi^*$ absorptions, a low energy Q band that is accompanied by a slight higher energy shoulder and a higher energy B band. For metalated porphyrazines, the symmetry of the chromophore is D_{4h} with the two LUMOs b_{2g} and b_{3g} giving rise to a two-fold degenerate e_g level resulting to an unsplit Q and B absorptions associated with transitions $a_{1u} \rightarrow e_g$ and $a_{2u} \rightarrow e_g$ [15-16].

The molecules from the porphyrazine class have gained interest from the scientific community due to both their potential in technological applications and their relationship to biological important porphyrins, such as chlorophyll and hemoglobin molecules, that play a vital role in life processes. The remarkable construction of porphyrazines, characterized by high symmetry, planarity, and electron delocalization, made these molecules attractive for theoretical studies as well.

Phosphonic acids bearing heteroatoms in the α and β positions have attracted considerable interests because of their well recognized interesting biological properties [17]. Most importantly, they act as inhibitors of proteolytic enzymes, such as rennin and human immunodeficiency virus (HIV) protease, as agents affecting the growth of plants or as haptens for the development of catalytic antibodies [18].

Biphosphonates have binding ability hydroxyapatite crystals in mineralized bone matrix for inhibiting function of osteoclasts which mediate bone resorption and osteoblast, which mediate new bone formation. It has been proposed that PDT might be useful in treating bone disorder by destroying osteoclasts or other cells involved in metabolic bone disorder [19]. Phorphyrinic molecules are used for PDT in many health problems [20]. Phosphonic acid substituted porphyrazines can be alternative to biphosphonic acids and phosphonates for the treatment of bone disorder by using PDT near the other application.

CHAPTER 2

SYNTHESIS METHODS OF AZAPORPHYRINS

2.1 GENERAL SYNTHESIS METHODS

The majority of TAP structures prepared from 1937 to 1990 have been collected by Luk'yanets and Kobayashi [21].

Since porphyrazines are analogs of phthalocyanines with the only differences of the absence of the fused benzene ring on the pyrrole units, the synthetic methods applied to phthalocyanines can be used to synthesize porphyrazines [21].

Porphyrazine can be synthesized from functionalized nitriles such as maleonitriles, fumaronitriles and phthalonitriles. Like benzoporphyrazines (phthalocyanines), the synthesis of porphyrazines is limited to Linstead macrocyclisation in which the dinitrile 1 or 2 undergoes a macrocyclisation reaction under reflux in the presence of a magnesium alkoxide in the corresponding alcohol (typically 1-butanol or 1-pentanol) or dimethylaminoethanol to yield 3 (Figure 2.1). Magnesium porphyrazines such as 3 are easily demetalated under acidic conditions to form the free-base porphyrazine such as 4 [4, 22].

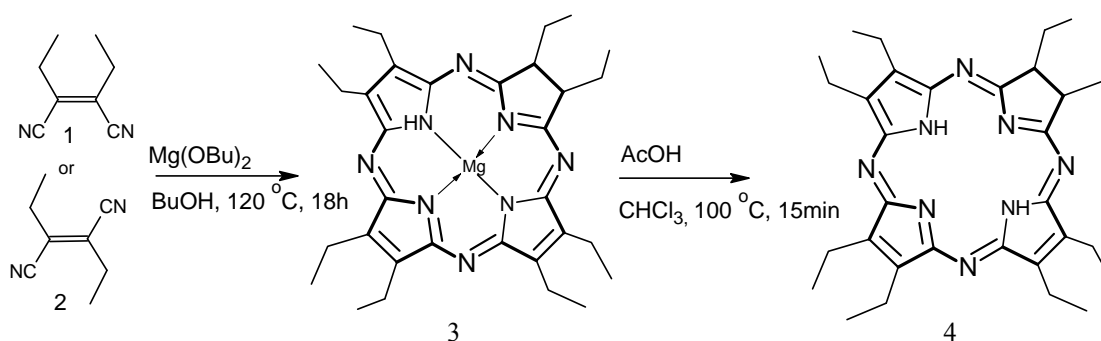


Figure 2.1 An example of porphyrazine synthesis [4].

Removal of magnesium can be achieved by treating a solution of magnesium octaethyltetraazaporphyrin 3 in chloroform and acetic acid for 15 minutes, to give free-base porphyrazine 4. The above synthetic method is known as Linstead magnesium template macrocyclisation. The same synthetic method is also applicable if two different precursors are macrocyclised to form different porphyrazine hybrids (Figure 2.2) [23].

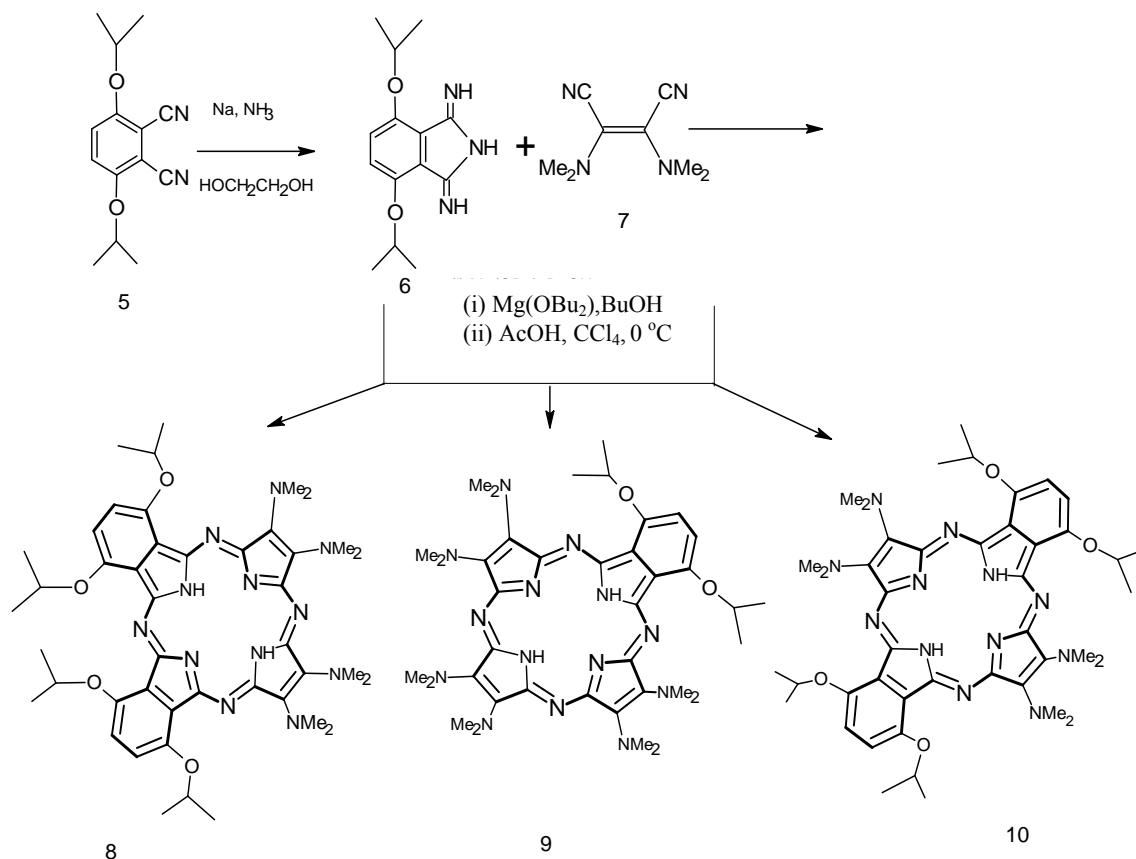


Figure 2.2 Synthesis of porphyrazine molecules from two different precursors [23].

Since phthalonitrile 5 is unreactive in the synthesis of either the phthalocyanine or porphyrazine, it is first converted into its corresponding 1,3-diiminoisoindoline 6 to increase its reactivity. A suspension of phthalonitrile 5 in 1,2-ethanediol is bubbled with ammonia gas in the presence of sodium metal. The 1,3-diiminoisoindoline 6 derived from hydroquinone isopropyl ether 5 is then reacted with dimethyl aminomaleonitrile 7 to give porphyrazine hybrids 8, 9, 10 (Figure 2.2) [23].

Some metal free porphyrazines can be prepared directly from succinoimidines by

heating in high boiling solvents such as chlorobenzene and nitrobenzene [21].

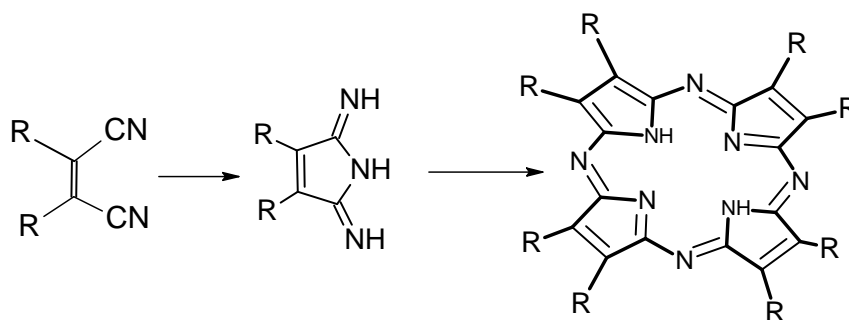


Figure 2.3 Synthesis of metal free porphyrazine directly from succinoimidine [21].

Nowadays metal-free porphyrazines are obtained by demetallation of corresponding magnesium porphyrazine with acid such as TFAA or HCl.

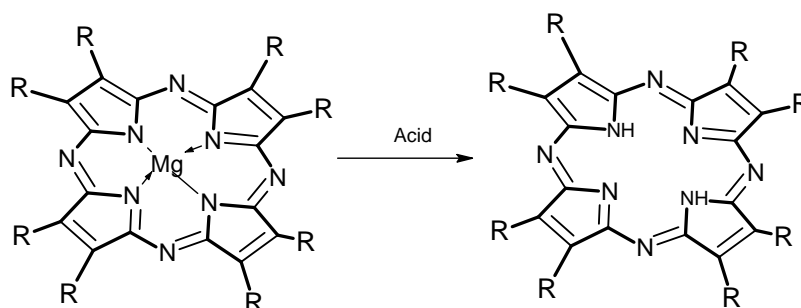


Figure 2.4 Synthesis of metal free porphyrazine by acid treatment [21].

Various substituents provide porphyrazines with substantial organic solubility compared to their porphyrin and phthalocyanine counterparts. Peripheral substitution among porphyrazines is becoming an increasingly popular strategy for the design of functional dyes and molecular devices. Porphyrazines with peripheral substitution of the form $M[Pz-(A_n:B_{4-n})]$, where A and B are functional groups fused to the β -position of the pyrroles, have the potential to exhibit magnetic and electronic properties [12, 24-25]. Due to peripheral substitution, these porphyrazines show unusual UV-visible spectra, redox chemistry and electrochemistry. In addition, they exhibit interesting coordination chemistry for binding of metal ions within the macrocyclic cavity and by peripheral ligating groups (N, S, O) [26]. Substituted amphiphilic and hydrophilic porphyrazines bearing both hydrophilic and hydrophobic moieties can be more potent as

photosensitisers in photodynamic therapy [27-29]. With acetylinic units as peripheral substituents, the π -systems of the chromophores are enlarged and bathochromic shifts in the electron absorption and emission spectra are induced. Alkyl groups also serve as covalent linkers for the assembly of delocalized multichromophore chains or two dimensional polymer networks [30].

The second method involves the macrocyclisation of substituted precursors, which may lead to a cleaner product of known substitution pattern. Peripheral substitution in porphyrazines is achieved by reacting a substituted phthalonitrile with a maleonitrile, or reacting two maleonitriles. However, as shown in Figure 2.5, this method also leads to the formation of isomers due to the symmetry involved in macrocyclisation. While macrocyclisation of substituted precursors has its drawbacks, it is still the method of choice for the synthesis of substituted porphyrazines with improved properties.

Trans-substituted porphyrazines can be synthesized by using a phthalonitriles with bulky groups. In this case, the bulky group appears once or twice due to steric hindrance in which the steric groups cannot be adjacent and co-planar (i.e. bulky groups are prevented from being adjacent to each other) as shown in Figure 2.5 [31].

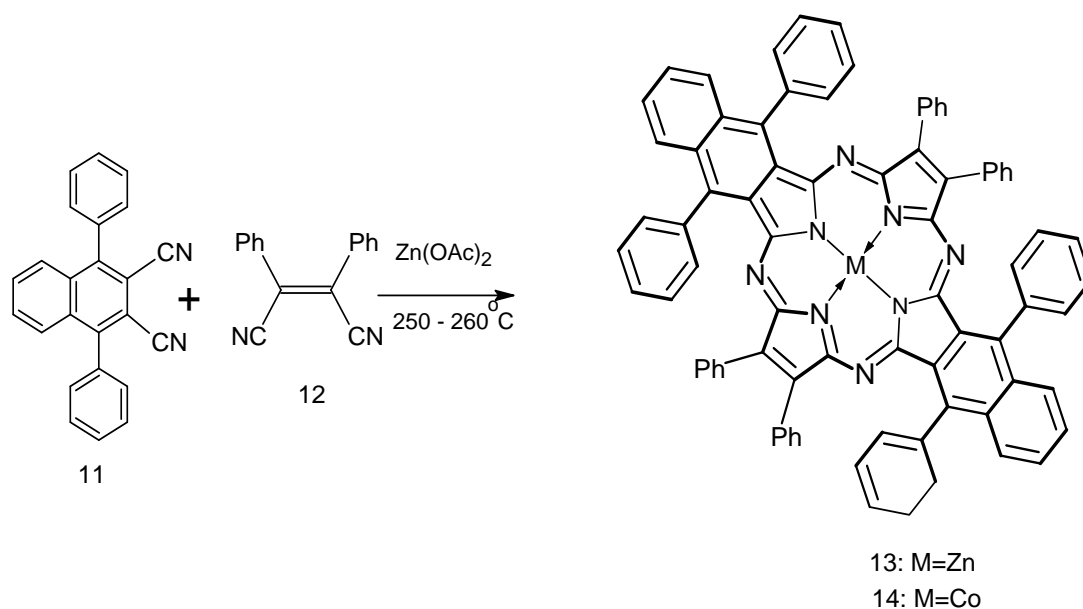


Figure 2.5 Synthesis of *trans*-substituted porphyrazine [31].

The most successful pathway of synthesizing unsymmetrical substituted porphyrazines is to use statistical condensation of two substituted precursors A and B in which the desired product can be isolated by column chromatography. Although the method also gives a mixture of six compounds, required compound can be isolated as a major product. If, for example, the reaction is done with the precursors A: B at a ratio of 1:8 or above, the major product is that in which A: B is incorporated into the pigment in the ratio of 1:3.

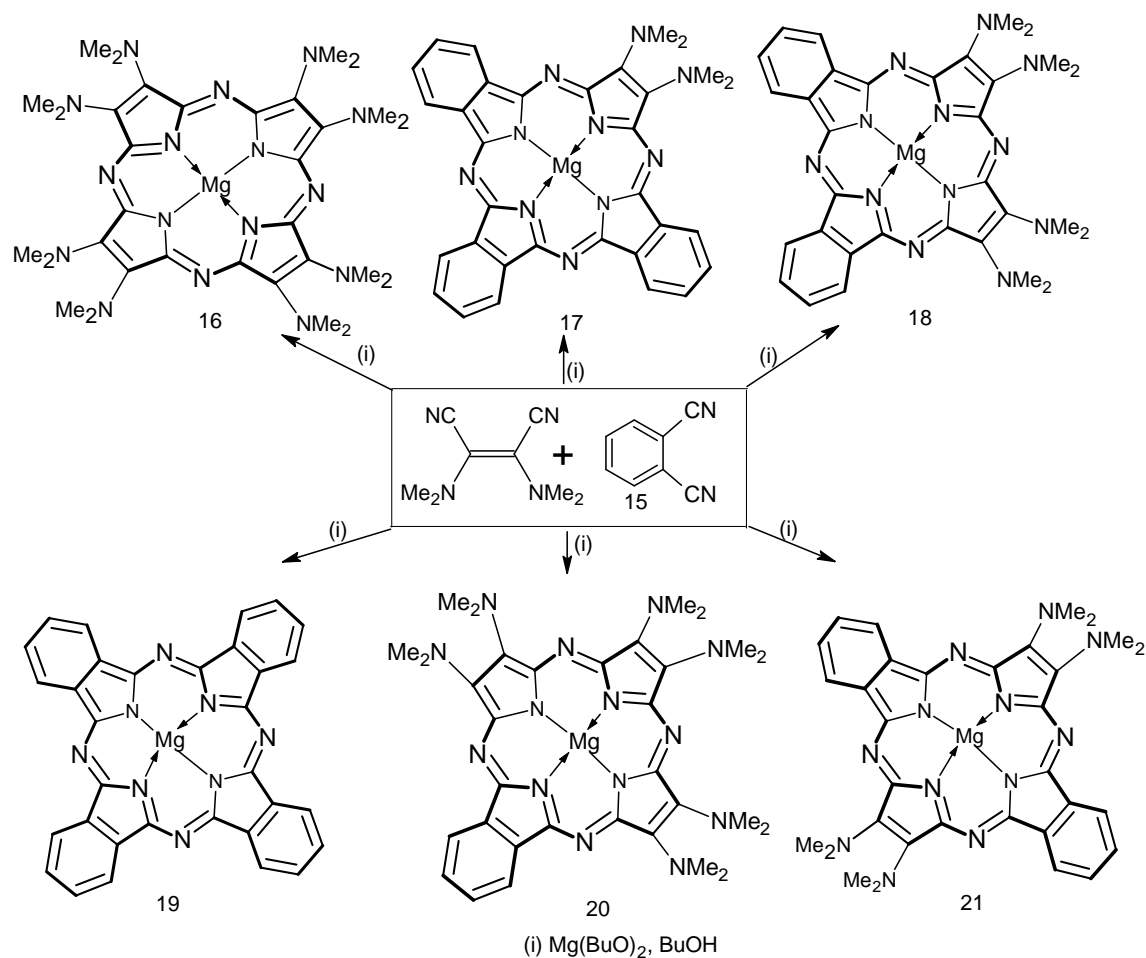


Figure 2.6 Synthesis of unsymmetrical porphyrazine [4].

2.2 TRANSITION METAL COMPLEXES OF PORPHYRAZINES

The porphyrazine macrocycle is a good ligand to most metals even though only few porphyrazine metal complexes have been reported compared to their phthalocyanine and porphyrin counterparts, where most research in this area has been

centered. This is because porphyrazines still represent a new field of research, with much research based on the selective incorporation of substituents. Even though metalations can be effected as an integral part of their synthesis, such as in cases in which the macrocyclisation in the presence of a templating transition metal salt or Li or Mg alkoxides, the best method that gives a product of high purity is the metalation reaction of a free-base ligand [32-39].

It has been already determined that a metal in the centre, or metal complexes to peripheral ligating groups can alter the physical and chemical properties of a porphyrin, phthalocyanine or porphyrazine. [39-40]. When the central metal is iron or cobalt, phthalocyanines make good electrocatalysts for the reduction of oxygen at a fuel cell cathode [41]. It has also been shown that iron (II) porphyrins decompose oxygen through a mechanism involving two porphyrins acting on oxygen molecule. Metal porphyrins have been also shown to catalyze carbene-type transformations with diazo reagents such as cyclopropanation of alkanes and C-H insertion of alkanes. Recently, it has been reported that iron (II) porphyrin complexes can catalyse the olefination of a selection of aldehydes with diazoacetate in the presence of triphenylphosphine [42]. With porphyrins, phthalocyanines and porphyrazines as photodynamic therapy agents, a metal in the centre may improve their photosensitivity, especially in the instances of the diamagnetic metals like zinc [43].

The normal charge of a porphyrin, porphyrazine or phthalocyanine is -2. Therefore, the metal ion to be accepted in order to form a stable complex is the one with a +2 charge. Metal ions with a charge of +1, requires an additional ion with +1 charge (Figure 2.7) [27].

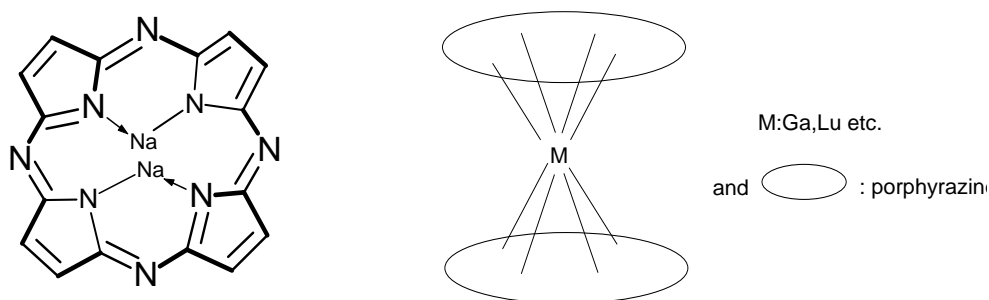


Figure 2.7 Metal complex formation of porphyrazine [27].

Metal ions with a charge of +3 or higher require additional “axial” ligands. In the case of larger ions, the phthalocyanine or porphyrazine or porphyrin cannot fully accommodate these ions within the core cavity and in this case the metal becomes surrounded by two phthalocyanines, porphyrins or porphyrazines, making a “sandwich” complex (Figure 2.7) [27].

Metalation in phthalocyanine and porphyrazine compounds can be incorporated into the synthesis [44, 45] as shown in Figure 2.8. In a metal-free porphyrazine, central metalation is mostly done by heating from 50 °C to reflux the metal-salt [Zn (OAc)₂, MnCl₂, etc.] in a mixture of chlorobenzene and DMF or in neat DMF, [46-48]. Peripheral metalation can be effected by heating the porphyrazine in a suitable solvent mixture (mostly using acetonitrile-trichloromethane) [44, 47].

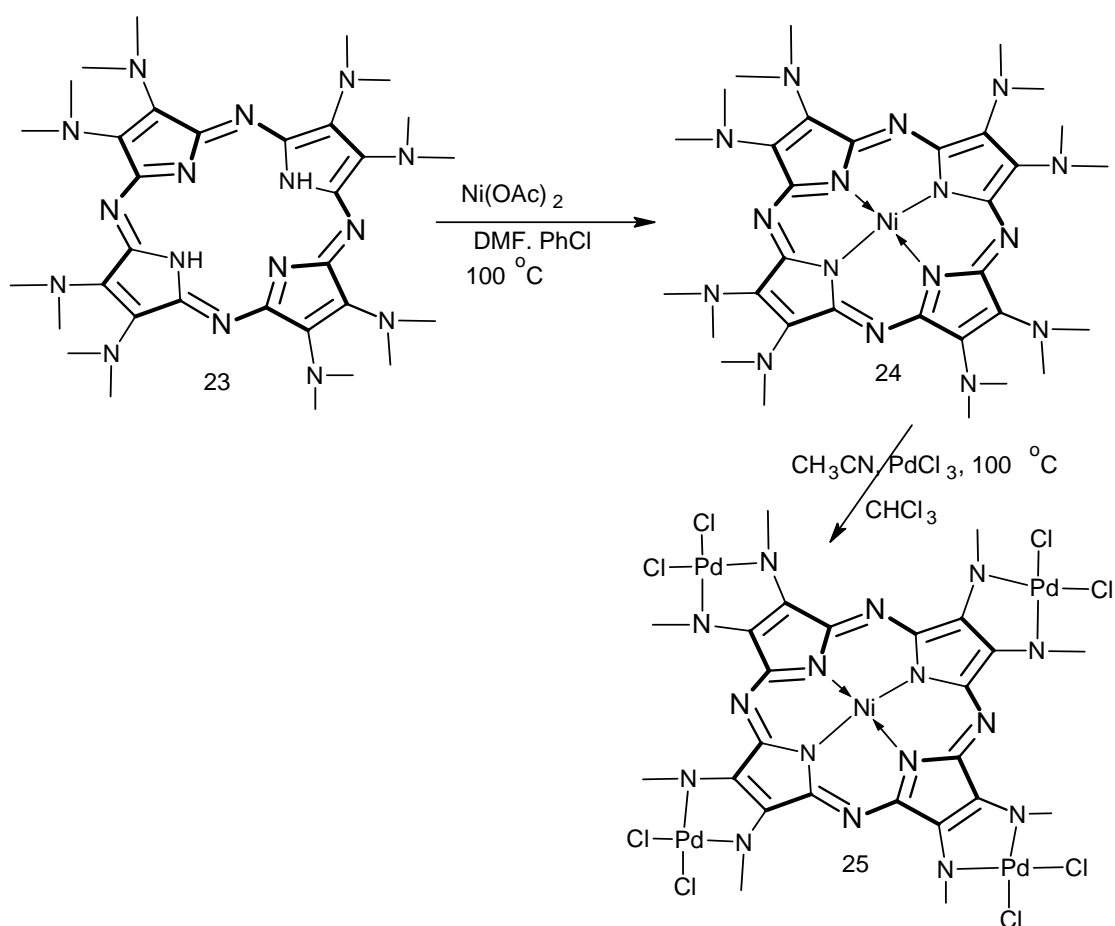


Figure 2.8 The synthesis of metal complex of porphyrazine 24 with Ni (central) and Pd (peripherally) metals [28, 47].

2.3 RECENT PROGRESS FOR PORPHYRAZINE SYNTHESIS

In recent study published by Giribau L. et al, [49] a novel single-step preparation of free-base and metalloporphyrazines from maleonitriles was studied for the first time by treatment with metal salts, hexamethyldisilazane (HMDS) and *p*-toluene sulfonic acid (PTSA) in DMF at 120 °C. This reaction provides a new preparative method under mild conditions for direct synthesis of metalloporphyrazines having a variety of metals and substituted maleonitriles.

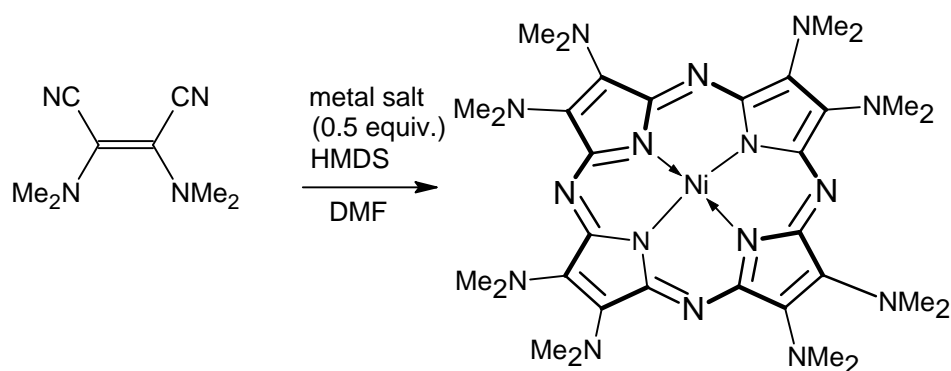


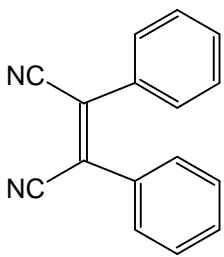
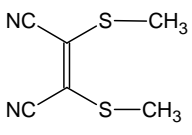
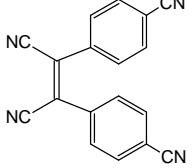
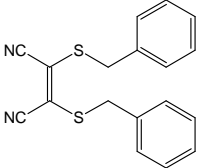
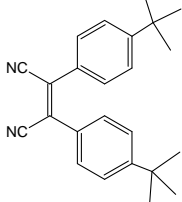
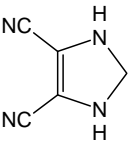
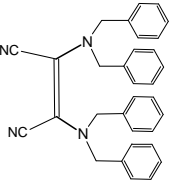
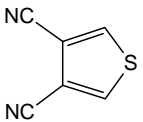
Figure 2.9 Synthesis of metalloporphyrazine with HMDS method [49].

Toru and co-workers have recently reported a simplistic method for the synthesis of metallophthalocyanines by hexamethyldisilazane (HMDS) method under mild conditions. [50]. Giribabu, L. et al. extended HMDS method to the synthesis of metalloporphyrazines. They reported for the first time a convenient method for the synthesis of porphyrazines on treatment of maleonitriles with metal salts and HMDS under mild conditions. By adopting this method it is possible to synthesize metalloporphyrazines directly. In the Table 2.1, the reaction of maleonitriles with $Zn(OAc)_2$ in the presence of HMDS and PTSA were summarized by Giribabu L. et al. Some of the maleonitrile derivatives do not give cyclization reaction with metal salt to prepare porphyrazines. The same maleonitrile precursor were reacted with the different metal salt such as $CuCl_2$, $CoCl_2$, $Mg(OAc)_2$ etc. The results were given in the Table 2.1 and Reference [49].

Toru and co-workers have published synthesis of porphyrazines with HMDS methods in microwave. Microwave-assisted reactions have attracted much interest because of their simplicity in operation and milder reaction conditions. The salient features of the microwave approach are enhanced reaction rates, formation of pure

products in high yields and ease of isolation. They extended the microwave technology to synthesize porphyrazines efficiently, in short reaction times, and improved yields using a laboratory microwave oven [51].

Table 2.1 Preparation of substituted porphyrazines by treatment of maleonitrile derivatives with $Zn(OAc)_2$ and HMDS in DMF [49].

Entry	Maleonitrile derivatives	Yield (%)	Entry	Maleonitrile derivatives	Yield (%)
1		40	5		35
2		31	6		28
3		29	7		-
4		38	8		-

When the microwave-assisted reactions were compared to oil-bath procedure for the synthesis of porphyrazine from the same precursors with HMDS, the microwave-assisted reaction has advantages for the reaction time and higher yield than oil-bath reactions. The time takes with microwave-assisted reaction 10-15 minutes where oil-bath reactions take for hours. The yields are 40-53% in the microwave-assisted and 28-43% for the oil-bath reactions [51].

CHAPTER 3

PROPERTIES OF PORPHYRAZINE

3.1 STRUCTURAL AND SPECTAL PROPERTIES OF PORPHYRINIC MOLECULES

Porphyryns, porphyrazines, phthalocyanines, and naphtholcyanines belong to a broad class of macroheterocyclic tetrapyrroles systems, which are of considerable interest from scientific and practical viewpoints, because their representatives are components of the most important natural compounds (hemoglobin, myoglobin, cytochromes, chlorophylls, and others) and are involved in such viable processes as photo-synthesis, cell respiration, electron transport, etc. Some synthetic analogs of porphyryns, especially phthalocyanine (Pc), have found wide practical applications dyes and pigments and, recently, in several new fields as well: as bleachable dyes in laser technique, discotic liquid crystals, components of electrochromic and electrophotographic materials, gas sensors, radiation protectors, catalysts of various processes (in particular, electrochemical), antimicrobial drugs in luminescent diagnostics and photodynamic therapy of cancer tumors, etc). The development of new fields of technique necessitated the creation of materials with physical and chemical properties different from those of Pc and porphyryns. For example, ecological problems associated with the removal of carbon monoxide in engine exhaust, of nitrogen oxides in the nitrogen fertilizer industry, and of sulfur compounds from oil mad natural gases and the technologically important problem of development of processes of mild oxidation of hydrocarbons require the creation of highly efficient and long lived catalysts. Positive properties of porphyrazines (Pzs), the closest synthetic analogs of Pc, especially their high stability against oxidation, favor their use in some of the aforementioned areas. Pzs are considerably less studied than Pc due to the absence of convenient methods for their synthesis.

Porphyrazine, tetraazaporphyrine or, according to the IUPAC nomenclature, 2,7,12,17,21,22,23,24octaazapentacyclo[16,2,1,13,6,18,11,12,26]tetracosaundecaene), in its structure, occupies an intermediate position between other well studied tetrapyrrole macrocyclic systems, porphyrine and Pc. The conjugation system of the H₂Pzs molecule is multicontour, and its internal chromophore n-electrons (8 double bonds and 2 π -electrons of internal nitrogen atoms) [52].

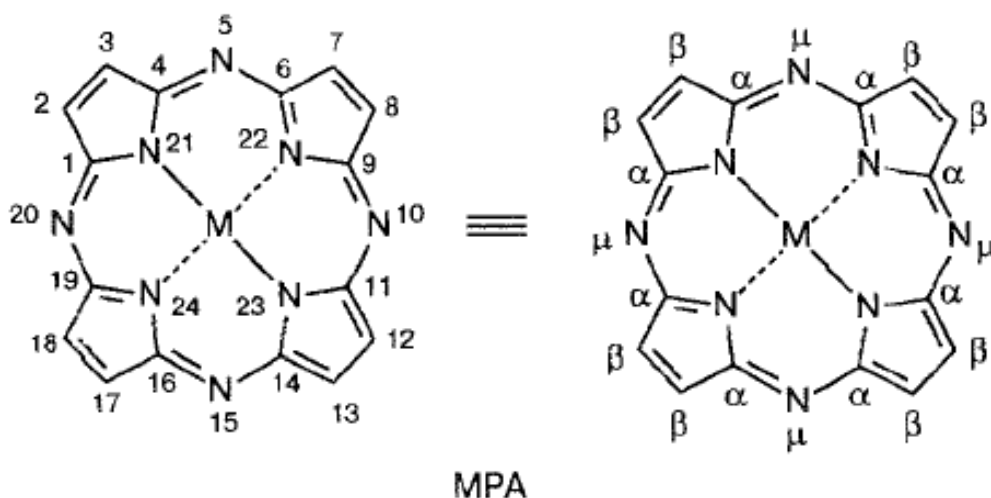


Figure 3.1 General structure of porphyrazine molecules [52].

The most important property of porphyrinic ligands is their ability to react with metal salts with the formation of chelate complexes:



The kinetics and mechanism of metal ion incorporation in porphyrinic ligands have been the subject of intensive studies and their results have been reviewed [53,54].

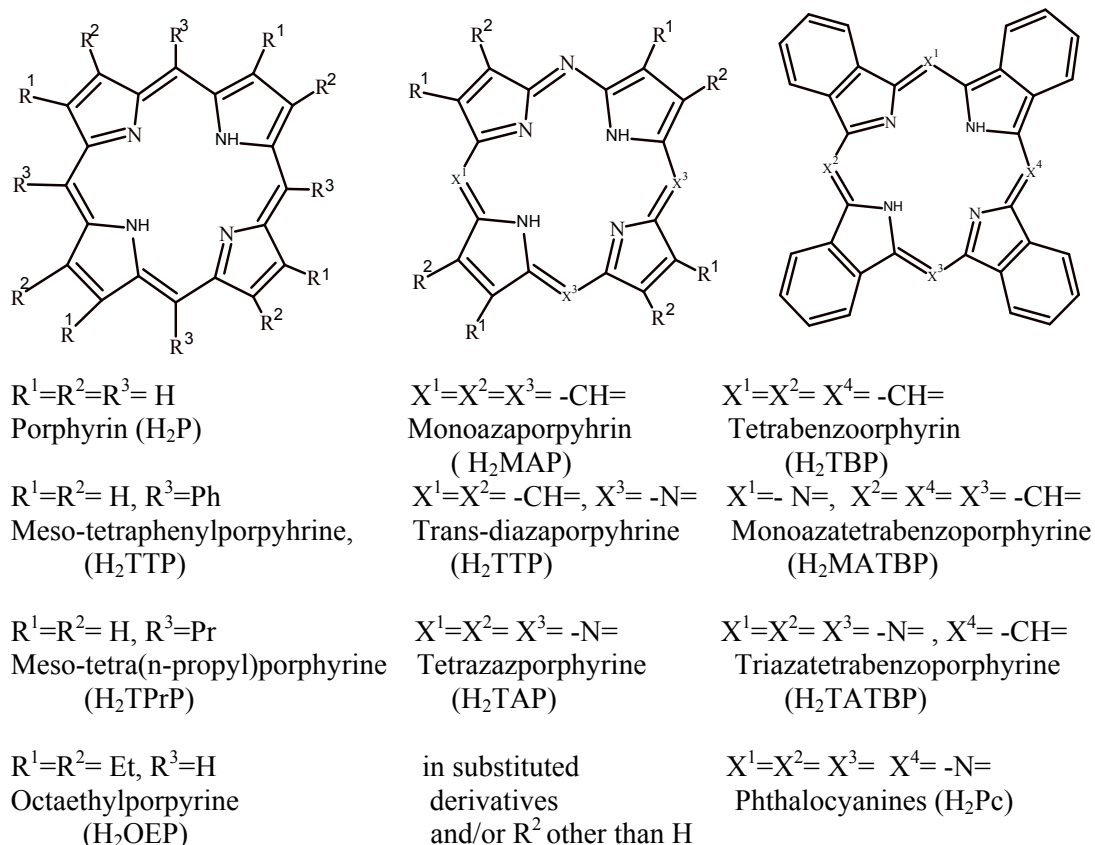


Figure 3.2 Some substituted porphyrinic molecules [55].

3.1.1 Reaction Center of Porphyrinic Molecules

The reaction center of porphyrinic ligands (N_4H_2) is composed of four nitrogen atoms and two imino-hydrogen atoms of the pyrrole rings which participate directly in complex formation. The structure of the reaction center, reflecting the geometry and electronic structure of the porphyrin molecule as a whole, has an important impact on the kinetic parameters of metalloporphyrin formation [56]. Its electronic structure dictates the state and stability of the N-H bonds and the solvation of the reaction center. The dimensions of the coordination cavity determine the degree of steric compatibility between the ligand and the metal ion.

The skeleton of common porphyrin ligands can be considered as almost planar since the deviations of the C and N atoms from the mean plane do not exceed 0.006 nm [57,58]. The symmetry of the skeleton is in most cases D_{2h} [57,58-60]. A D_{4h} skeletal symmetry was found for monoclinic H_2P [61] and tetragonal H_2TPP [62]. D_{2h} distortion of the porphyrin ligands is connected above all with the inequivalency of the five-

membered rings composing the macrocycle. In two translocated pyrrole type-rings (A) the bonds C_α - C_β are about 0.002-0.003 nm shorter, C_β - C_β bonds are about 0.002 nm longer and the inner angle formed by the nitrogen atom is 2.5-4° larger compared with a pair of the neighbouring pyrrolenine type rings (B) (Figure 3.3). At the same time the bond lengths between C_α atoms and the inner nitrogen atoms vary only slightly in these two ring types and are 0.002-0.003 nm shorter than the bonds of C_α atom with C_{meso} atom. The symmetric alkyl or aryl substitution in the meso or β positions has little influence; the changes in the bond lengths and values of the angles do not exceed 0.002 nm and 2°. The dimensions of the central coordination cavity (measured as a distance between the intracyclic N atoms N_{pyr} and the macrocycle center C_t) vary slightly in the range 0.204-0.206 nm. One can expect that the direct substitution of the carbon atom in the conjugated π system of the porphyrin with a heteroatom, namely aza substitution in the meso positions, should produce significantly greater changes in the geometry of the reaction center and that is the case in fact [55].

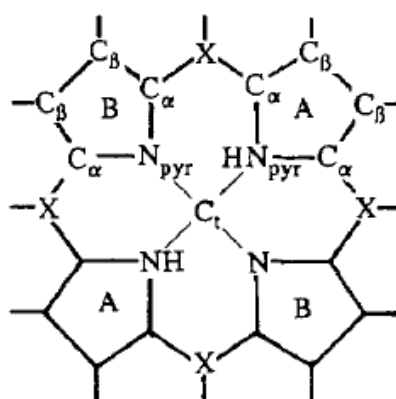


Figure 3.3 The skeleton of **A**, pyrrole type **B**, pyrrolenine-type rings [55].

The only X-ray study of metal-free phthalocyanine made by Robertson [63] in 1936 showed that the H_2Pc molecule is planar and has D_{2h} symmetry. Unlike porphyrins this D_{2h} distortion of the tetragonal symmetry of the skeleton owes its origin not to the inequivalence of pyrrole rings but to the difference in the angles formed by neighbouring meso-nitrogen atoms (115 and 119°). The bonds composing the inner 16-membered macrocycle in H_2Pc are shorter than in the porphyrins. The bonds formed by the bridge atoms (meso-nitrogen atoms) are considerably shortened. Thus the alternation of the bonds of the inner macrocycle which is noticeable in porphyrins (about 0.137 nm for C_α - N_{pyr} and 0.139-0.140 nm for C_α - C_{meso} bonds) is barely perceptible in

phthalocyanine ($C_{\alpha}-N_{\text{pyr}}$, 0.134 nm; $C_{\alpha}-N_{\text{meso}}$, 0.133-0.134 nm). The values of the angles formed with participation of the bridge atoms also change. In comparison with porphyrins the angle $C_{\alpha}-X_{\text{meso}}-C_{\alpha}$ is decreased by 10° and the angle $N_{\text{pyr}}-C_{\alpha}-X_{\text{meso}}$ increased by 6° . These changes in bond lengths and angles lead to a significant shrinkage of the central coordination cavity, by 0.026 nm compared with porphyrins. The geometry data for H_2Pc obtained by Hoskins et al. [64] by a neutron diffraction method differ somewhat from the data of Robertson [63]. However, the observed change in the dimensions of the reaction center as one goes from porphyrins to phthalocyanine is the same. To what can these changes be attributed: to the influence of aza substitution or rather to benzo substitution [55].

3.1.2. The Influence of Benzo and Aza Substitution

Unfortunately structural data on unsubstituted H_2Pz and H_2TBP ligands which could provide a direct answer to this question are lacking until now. Although preliminary X-ray studies on H_2TBP and its monoaza- and triaza-substituted derivatives made by Woodward [65] and Robertson [66] did not resolve the structures of these molecules; yet on a basis of the crystal parameters they supposed that the structure of the monoaza derivative (H_2MATBP) should be like the structure of H_2TBP and differ essentially from the structure of the triaza derivative (H_2TATBP) which should be more like the phthalocyanine. Later Das and Chandhuri [67] evaluated the structure of H_2MATBP and showed that monoaza substitution provokes a significant distortion of the molecule. The deviations from the mean plane reach 0.0311 nm. The bond lengths and bond angles formed by the meso-nitrogen atom (0.125 nm and 111°) are significantly less than formed by the meso-carbon atoms (average values of 0.139 nm and 143°). The inner angle formed by the bridge atom with the isoindole rings ($X_{\text{meso}}-C_{\alpha}-N_{\text{pyr}}$) is larger in the case of meso-nitrogen (132°) than of meso-carbon (123°). A similar but weaker effect of monoaza substitution on the geometry of the macrocycle was observed for the Fe complex of octaethylmonoazaporphyrine ($ClFeMAPEt_8$) [68].

Recently the results of the first X-ray investigations of complexes of tetraazaporphyrins were published [68, 69]. Comparison of these structural data with the data on corresponding complexes of porphyrins [70], tetrabenzoporphyrine [71] and phthalocyanine [72] reveal the separate influence of aza and benzo substitution. Figure 2.3 displays changes in the geometry produced by tetrabenzo substitution in porphyrins

and tetraaza-porphyrins and by tetraaza substitution in porphyrins and tetrabenzoporphyrins. Aza substitution reduces the angles formed by a bridge atom and shortens the bonds composing the inner 16-membered ring. In the case of porphyrins the bond between C_{α} atom and meso-atom is especially shortened. Only the $N_{\text{pyr}}-C_{\alpha}$ bonds change significantly in the isoindole fragments, whereas in the pyrrole fragments the isolation of ethylene double bonds is distinct and their geometry changes drastically. Benzo substitution has little impact on the geometry of the inner macroring in tetraazaporphyrins, while in the porphyrins the bonds and angles formed by the bridge carbon atom are significantly reduced.

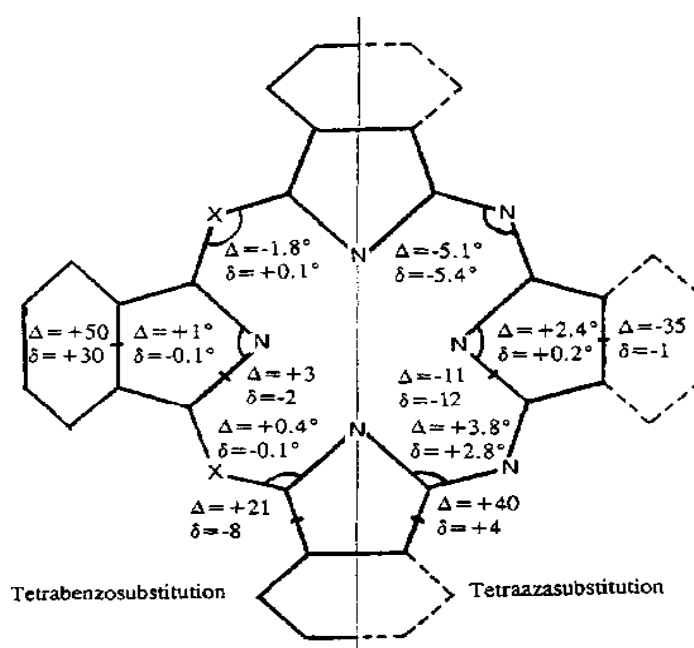


Figure 3.4 Changes in the geometry of the CN skeleton produced by tetrabenzo substitution (left side) in porphyrins (Δ) and tetraazaporphyrins (δ) and by tetraaza substitution (right side) in porphyrins (Δ) and tetrabenzoporphyrins (δ). The angles are in degrees and the bond lengths in 10^4 nm [55].

Aza substitution affects the geometry more strongly than benzo substitution and that its effect is more pronounced in porphyrins (and their alkyl and aryl derivatives) than in tetra benzoporphyrins. One can expect that in the free ligands, in the absence of a central metal ion rigidly bonding the inner nitrogen atoms, the effect of aza substitution will be greater.

The influence of aza substitution in porphyrins on their electronic structure was

intensively studied by quantum chemistry methods [73-75]. The most comprehensive review of this area was published by Solovyov and co-workers [76]. Calculations of the H₂Pz molecule were based on the geometry of H₂P, H₂Pc or an idealized geometry [75]. They all show poor consistency with experimental data (for example with UV-visible spectra) than in the case of H₂P or H₂Pc, where the experimental geometry based on X-ray data were available. No successful optimization of the H₂Pz skeleton geometry was made in these studies to achieve better consistency. On the basis of X-ray structural data for porphyrines, tetrabenzoporphyrine and its monoaza, triaza and tetraaza substituted derivatives in Reference [77] empirical structural parameters for H₂Pz were suggested.

3.1.3 The Location of the NH Hydrogen Atoms and the State of the N-H Bonds

There are four possible structures for the N₄H₂ center in porphyrin-like ligands are usually debated (Figure 3.5); LS, localized (bonded) structure in which the H atoms are located on the line combining the opposite N atoms of the pyrrole rings and bonded with them with two-center covalent bonds; US, unlocalized structure (known also as shared or bridged) in which the H atoms form three-center bonds with two N atoms of adjacent pyrrole rings and are located on the line combining the opposite meso atoms; HS, hydrogen-bonded structure which is intermediate between LS and US (each H atom forms a mostly covalent bond with one N atom and a strong H bond with the neighbouring N atom); IS, ionized structure in which two protons are located in the field of the ligand dianion (Figure 3.5). One can see that in the LS and HS structures the internal nitrogen atoms are inequivalent: two atoms of aza (pyridine) type and two of imino (pyrrole) type. In the US and IS structures all four internal nitrogen atoms are equivalent.

X-ray data defining the atoms of the CN skeleton are not sufficiently reliable in the case of hydrogen atoms. Neutron diffraction can give more reliable data about the H atom positions. However, it is well to bear in mind that these methods can reveal only the static structure of the molecule in the solid state which can differ significantly from the structure in the vapor phase and especially in solution. Thus the N₄H₂ center structure must be resolved by a combination of diffraction methods, spectroscopic methods and quantum chemistry methods. The acid-base properties also provide important information about their structure in solution.

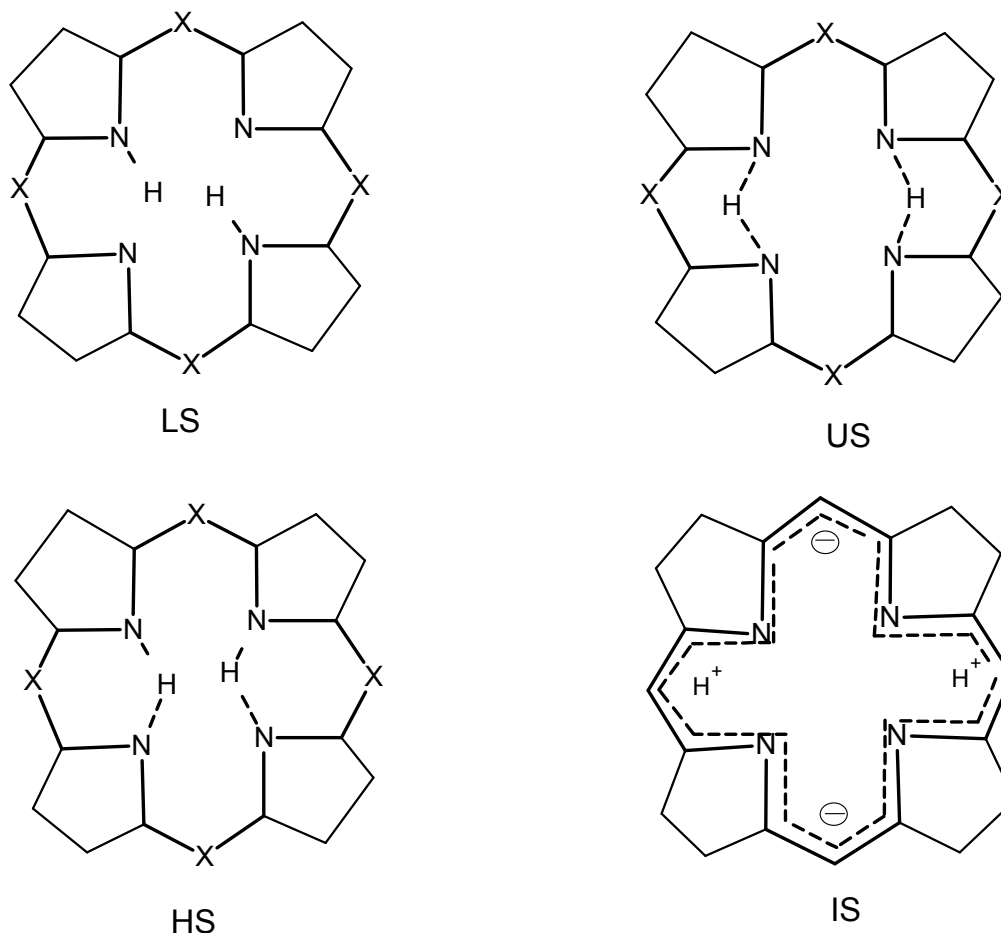


Figure 3.5 The possible structures of the N_4H_2 reaction center in porphyrin-type ligands, where $X = CH$ in porphyrins, $X = N$ in azaporphyrins: LS, localized (bonded) structure; US, unlocalized (shared or bridged structure); HS, hydrogen-bonded structure; IS, intraionized structure [55].

According to X-ray studies of common porphyrinic ligands, two internal H atoms are most probably localized near the line connecting two opposite N atoms [57-62] or are equally distributed between all four nitrogen atoms (each bears half a hydrogen atom) as in the case of tetragonal H_2TPP [62] with an N-H distance of 0.092-0.096 nm. The X-ray photoelectron spectra of H_2TPP [78] and benzo-substituted porphyrins [79] shows the existence of two types of nitrogen atom with different N 1s binding energies, which is also consistent with the LS structure. Schaffer and Gouterman [74] used the EHMO method to investigate the location of the inner protons in porphyrine and found better agreement with the experimental UV-visible spectrum for the LS than for the US structure. IR spectroscopy data give evidence of intramolecular H bonds [80]. The complete neglect of differential overlap 2 (CNDO/2) calculations [81] also substantiate

the tendency for H bonding in porphyrins which can be achieved without displacement of H atoms from the line connecting the opposite nitrogen atoms when each of the H atoms forms two equivalent H bonds with both of the neighbouring aza atoms.

The static model is not adequate to describe the reaction center. Early studies of the ^1H NMR spectra of porphyrins [82] showed the existence of fast NH tautomerism (the lifetime of each tautomer at ambient temperature is not more than 0.02 s) which can be inhibited only at low temperatures. Different dynamic models for the N_4H_2 center structure in porphyrins and mechanisms of NH tautomerism were suggested on the basis of ^1H , ^{13}C , and ^{15}N nuclear magnetic resonance (NMR) spectroscopy and on quantum-chemical calculations and were reviewed by Mamaev et al. [83] in 1989. The porphyrin reaction center can be conceived as two tautomeric LS structures. Weak intramolecular H bonding of the H atoms with both aza atoms promotes tautomerism which proceeds according to the asynchronous tunnel mechanism at 150-300 K and according to the synchronous mechanism at lower temperatures. Such a structure is also in agreement with the behavior of porphyrin ligands in complex formation reactions and with their acid-base properties [54].

Neither Das and Chandhuri (for H_2MATBP [67] nor Robertson (for H_2Pc [63] speculated about the position of the internal hydrogen atoms on the basis of their X-ray data.

Berezin [84], using the X-ray data of Robertson [63] and his own investigation of the behaviour of H_2Pc and its complexes in acid media, suggested the inner ionized IS-type structure "which explains practically all physicochemical properties of phthalocyanine in solution" [84, p. 50]. Later Fleischer [85] reanalyzed the X-ray data of Robertson and proposed the bridged US-type structure for H_2Pc . In a neutron diffraction study made by Hoskins et al. [64] the two internal hydrogen atoms "appeared as ... four half-hydrogen atoms, one associated with each of pyrrole nitrogen atoms ... with an average distance 0.094 nm". As with tetragonal H_2TPP [60] this result favoured the LS structure.

Apart from these data, only IR and UV-visible data were available for H_2Pc and H_2Pz for a long time. The observed shift in the ν_{NH} frequencies in the IR spectra of the solid samples in the order H_2P (3305 cm^{-1}) > H_2Pz (3300 cm^{-1}) > H_2Pc (3290 cm^{-1}) was

considered by Berezin [56, p. 57] as evidence of N-H bond polarization. However, it is indicative rather of the strengthening of intramolecular H bonding, i.e. of the HS or US structures than of the IS structure. Sharp and Lardon [86] explained the observed red shift in the ν_{NH} frequency in (3-H₂Pc (3284 cm⁻¹) compared with oc-H₂Pc (3302 cm⁻¹) as a result of the intermolecular H bonding in the β form.

3.1.3.1 Quantum- Chemical Investigations

UV-visible [86] and structural [63,64] data provided the experimental basis for numerous efforts to solve the problem using quantum-chemical methods [38]. Usually the agreement between the experimental UV-visible spectra and the calculated spectra was used as a criterion of goodness of the implied model. Orti et al. [87] have calculated the UV-visible spectrum of H₂Pc assuming the LS model on the basis of the geometry employed by Hoskins et al. [64] and using a valence effective hamiltonian non-empirical pseudopotential method. The results were in good agreement for $\Delta E(Q)$ only for the vapor spectra of H₂Pc but the energy of the Q_x transition was greatly underestimated. Berkowitch-Yellin and Ellis [88] used a one-electron Hartree-Fock-Slater model in their calculations and supported the US structure for H₂Pc. The most comprehensive studies of the influence of the CN skeletal structure on the location of the internal hydrogen atoms in H₂Pc were made in Reference [74].

Schaffer and Gouterman [74] used the extended Huckel method and found that the bonded model with the D_{4h} skeleton (LS structure) gives a calculated energy gap between Q_x and Q_y transitions $\Delta E(Q)=1440\text{cm}^{-1}$) which is very close to the experimental value of the H₂Pc spectrum in the vapor (1490 cm⁻¹) or in the solid (1530 cm⁻¹). However, the splitting parameter of the solution spectrum $\Delta E(Q)=730\text{cm}^{-1}$) could not be achieved for the bonded model and was obtained only on the basis of the bridge (US) model with significant distortion of the CN skeleton. In all cases the calculations gave a lower energy for the Q_x transitions (12300-13300 cm⁻¹) than experimental values. Schaffer and Gouterman [74] also concluded that the structure of H₂Pc depends strongly on environment and can differ in vapor, in solid state and in solution.

Mamaev et al. [89] investigated the structure of the H₂Pc reaction center with CNDO/S using dynamic models. As in Reference [74] the experimental geometry of the

CN skeleton [63] was preferable for the LS structure which is about 120 kJ mol^{-1} more stable than the US structure. The spectrum observed in solution was well reproduced (calculated; $Q_x=14026$; $\Delta E(Q)=711 \text{ cm}^{-1}$) when the $N_{\text{meso}}\text{-C}_\alpha\text{-N}_{\text{pyr}}$ angle was reduced from the experimental value in the solid state (131° to 127° and all other parameters remained unchanged. The location of the internal hydrogen atoms has only a small effect on the Q band splitting (608 and 711 cm^{-1} for LS and US structures respectively) but greatly influences the splitting of the B band located in the UV region. This splitting is predicted to be two and a half times larger for the LS structure (1613 and 632 cm^{-1} for the LS and US structures respectively). Since for this distorted skeleton the total energy for the US structure was calculated to be 50 kJ mol^{-1} less than for the LS structure and no splitting (only broadening) is observed for the B band in the experimental solution spectrum, the US model is favored for solution. Mamaev et al. [89] concluded that the transition from the solid state to the solution causes deformation of the CN skeleton and the structure of H_2Pc changes from LS to US which is about 80 kJ mol^{-1} more stable. However, since the energy difference between the LS and US structures is not large, small changes in the intermolecular interactions can lead to distortion of the H_2Pc geometry and to the transition from one structure to another. On the basis of the dynamic model of the reaction center the adiabatic potential surface for the synchronous movement of protons in the reaction center was calculated [89]. For the LS structure, this surface has four potential wells with barriers of 120 and 230 kJ mol^{-1} which is less than for H_2Pz (300 kJ mol^{-1} [90]) and for H_2P (394 kJ mol^{-1} [83]). For the US structure the surface has only two potential wells with a barrier of 660 kJ mol^{-1} .

Theoretical consideration of the H_2Pz reaction center has received less attention. Schaffer and Gouterman [74] calculated the spectrum of H_2Pz but neither a bonded nor a bridged model gave results comparable with experimental spectroscopic values of Q_x and $\Delta E(Q)$. Orti et al. [87] used the LS model and their results also show poor agreement. The theoretical UV-visible spectrum of H_2Pz obtained by Berkowitch-Yellin and Ellis [88] gave good agreement in the case of the US structure. Since all these calculations were based on the H_2Pc geometry, they should be considered with caution.

Table 3.1 UV-visible spectra of H₂Pz: Experimental and calculated parameters [55].

Conditions	Structure of reaction center	Energy of electronic transitions (cm ⁻¹)				Splitting(cm ⁻¹)	
		Q _x	Q _y	B _x	By	Δ _Q	Δ _B
Experimental							
In KBr at 10 K		16155	18210	30210sh	32470	2055	2260
In EtOH		16320	18500	30120	31350sh	2180	1230
In AcOH		16290	18440	30160	31550sh	2150	1390
In pyridine		16220	18290	29605	30170sh	2070	565
Calculated							
	US	16800	19100			2300	
	LS	15500	20600			5100	
	US	11510	13032			1522	
	LS	12740	14190			1110	
	LS	12324	13864			1450	

3.1.3.2 Nuclear Magnetic Resonance Spectroscopy

Solid samples of H₂Pc were also investigated by ¹H [91], ¹³C [92]] and ¹⁵N [93] NMR spectroscopy. Dudreva and Grande [91] measured the dependence of the spin-lattice relaxation time in the temperature range from -140 to +150 °C for different crystalline modifications of H₂Pc (α, β and γ) and for D₂Pc using the ¹H NMR method. They came to a conclusion about intramolecular H bonds and about intramolecular proton exchange at low temperatures and supposed the diffusion of protons among the molecules of solid substance above room temperature. The potential barrier was estimated as 28kJmol⁻¹.

Meyer et al. [92] using ¹³C NMR spectroscopy observed the tautomerism process for H₂Pc and determined the rate of proton exchange which appears to be higher than for solid H₂P [94]. The data presented allow one to estimate roughly the activation energy to be 33 kJ mol⁻¹. It was concluded [90] that the existence of two types of C_α and C_β atom provides evidence for two inequivalent isoindole fragments and therefore for the LS structure. We should like to mention that in the HS as well as in the US and IS structures there are also two pairs of inequivalent C_α and C_β atoms in each isoindole fragment and two tautomeric forms are also possible.

Kendrick et al. [93] reported ¹⁵N NMR spectra for H₂Pc. The spectral changes

observed with temperature were interpreted as double-proton transfer in the LS structure which is fast on the NMR time scale at 300 K and slow at 153 K just as it is in solid H₂P [94]. Such an interpretation seems inappropriate for H₂Pc. As one can see (Figure 3.5) in the LS structure of H₂Pc there are three types of nitrogen: two imino-nitrogen atoms, two internal aza-nitrogen atoms and four meso-nitrogen atoms which are also of the aza type. Meso-nitrogen atoms in the LS structure of H₂Pc are equivalent, do not take part in proton exchange and should give a singlet at any temperature. Internal aza and imino-nitrogen atoms in the LS structure should give two signals at low temperatures and one broadened signal at high temperatures when the exchange process is fast. Such behavior was observed for H₂P [94] when the doublet for imino and aza-nitrogen atoms at 192 K (107 and 215 ppm respectively) coalesces without combination of the doublet peaks into a broad singlet at 161 ppm, at ambient temperature. This singlet becomes sharp at higher temperatures. In the spectrum of H₂Pc at 153 K the signal at 195 ppm corresponds to the four meso-nitrogen atoms, the shoulder at 191 ppm to two internal aza-nitrogen atoms and the singlet at 104 ppm to two imino-nitrogen atoms as might be expected for a localized structure with a slow exchange rate. However, at 300 K, contrary to expectation for the LS structure, two sharp singlets are not observed but rather two doublets: the first at 141 and 160 ppm and the second at 190 and 194 ppm. Such a view of the spectrum corresponds best to the HS structure for H₂Pc with a slow exchange rate. In this structure the meso-nitrogen atoms are inequivalent; one pair, which are due to the weak interaction with the internal hydrogen atoms, resonate slightly more upfield (190 ppm) than the other pair (194 ppm). Two pairs of internal nitrogen atoms also differ; the signal of two aza-nitrogen atoms shifts upfield to 161 ppm owing to the strong H bonding compared with the LS structure (191 ppm) and the signal of two imino-nitrogen atoms shifts downfield to 141 ppm (104 ppm in the LS structure) owing to the weakening of NH bonds. With increasing temperature the LS structure of H₂Pc transforms to the more stable HS structure. Proton exchange in the HS structure is also slow on the NMR time scale at 300 K. This interpretation is also consistent with the above mentioned calculations of Mamaev et al. [89] who showed that proton transfer processes for the delocalized structure of H₂Pc should proceed through a double-minimum potential with an activation energy three times higher than for the LS structure with a four-minimum potential.

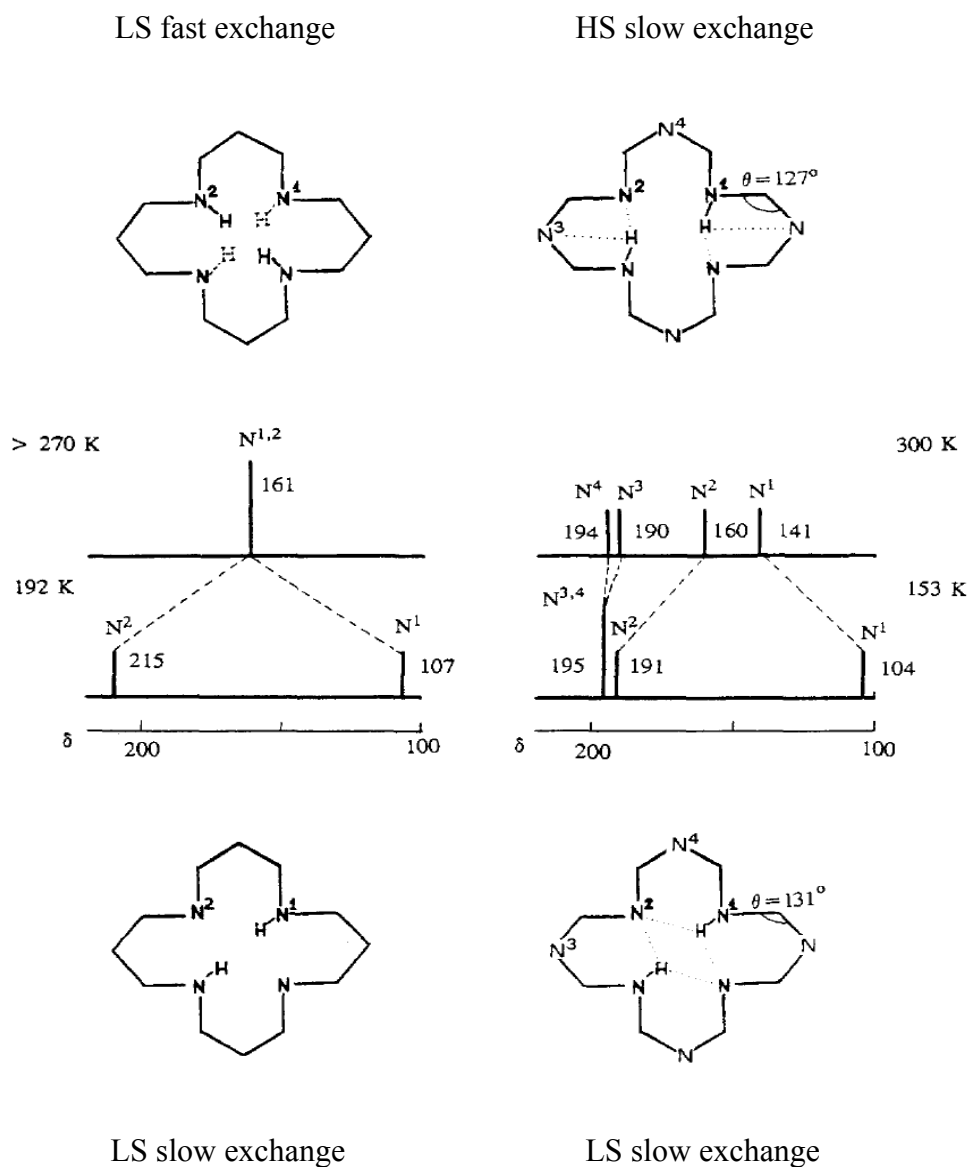


Figure 3.6 Interpretation of the ^{15}N NMR spectra of solid H_2P and H_2Pc . Values of the chemical shifts are from [93] for H_2Pc and from [94] [60] for H_2P [55].

Andronova and Luk'yanets [95] first reported the ^1H NMR spectrum of the soluble substituted derivative, tetra (4-tert-butyl)phthalocyanine ($\text{H}_2\text{Pc}^t\text{Bu}_4$). They observed a broad peak of the internal NH protons in the strong field (-5.3 ppm) in CCl_4 solution at room temperature, together with the signal of the tert-butyl group protons (1.72 ppm) and the multiplet of the benzene rings protons (7.5-8.4 ppm). Later Hanack et al. [96] reported the ^1H NMR spectrum of $\text{H}_2\text{Pc}^t\text{Bu}_4$ in CDCl_3 . Although the chemical shifts of the benzene and tert-butyl protons have similar values as in [95], the NH-proton singlet was observed at 2.0 ppm. The reason for such a large difference in the chemical shift of the NH protons reported in these studies became clear when Leznoff

and coworkers [97] investigated the ^1H NMR spectra of the monomeric and dimeric alkyloxy derivatives of phthalocyanine and found that aggregation had a great impact on the NH-proton signal, resulting in its upfield shift. With a solution of tetra(4-*r*-ceopentoxy)phthalocyanine ($\text{H}_2\text{Pc}(\text{OCH}_2^t\text{Bu})_4$) in CDCl_3 the signal shifts from -5.5 ppm at 10^{-1} M to -3.0 ppm at 10^{-3} M and does not change upon further dilution. The 10^{-4} - 10^{-3} M solutions most probably represent free non-aggregated phthalocyanines at room and even at lower (down to -80°C) temperatures [97]. Although the $\text{H}_2\text{Pc}^t\text{Bu}_4$ concentrations in the solutions investigated were not reported, one can suppose that Andronova and Luk'yanets [95] using an 80 MHz spectrometer obtained the spectrum of the aggregated form whereas Hanack et al. [96] using a more modern 360 MHz spectrometer were able to study a dilute solution containing the non-aggregated compound.

Experimental data show that aza substitution in the tetrabenzoporphyrin molecule induces considerable deshielding of the internal protons and their resonance is shifted downfield from 4.13 ppm for $\text{H}_2\text{TBP}^t\text{Bu}_4$ [98] to -2.0 ppm for $\text{H}_2\text{Pc}^t\text{Bu}_4$ [96]. Borovkov and Akopov [99] investigated the triaza derivative ($\text{H}_2\text{TATBP}^t\text{Bu}_4$) and observed resonance of the internal protons as a multiplet in the range between -2.5 and -3.2 ppm at room temperature. Vysotsky et al. [98] using the molecular orbital self-consistent atomic orbital self-consistent field method and supposing the LS structure of the reaction center, calculated NMR shifts for porphyrins and their aza and benzo derivatives and predicted a much smaller effect of aza substitution. The calculated value of the NH-proton resonance of H_2Pc ($\delta_{\text{NH}} = -3.37$ ppm) is shifted downfield only slightly compared with H_2TBP ($\delta_{\text{NH}} = -3.76$ ppm). These calculations give good agreement with experimental values of the NH-proton shifts for porphyrins where the bonded LS structure of the reaction center is the case (H_2P ; calculated -3.82 ppm; experimental, -3.94 ppm); (H_2TBP ; calculated, -3.76 ppm; experimental, -4.13 ppm (for $\text{H}_2\text{TBP}^t\text{Bu}_4$) [100], whereas for H_2Pc the calculated value ($\delta_{\text{NH}} = -3.37$ ppm) is lower than experimentally observed even for derivatives with substituents having a strong shielding effect ($\text{H}_2\text{Pc}(\text{SiMe}_3)_4$, $\delta_{\text{NH}} = -2.7$ ppm [96]).

Borovkov and Akopov [99] studied the temperature dependence of the ^1H NMR spectra of triazatetra(4-*t*-butylbenzo)porphyrine ($\text{H}_2\text{TATBP}^t\text{Bu}_4$) and concluded that, at ambient temperatures, $\text{H}_2\text{TATBP}^t\text{Bu}_4$ exists in CS_2 as a mixture of two US structures,

an asymmetric structure and a symmetric structure as follows;

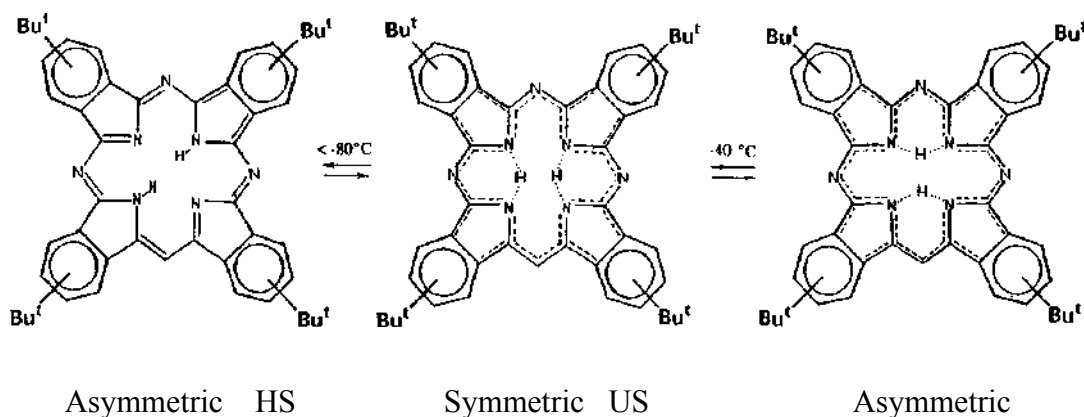


Figure 3.7 The state of NH protons depending on temperature [55].

Lowering of the temperature to -40°C shifts the equilibrium to the symmetric US structure. Further reduction in the temperature leads to conversion of the symmetrical US structure to the LS structure which has lower symmetry and was also supposed by Niwa et al. [101] for solid H_2TATBP on the basis of X-ray PES measurements. The solvent also influences the equilibrium of the two US forms. Replacement of CS_2 by solvents with better solvation abilities (pyridine) shifts the equilibrium to the symmetric US structure. Connecting the influence of solvent and temperature on the NH-resonance form with the structure of the reaction center, Borokov and Akopov [99], however, did not take into account that the same factors also have an impact on the extent of aggregation [97] which may be reflected in similar changes of the NH absorbance.

Kopranenkov and coworkers [102] reported the ^1H NMR spectra of tetra(tert-butyl)-tetraazaporphyrine ($\text{H}_2\text{PZ}^t\text{Bu}_4$) and for its randomers. At ambient temperature the β -CH proton singlet was observed at about 8.90 ppm and the NH-proton signal in the range -2.45-2.59 ppm depending on solvent. Lowering of the temperature causes a downfield shift in the NH protons to -2.87 ppm (-88°C). At the same time the β -CH proton singlet splits into two signals owing to NH tautomerism (8.69 and 9.08 ppm) with a coalescence temperature of -69°C . The value determined for ΔG^\ddagger of 41.4 kJ mol^{-1} is less than for porphyrins (H_2TPP , $\Delta G^\ddagger=47.7 \text{ kJ mol}^{-1}$ [103a]) but higher than for H_2Pc in the solid ($28\text{-}33 \text{ kJ mol}^{-1}$ [91, 92]). The same order of potential barriers was predicted by Mamaev and coworkers [83, 89-90].

^1H NMR spectra of the unsubstituted H_2Pz were obtained by Stuzhin [77]. In pyridine the β -CH proton singlet (9.24 ppm) is located at higher field than in H_2P (9.53 ppm [103b]). This upfield shift is not due to loss of aromaticity but can be explained by the larger isolation of the ethylene double bonds from the main 16-membered conjugation contour in which the π -electron ring current is stronger than porphyrine [98]. This is also substantiated by the ^{13}C NMR spectroscopy data which have shown a downfield shift for the C_α signal and an upfield shift for the C_β signal for $\text{H}_2\text{Pz}^t\text{Bu}_4$ compared with porphyrins [103a]. The singlet of the internal NH protons in H_2Pz is observed at -0.97 ppm and is located in a substantially weaker field than for H_2P (-3.94 ppm [103b]). In as much as the higher aromaticity of H_2Pz [73-75, 98] and the smaller diameter of its central cavity compared with H_2P should lead to the opposite upfield shift of the internal proton signal, this strong downfield shift is explained by changes in the state of the N-H bonds themselves. The polarization of the N-H bonds and the increase in the positive charge on the internal hydrogen atoms in H_2Pz reduces their shielding by the π -electron ring current and this manifests itself as a downfield shift. The state of the N-H bond is very sensitive to substituents in the pyrrole rings. Electron donors such as butyl or ethyl groups reduce the ionic character of the N-H bonds and cause an upfield shift of the NH-proton signal to between -2.1 and -2.6 ppm [102]; Br atoms as electron-acceptors increase the ionic character of the N-H bonds and the signal shifts downfield to +1.43 ppm [104].

The NH-proton resonance in H_2Pz and in its substituted derivatives is observed at a substantially lower field than was predicted by Vysotsky et al. [98] for the LS bonded structure ($\delta_{\text{NH}}=-4.62$ ppm). Therefore the delocalized US or HS structure of the reaction center is favored for H_2Pz in solution as well as for H_2Pc . Such a structure of the reaction center with a high degree of ionization of the N-H bonds is also supported by direct measurement of the acid properties of porphyrins, phthalocyanine and tetraazaporphyrins [105].

3.2 ACID-BASE PROPERTIES OF AZAPORPHYRINS

Quite valuable information on the structure of porphyrazines and their analogs can be obtained while studying their behavior in the proton donor media [106-

107]. In addition, the possibility of practical application of porphyrazine metal complexes and their analogs significantly depends on their stability in solutions. In this connection, the study of the acid-base interactions of porphyrazines and their complexes is of interest in both theoretical and practical aspects.

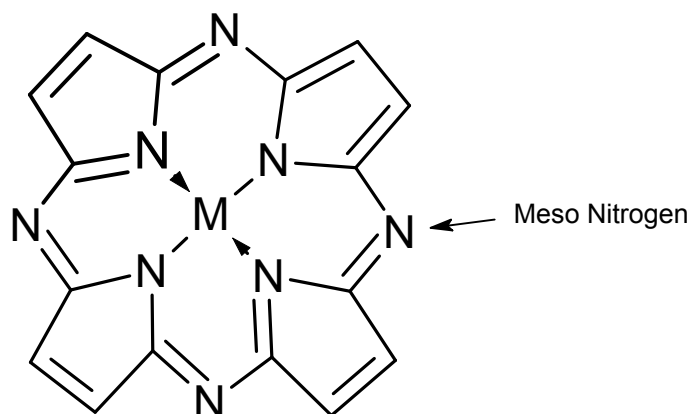


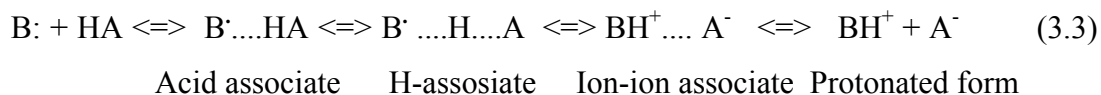
Figure 3.8 Porphyrazine metal complex [111].

Porphyrazines are weak multicenter conjugated bases. The number of porphyrazine donor centers involved in the acid–base interaction with acids, the character of the interaction, and the stability of the acidic forms obtained depend on the porphyrazine structure and the properties of the proton donor medium [108-110]. The π orbitals of endocyclic N atoms in metal complexes of porphyrazines participate in formation of bonds with a central metal atom. Therefore, only the exocyclic meso-nitrogen atoms are involved in the acid–base interaction.

The long-wavelength region of the electronic absorption spectra of porphyrazine complexes in a neutral solvent contain intense Q-band due to the $\pi \rightarrow \pi^*$ electronic transitions $a_{1u} \rightarrow e_g^*$ of a macrocyclic ligand. The interaction of porphyrazines with acids is attended by the spectral changes in a visible region corresponding to the formation of different acidic-basic forms. In the case of porphyrazine complexes, the acid-base inter-actions occur in two stages, which are attended by bathochromic shift of the Q-band [108-110].



The transfer of a proton from acid HA to base B: proceeds through the stages of formation of the acid associate, H-associate, ion-ion associate and fully ionized protonated form:



The acidic forms thus obtained differ from one another in a degree of a proton transfer from the acid molecule to the donor center. In media with a low ionizing capability, the electron-donor centers of porphyrazine participate in a weak acid-base interaction and form H-associates and ion-ion associates. The complete transfer of a proton can be observed in strongly ionizing medium only [111].

3.2.1 Acid Ionization of Azaporphyrins

Molecules of porphyrins can exhibit acidic properties and the two NH groups of the pyrrol-type fragments can be ionized in strongly proton-accepting media with the formation of monoand dianions:



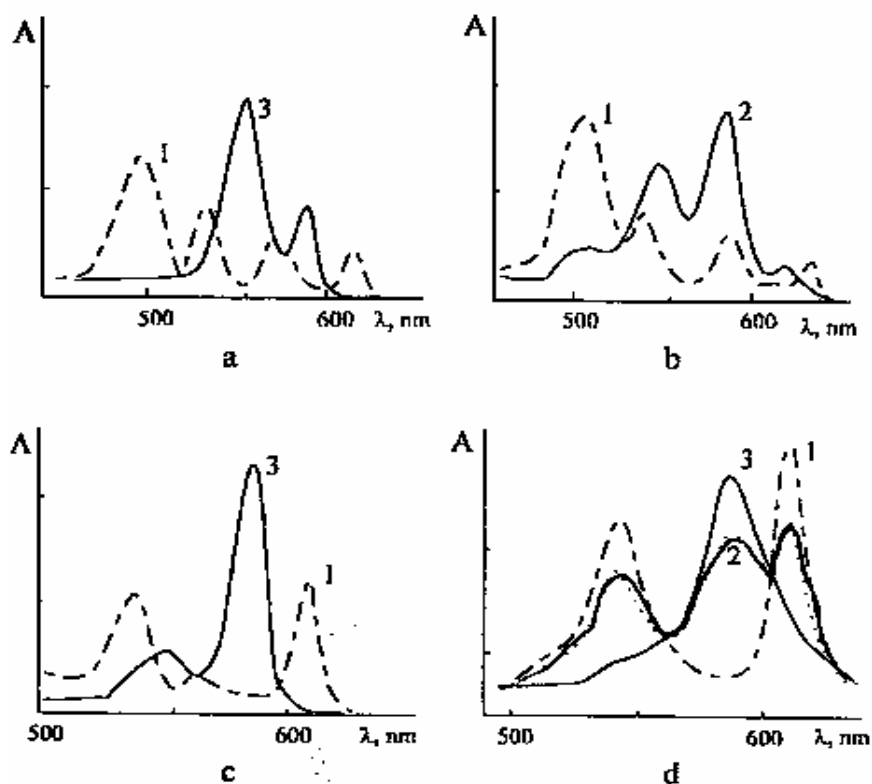


Figure 3.9 Absorption spectra of the neutral form (I), monoanion (2) and dianion (3) of H₂EP (a), H₂(Me)PEt₈, (b), H₂MAEP (c) and H₂Pz (d) in DMSO-H₂O-PhMe(82:10:8)(a-c) and in DMSO[9].

3.2.2 Spectral Picture of the Acid Ionization

The process of acid ionization is attended with changes of the symmetry and energy of the the π -molecular orbitals and can be easily followed by means of UV-visible spectroscopy. The spectral changes accompanying the acid ionization of aetioporphyrine (H₂EP), N-methyloctaethylporphyrine (H₂(Me)PEt₈), monoazaetioporphyrine (H₂MAEP) [112] and tetraazaporphyrine (H₂Pz) [113] are depicted in Figure 3.9[9].

The changes in the UV-visible spectra can be qualitatively explained on the basis of the "four-orbital" Gouterman's model [114], and the first order perturbation theory. The absorption bands in the visible and UV regions of the spectra of porphyrins and azaporphyrins (Q and B bands respectively) are due to the electronic transitions between two highest occupied molecular orbitals (HOMO, π_1 and π_2) and two lowest unoccupied molecular orbitals (LUMO, π_1^* and π_2^*) [115,116]. These orbitals are presented

schematically in Figure 3.9 [9].

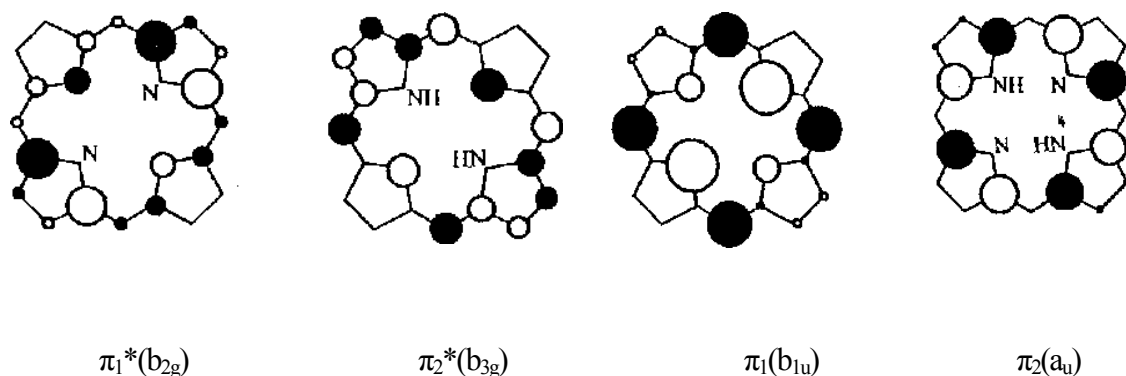


Figure 3.10 Symmetry properties of HOMO (π_1 and π_2) and LUMO (π^* and π_2^*) for the porphyrin type macrocyclic chromophore having D_{2h} symmetry [9].

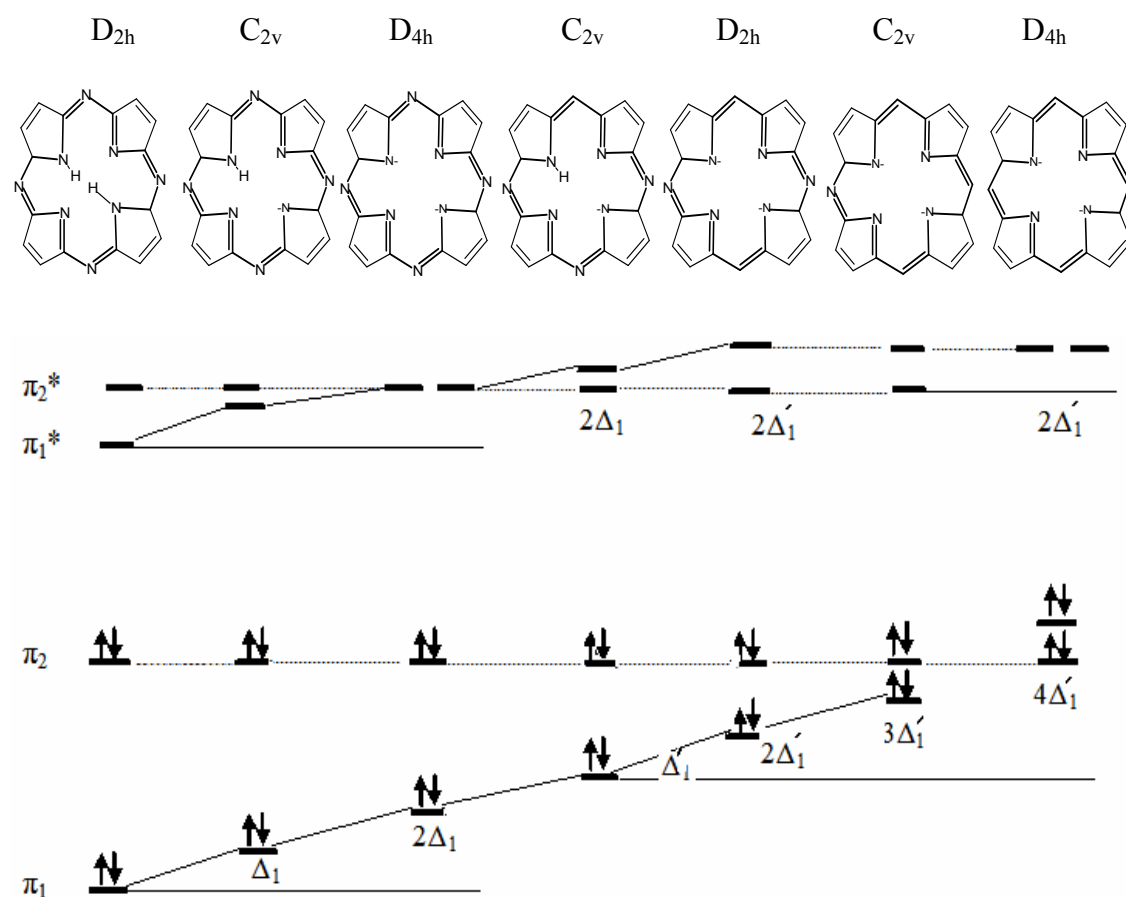


Figure 3.11 Schematic representation (first order perturbation theory approximation) of the HOMO and LUMO energy changes of H_2Pz during formation of the monoanion HPz^- , dianion Pz^{2-} and successive substitution of meso-nitrogens with methine bridges in the dianion [9].

In the case of free ligands having D_{2h} , symmetry (H_2P , H_2Pz) the transitions $\pi_2 \rightarrow \pi_{1,2}$ ($a_u \rightarrow b_{2g}, b_{3g}$) and $\pi_1^* \rightarrow \pi_{1,2}^*$ ($b_{1u} \rightarrow b_{2g}, b_{3g}$) give Q and B bands respectively. In the first approximation acid ionization can be considered as a one-center perturbation



which results in the change of the π -molecular orbitals energies by an amount $\Delta = \delta\alpha_N a_{Ni}^2$, where $\delta\alpha_N$ is the difference in the coulomb integrals of the pyrrole ($>N-H$) and aza-type ($=N-$) nitrogens and a_{Ni} - the atomic coefficient of the molecular orbital i . The $\pi_1(b_{1u})$ and $\pi_2(b_{2g})$ orbitals having non-zero coefficients on the pyrrole type nitrogens (Figure 3.10) are destabilized by an amount $\Delta_1 = \delta\alpha_N a_{N1}^2$, and $\Delta_3 = \delta\alpha_N a_{N3}^2$ on each of the acid ionization respectively (Figure 3.11). The $\pi_2(a_u)$ and $\pi_2^*(b_{3g})$ orbitals with nodes on the pyrrole-type nitrogens (Figure 3.10) are destabilized much less only due to the second order perturbations ($\Delta_2 \ll \Delta_1 \ll \Delta_4 \ll \Delta_3$) which can be neglected in the first order approximation. Formation of the dianion raises the orbital $\pi_1^*(b_{2g})$ by an amount $2\Delta_3$, whereas $\pi_2^*(b_{3g})$ remains constant. As a result these orbitals closely approach each other and in the case of D_{4h} symmetry of the dianion (Pz^{2-} , P^{2-}) they give two degenerated $\pi_{1,2}^*(e_g)$ orbitals. Two components of the absorption bands B and Q should therefore merge and the low energy Q band should be shifted hypsochromically. This is in fact observed for the dianion formation (Figure 3.9a, d). Formation of the monoanion destabilizes the $\pi_1^*(b_{1u})$ orbital by an amount Δ and lowers the symmetry to C_{2v} . As a result the monoanion has a similar spectral pattern (number of absorption bands) as the neutral form (Figure 3.9b) but the splitting of the Q band is decreased due to the hypsochromical shift of its long-wave component Q_x . The substitution of the bridging atom X in the meso-position change the energy of the molecular orbitals by amount $\Delta_i = \delta\alpha_X a_{Xi}^2$. The $\pi_1(a_{2u})$ and $\pi_{1,2}^*(e_g)$ orbitals raise their energy gradually in passing from Pz^{2-} to P^{2-} through monoaza, diaza and triazasubstituted porphyrin dianions [115, 117]. As can be seen from the right side of Figure 3.11, two LUMO are degenerated only for the most symmetrical Pz^{2-} and P^{2-} dianions having D_{4h} symmetry. For monoaza, diaza- and triazasubstituted species the Q and B bands should remain split for the dianions as well for the monoanions. Acid ionization in this case doesn't simplify the spectral pattern (MAEP²⁻ - (Figure 3.9c). Data for diaza and triaza substituted species have been also obtained [118,119]) and results only in the smaller splitting and the hypochromic shift of the Q_x band [9].

3.2.3 Methods of the Quantitative Estimation of Acidity

McEwen [120] was the first person, who 50 years ago, has estimated the acidity constants of aetioporphyrin (H_2EP) and of its N-methylated derivative ($H(Me)EP$) using a spectrophotometric titration method. Rochester et al. [112] have reinvestigated these compounds and also reported data for monoaza-aetioporphyrene (H_2MAEP). Andrianov [121] has used a solubility method for the determination of the acidity constants of several natural and synthetic porphyrins. These and some other early works have been critically reviewed in 1977 by Berezin [122] and it was pointed out that all acidity constants reported to that time can be considered only as relative and conditional [9].

Table 3.2 Thermodynamic parameters of the acid ionization of porphyrins and azaporphyrins. (Obtained by the solubility method) [9].

Compound	Medium	T, K	pK_{a1}	pK_{a2}	$\Delta H kJ mol^{-1}$	$\Delta S J mol^{-1} K^{-1}$
H_2P	DM SO	298	22.35		121	-23
H_2TPP	DMSO	298	21.15		120	-2
	DMF	298	17.0			
H_2TBP	DMSO	298	18.53		82	-79
	DMF	298	12.05		192	+414
H_2PEt_8	MeOH	298	16			
	MeOH ⁸	298	15.80			
$H_2DAP(MeBu)_4$	DMF	298	12.56		63	-30
		308	12.25			
H_2PZ	DMSO	298	12.36	12.43	232	+544
	DMF	298	9.68		105	+168
H_2PZBr_4	DMSO	298	7.26			
H_2PZPh_8	DMF	298	12.79		169	+37
H_2MATBP	DMF	298	12.11		53	-74
H_2TATBP	DMF	298	12.91		56	-60
$H_2Pc(SO_3H)$	DMSO	298	10.73		70	+28
$H_2Pc(SO_3H)_{..}$	H_2O	293	9.6	>12		

Since then Sheinin and Andrianov [123, 124] have studied the acid properties of porphyrins and azaporphyrins most systematically. They were the first who combined a spectrophotometric titration method with a potentiometric pH control of media [125]. That allowed them to evaluate thermodynamical acidity constants K_{a1} and K_{a2} in non-aqueous media. Solution of porphyrin or azaporphyrin in dimethylsulfoxide (DMSO) or

dimethylformamide (DMF) was titrated with tetraalkylammonium hydroxide and the current pH value was measured potentiometrically. Depending on the free base porphyrin and on the conditions, a monoanion or a dianion was formed at once. The concentration of the non-ionized and ionized forms was determined spectrophotometrically and the acidity constants were calculated from the equation

$$pK_a = npH - \log I_n, \quad (3.7)$$

where I_n is a concentration ratio of the neutral and ionic forms and n indicates the formation of the monoanion ($n=1$) or dianion ($n=2$) in a single step reaction [9].

3.2.4 Acidity of Common Porphyrins

Porphyrins appear to be less acidic than water and have a close acidity with alcohols. That is why acid ionization of porphyrins does not proceed in aqueous alcoholic solutions and formation of the dianionic forms can be observed only in absolutely dry alcohols. The solvents with higher pK_a values such as DMSO or DMF are more appropriate for the investigation of weak acids such as porphyrins [9].

Sheinin and co-workers [126] have investigated the acid ionization of porphyrin (H_2P) and of some natural and synthetic porphyrins in DMSO in the presence of tetraalkylammonium hydroxide using spectrophotometric titration with potentiometric pH control. In the conditions used for the spectrophotometric titration (the OH^- ion concentration is less than 0.1 M) common porphyrins undergo only the first ionization stage (3.4). The formation of the dianion P^{2-} can be observed only in a more basic media. The dianion exists as an associate with two cations of alkali metals. It was found that an associate with Li^+ has the highest stability [127]. The first acidity constant pK_{a1} and the thermodynamic parameters of the monoanion formation have been determined for porphyrine and for several of its substituted derivatives [126, 127] in (Table 3.2). It is remarkable that the $pK_{a1}^{298} = 22.35$ determined in DMSO for porphyrin is only slightly lower than that of pyrrole ($pK_a^{298} = 22.05$ in DMSO [127]). Comparison of the ν_{NH} frequencies in the infrared spectra (3305 and 3495 cm^{-1} for porphyrin and pyrrole, respectively) suggests a much stronger ionization of the N-H bonds in porphyrin than, in pyrrole. This large difference in the ν_{NH} frequencies can be only partially explained by the intramolecular H-bonding in the porphyrine molecule. The proximity of the acidity constants in porphyrine

and pyrrole is indicative about strong steric and π -electron shielding of the reaction center in porphyrins which hinders the interaction of the base anion with the protons and counteracts their removal from the porphyrin plane [9].

The acidity constant pK_{a1} depends on substituents in the pyrrole rings or in the meso-positions of the porphyrin molecule and vary between 25.3 for alkyl substituted derivatives (dimethyl ester of deuteroporphyrin) to 20 for meso-substituted tetraphenylporphyrine derivatives in accordance with the inductive electronic effects of the substituents (Table 3.2). Benzosubstitution and especially azasubstitution have much stronger impact on the acidity [9].

3.2.5 Azaporphyrins

Rochester and co-workers [112] observed the formation of the dianion of monoazaaetioporphyrine MAEP²⁻ in the DMSO:H₂O:PhMe mixture in the presence of NaOH (Figure 3.9c) and found that substitution of one meso-CH- group in aetioporphyrine with a nitrogen atom increases an acidity by ten times (the relative net constants of the dianion formation is $pK_{1,2} = -2.94$ and -4.00 , respectively).

Sheinm et al. [113] have investigated acid ionization of tetraazaporphyrine (H₂Pz) in DMSO. Replacing four meso-CH= groups with nitrogen atoms (tetraazasubstitution) leads to a drastic increase of acidity. H₂Pz has an acidity ten orders of magnitude stronger than H₂P (pK_{a1} values 12.36 and 22.35 respectively). Meso-nitrogen atoms in H₂Pz stabilize the anionic forms and H₂Pz unlike common porphyrins (H₂P, H₂TPP, H₂TBP) undergoes also the second ionization stage (3.5) in the conditions of the spectrophotometry titration in DMSO (concentration of OH⁻¹ less than 0.1 M) forming successively monoanion HPz⁻ and dianion Pz²⁻ (Figure 3.9d). The spectral changes observed during these two ionization stages reflect the reduction of the molecular symmetry from D_{2h} in H₂Pz to C_{2v} for HPz⁻ and its subsequent increasing in Pz²⁻ (D_{4h}). The UV-visible spectrum of the dianion resembles the spectra of metal complexes. The acidity constants of both steps (3.4) and (3.5) pK_{a1} and pK_{a2} were obtained for H₂Pz in DMSO and were found to be very close to one another (12.36 and 12.43 respectively) [113]. The enthalpy of the first stage (3.4) of the acid ionization of H₂Pz is two times higher than for common porphyrins and the entropy value is strongly positive (Table 3.2) [9].

It was supposed that N-H bonds in H₂Pz are ionized and that the reaction center of the H₂Pz molecule can be regarded as an unique "associate" of two protons with the macrocyclic dianion (so called intraionized IS structure, Figure 3.5). This associate is strongly stabilized by solvation. It is unlike common porphyrins in which protons are localized on the two nitrogen atoms of the pyrrole type and form only weak H-bonds with the nitrogen atoms of the adjacent pyrroline rings (localized LS structure) (Figure 3.5). Such a difference in the solvation of porphyrins and azaporphyrins was substantiated by the recent studies on the, thermodynamics of their dissolution. Vyugin and co-workers [128] have shown that appreciable solvation of the N-H bonds in porphyrins is absent contrary to tetraazaporphyrins for which specific solvation of N-H bonds was observed by Trofimenko [129].

Recently, Tsvetkova has studied the acid ionization of H₂PZ, its octaphenyl derivative (H₂PzPh₈) and tetramethyltetrabutyl diazaporphyrine (H₂DAP(MeBu)₄) in DMF. Values of pK_{a1} obtained in DMF [118,119] are lower than those obtained in DMSO [113] (Table 3.2). Probably, that can be explained by the difference in the solvation of the neutral and anionic forms in these two solvents [9].

Substituents in the pyrrole rings of the tetraazaporphyrin molecule can change its acidity greatly. Eight phenyl groups in H₂PzPh₈ reduce the acidity due to their positive inductive effect and steric hindrances (pK_{a1}²⁹⁸ = 12.79 in DMF [118, 119]). At the same time four Br atoms in H₂PzBr₄ acting as electron-acceptors stabilize the anionic form and acidity increases by 5 orders of magnitude as compared with H₂Pz (pK_a²⁹⁸ = 7.26 in DMSO [130]).

Recent analysis [131] of the spectral and structural data of porphyrins and azaporphyrins showed that properties of H₂Pz in basic media can be most adequately described as an unlocalised structure (US) of the reaction center (Figure 3.5). The internal hydrogen atoms form strong H-bonds with two adjacent internal nitrogens and with meso-nitrogen and the partial negative charge is strongly delocalized on the π -orbitals of the conjugated system of the macrocycle [9].

3.2.6 N-base Adducts of Tetraazaporphyrins

Due to their high acidity tetraazaporphyrins and phthalocyanines can form unique adducts with N-bases. Whalley [132] was the first who observed the formation of so called "pyridine salts" of tetraazaporphyrine and of some its alkyl and benzo substituted derivatives. Tribenzotetraazaporphyrine and phthalocyanine give such adducts on refluxing of their pyridine solution. Vul'son et al. [133] have investigated the interaction of H_2Pc with different amines and found that the "amine salts" can form only in nonprotonating polar solvents. According to Whalley [132] tetraazaporphyrine, its tetramethyl, octamethyl and tetra (tetramethylen) derivatives yield adducts with pyridine during anaerobic irradiation of their pyridine solutions. Octaphenyltetraazaporphyrine give salts with pyridine and piperidine on heating of its solutions in these N-bases for several hours or on their long standing at room temperature [134]. Tetrahalogenetetraazaporphyrins, such as H_2PzBr_4 , having higher acidity forms N-base salt in one hour at room temperature [130].

Although such species are commonly named "salts", very little is known about their structure and there are many doubts about their ionic character. Changes in UV-visible spectra accompanying the formation of the "pyridinium salts" resemble those during an acid ionization or metal ion incorporation processes (Figure 3.12. a) and therefore, being characteristic of the increase of the molecular symmetry from D_{2h} to D_{4h} , they confirm withdrawing of the two protons from the plane of the molecule [9].

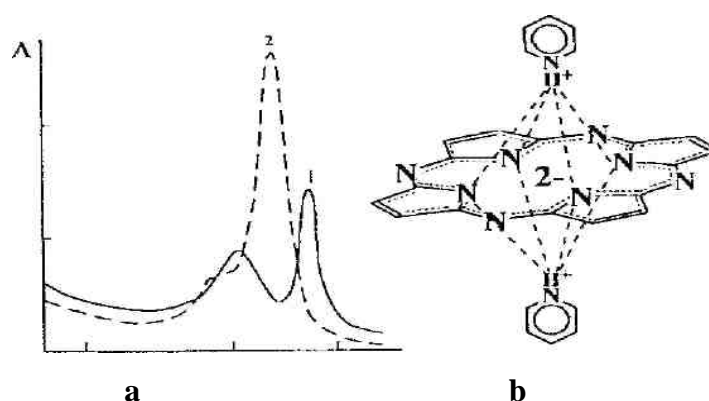


Figure 3.12 (a) Absorption spectra of H_2PzPh_g (1) and its "pyridinium salt" (2); (b) Possible structure of the "pyridinium salt" [9].

3.2.7 Basic Properties of Azaporphyrins

Molecules of common porphyrin ligands H_2P contain two pyrroline type nitrogen atoms in the reaction center that can be protonated in acid media with formation of the monocation H_3P^+ or dication H_4P^{2+}



Azasubstitution introduces additional nitrogen atoms in the meso-positions of the porphyrin molecule, which are of the pyridine-type and can also exhibit basic properties. In the azaporphyrin ligands H_2AP two internal pyrroline and from one to four meso - nitrogens can take part in the acid-base interaction with acids in principle. Because of this, the pattern of acid-base interaction can be very complicated for free-base azaporphyrins:

It is simpler for metallo-azaporphyrins in which ϕ_n orbitals of the internal nitrogen atoms are involved in the formation of strong donor-acceptor bonds with metal and only meso-nitrogens can participate in the acid-base interaction:

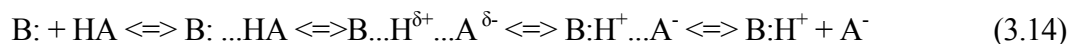


All electron donating nitrogen atoms of azaporphyrins are integrated in the π -conjugated aromatic system of the macrocycle and their properties are strongly interconnected and interdependent. Azaporphyrins can be considered as unique multi-center conjugated bases.

In the studies of basic properties of the multi-center bases such as azaporphyrins three main problems should be solved:

(i) Determination of the number and location of donor centers participating in the acid-base interaction in the media of different acidity;

(ii) Determination of the character of interaction of the donor centers with acid molecules, taking in account that according to the modern theory of acid-base interaction the proton transfer from acid HA to base B: is a complex process in which stages of the acid associate, H-associate, ion-ionic associate and finally fully ionized protonated form can be distinct:



Acid associate H-associate Ion-ionic associate Protonated form

These forms differ by the "depth of protonation" by the degree in which the proton is transferred from the acid molecule to the donor center.

(iii) Reliable quantitative estimation of the basicity.

These problems can be solved only by combined use of the different investigation methods - spectroscopical, thermodynamical and quantum-chemical [9].

CHAPTER 4

APPLICATIONS

4.1 BIOMEDICAL APPLICATIONS OF SOME WATER SOLUBLE PORPHYRINIC MOLECULES

4.1.1 Developing a Structure–function Relationship for Anionic Porphyrines Exhibiting Selective Anti-tumor Activity

Beginning with photodynamic therapy (PDT) the use of optical agents is becoming increasingly popular for the detection and treatment of tumors [135-138]. PDT optimally employs dye (a photosensitizer) that preferentially accumulate in tumors and absorbs light in the near-infrared (NIR), at wavelengths penetrable to mammalian tissue (700–900 nm). Upon excitation, such a dye can react with endogenous oxygen to produce cytotoxins, initially through singlet oxygen, that can eventually lead to cell death and. A NIR-absorbing/emitting dye also can act as an optical imaging agent, especially if it is a poor singlet oxygen sensitizer. First-generation efforts at PDT focused primarily on developing porphyrins for these uses [139], and included the preparation of Photofrin (hematoporphyrin derivative, HpD) [140]. However, while Photofrin is somewhat effective for treating tumors, because Photofrin has the relatively poor optical properties of porphyrins in general poor tumor selectivity, long retention time, and synthetic difficulties [141], better photosensitizers are needed. Likewise, optical tumor imaging, while of great potential promise, requires better contrast agents than the currently approved indocyanine green [142]. Recent interest has shifted to studying porphyrin variants to overcome these limitations for both applications [143]. To this end, the porphyrines (Pzs) – porphyrin derivatives in which the *meso* (CH) groups are replaced by nitrogen atoms linking the pyrrole rings (see Figure 4.1) show extreme promise as potential imaging therapeutic agents [144].

Recently examined the effect of charge differences on the biological behavior of a suite of three structurally similar porphyrazines of the form $H_2[Pz(A_n;B_{4-n})]$ (illustrated by **11** in Fig. 4.1 where $n = 2$ (*trans*), **A** is $[S-R]_2$, and **B** is fused β,β' -dialkoxybenzo group [144]. In that study, the three Pzs had R groups with different charge (positive, negative, or neutral), and we identified an anionic porphyrazine with carboxylic acid R-groups, **11** as $R=(CH_2)_3CO_2^-$ having selective anti-tumor activity [145].

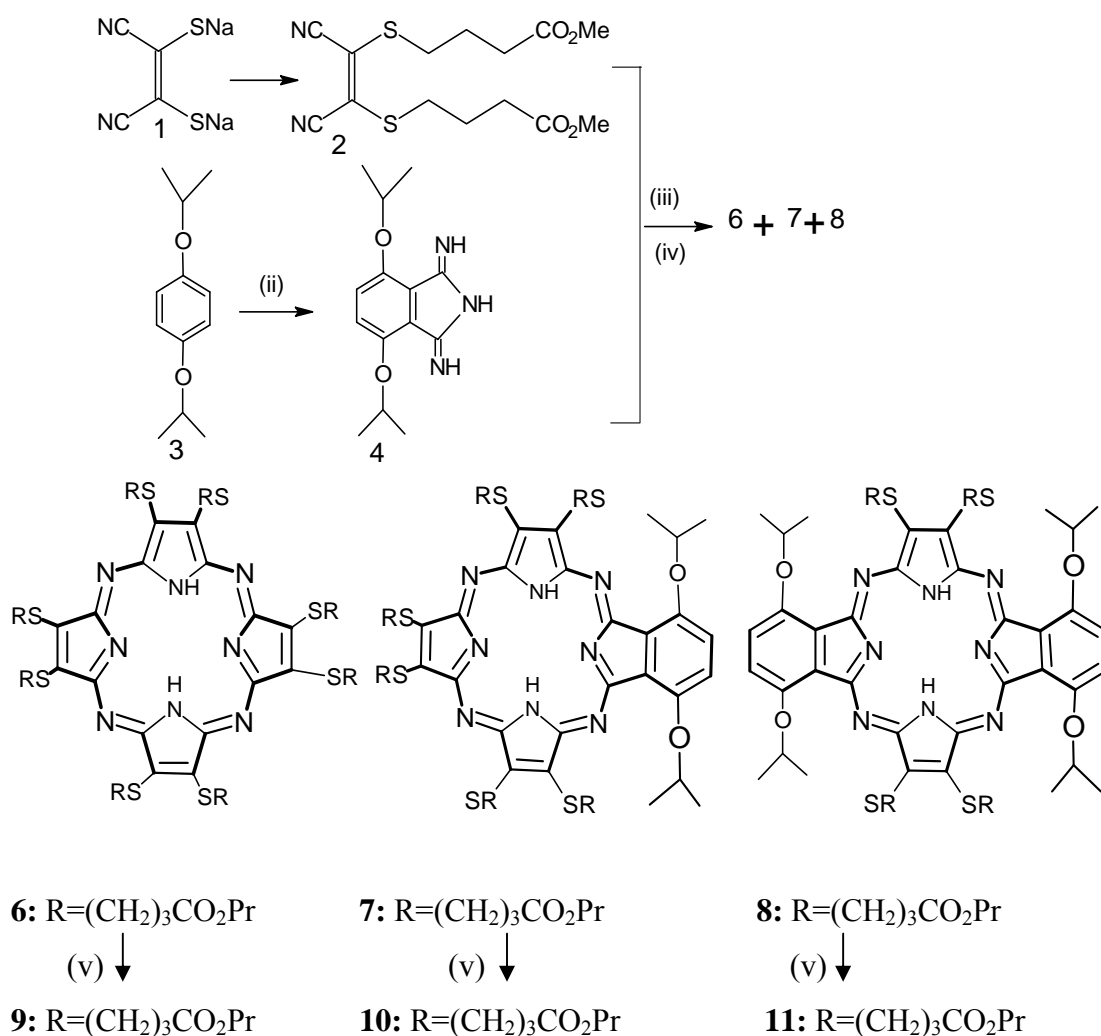


Figure 4.1 Synthesis of $H_2[Pz(A_n;B_{4-n})]$, where **A** is $[S(CH_2)_3COOR]_2$ ($R = n\text{-Pr, H}$) and **B** is a fused β,β' -diisopropoxybenzo group, including the compounds with $n = 4$ (**6**), $n = 3$ (**7**) and the *trans* compound with $n = 2$ (**8**) [145].

Key: (i) $Cl(CH_2)_3CO_2CH_3$, NaI, acetone at reflux, 24 h; (ii) $NH_3(g)$, Na, $n\text{-PrOH}$ at reflux, 12 h; (iii) $Mg(OPr)_2$, $n\text{-PrOH}$ at reflux, 7 h; (iv) TFA, CH_2Cl_2 , 20 °C, 1 h; (v) LiOH, THF/ H_2O , 20 °C, 4-5 days.

4.1.2 Studies on Photodynamic Activity of New Water-Soluble Azaphthalocyanines

Pc's and also AzaPc's possess one undesirable property. Owing to the extended π system, these macrocyclic compounds exhibit a high aggregation tendency forming dimeric and oligomeric species in solution [146,5a]. This causes insolubility, hinders purification and characterisation of the compounds and precludes their use in PDT. The introduction of either long chains or bulky substituents to the periphery of the macrocycle should prevent the aggregation [147, 148].

The aim of synthesis of aza analogues of phthalocyanines (AzaPc's) bearing four long chains with carboxy groups at the end and four "bulky" diethylamino groups on periphery was to prepare water-soluble AzaPc **5-7**. The long chain substituent (6-aminohexanoic acid) carries carboxy group that enables solubility in water (as a sodium salt) and is also suitable for a conjugation to the biomolecules.

The AzaPcs were prepared by the Zimcik P. et al. [149] according to following scheme and characterized. The second, bulky, substituent (diethylamine) was chosen to prevent the aggregation even more. Designing a substituent structure, we considered not only an aggregation behaviour but also lipophilicity. It was found that Pc with four carboxy groups is more photodynamically active than with eight carboxy groups or, on the other hand, completely hydrophobic [150].

Photodynamic activity depends also on introduced central metal. Metal-free Pc does not exert any photodynamic activity. Diamagnetic central metals, such as Zn or Mg enhance phototoxicity of Pc's and therefore their potential for PDT. Since PDT activity is mainly based on singlet oxygen, its production was determined by the dye-sensitised photooxidation of 1,3-diphenylisobenzofuran (DPBF), a specific scavenger of this toxic species [151].

Toxicity and photodynamic activity of the AzaPc's **5-7** were measured on the protozoa culture of *Paramecium caudatum*. Growth curve, morphology of cells and percentage of died cells were measured. Neither toxicity nor photodynamic activities were detected. Tests on cells, surprisingly, did not show any photodynamic activity. It can probably be due to the aggregation in water. These aggregates can be detected on UV-Vis spectra (Figure 4.3). While UV-Vis spectra in pyridine show sharp absorption

peaks in the Q-band region the spectra in 0.2% aqueous NaHCO₃ show broadening and significant decrease of extinction coefficients due to the presence of the aggregates.

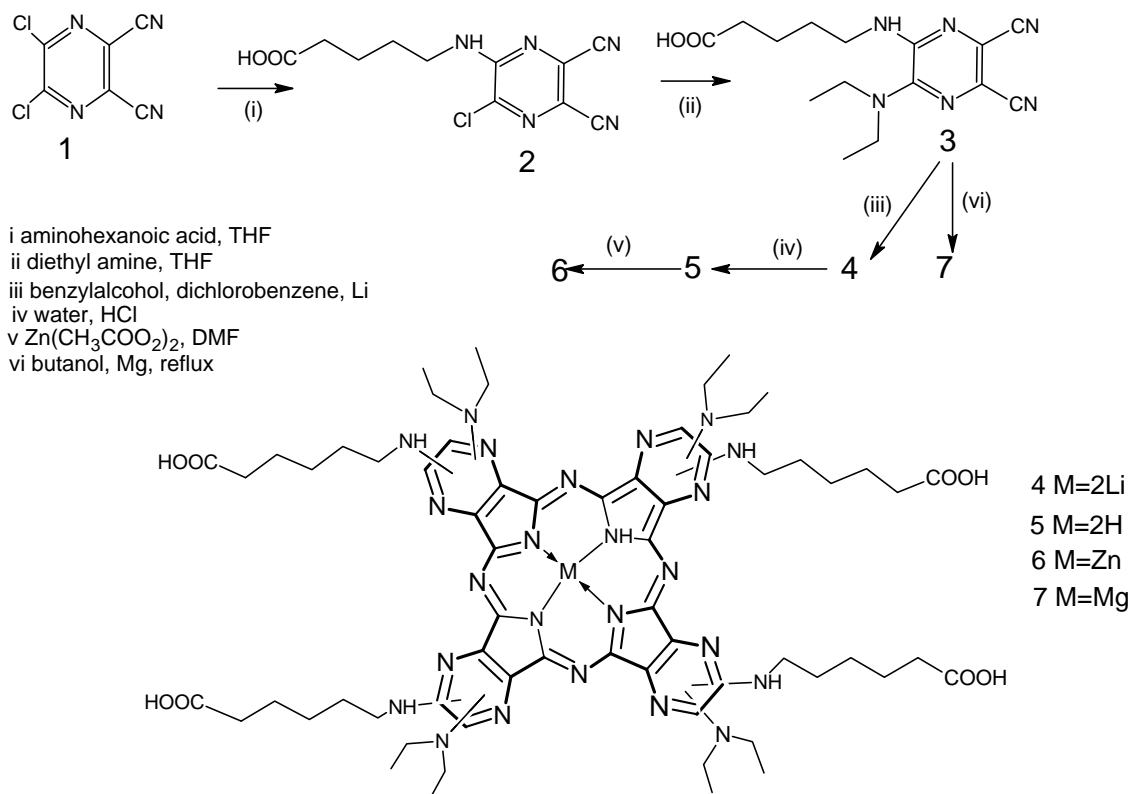


Figure 4.2 Synthesis of water soluble AzaPcs [149].

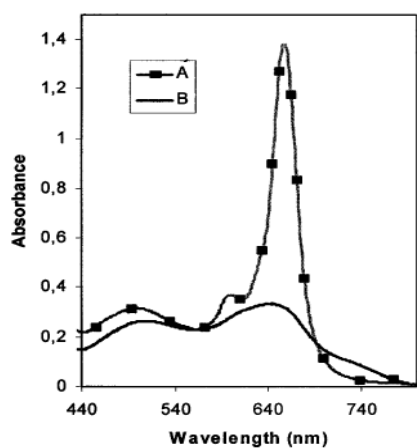


Figure 4.3 Absorption spectra of **6** in pyridine (A) and in 0.2% aqueous NaHCO₃ (B). Concentration was 12.5×10^{-6} mol dm⁻³ in both cases [149].

Singlet oxygen measurement was carried out by a DPBF decomposition reaction. AzaPc (5.0×10^{-6} mol/dm³) and DPBF (5.0×10^{-6} mol/dm³) were dissolved in pyridine,

transferred to a glass tube in the dark, and during vigorous stirring irradiated from distance 0.5m for different times. As the light source a halogen lamp (OSRAM, 500 W) was used. A decrease of DPBF concentration was followed by an absorbance at 417 nm.

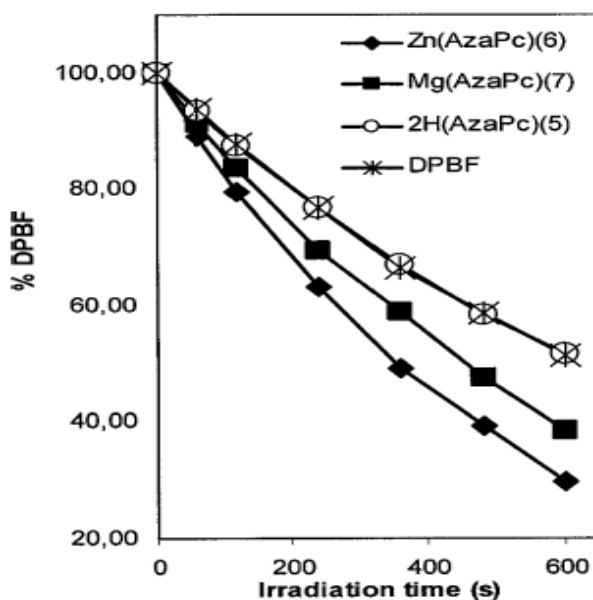


Figure 4.4 Degradation of DPBF by singlet oxygen generation [149].

It can be seen in Figure 4.4 that in the presence of metal-free **5**, DPBF decomposes at the same rate as without any AzaPc. On the other hand, in the presence of **6** or **7**, the rate of the DPBF decomposition is higher, thus suggesting they release singlet oxygen after illumination. It is in a relation with findings for Pc's, where metal-free Pc does not exert any photodynamic activity while ZnPc belongs to the most potent photosensitisers [151].

4.1.3 Super-Charged Porphyrazines: Octacationic Tetraazaporphyrins and Investigation Binding Properties of Octa-plus Porphyrazines to DNA

Cationic tetraazaporphyrins, or porphyrazines, represent an alternative and highly under-developed class of cationic porphyrinic compounds. Macrocycles based on the porphyrazine core, including phthalocyanines, exhibit many of the same properties as porphyrins, but the replacement of the *meso* methylene carbons of porphyrins with

nitrogen in porphyrazines creates profound differences [152-153]. For example, porphyrazines absorb more strongly at longer wavelengths a critical feature in biological and medical applications. Furthermore, the synthetic route to porphyrazines, which involves cyclization of functionalized maleonitriles, rather than condensation of aldehydes and pyrroles, gives opportunities for generating new types of functionalization at the peripheral β -carbons [154]. The binding of tetracationic, fused methylpyridino porphyrazines to DNA has been reported [155].

Anderson M.E. published the preparation of a new class of cationic tetraazaporphyrins, the octa-methyl-pyridyl porphyrazines, including CuPz^{+8} and ZnPz^{+8} [156]. These octacationic macrocycles are directly functionalized at the β -pyrrole carbons with pyridyl groups to provide a higher charge per macrocycle, to decrease aggregation, and to avoid problems of isomer purification. Possessing eight positive peripheral charges, these macrocycles should bind strongly to the negatively charged double-stranded DNA polymer, and they reported preliminary electronic absorption and emission spectroscopic investigations into the binding of CuPz^{+8} and ZnPz^{+8} to double-stranded calf thymus (CT) DNA.

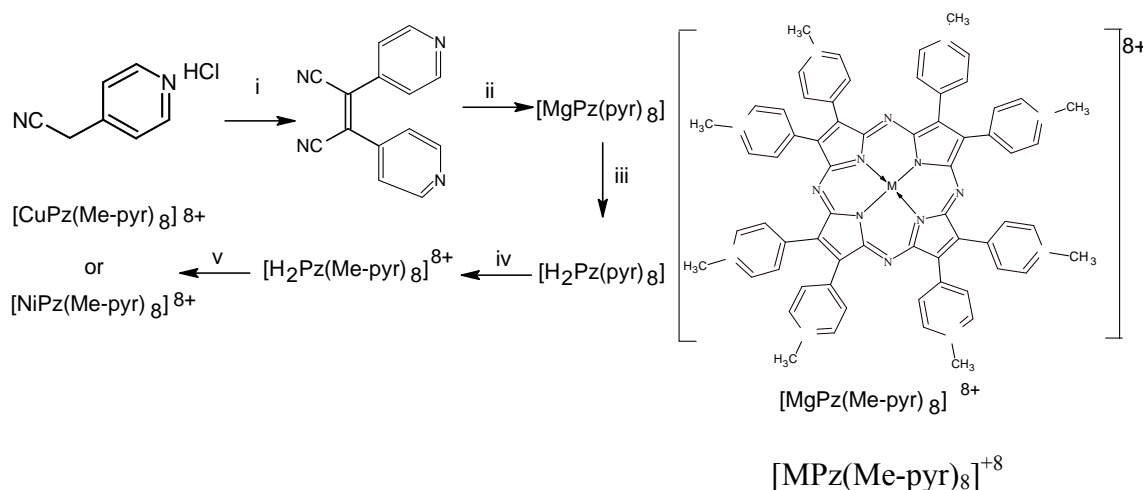


Figure 4.5 Synthesis octa-methyl-pyridyl porphyrazines [156].

Key: (i) 1:1 Et₂OMeOH, I₂, NaOMe, reflux (37% yield); (ii) Mg(O-nBu)₂, n-BuOH, reflux (20% yield); (iii) dilute aqueous HCl; (iv) MeOTf, DMF, 3 days, 100 °C (65% yield); (v) MCl₂, 2.0 M NaCl, H₂O.

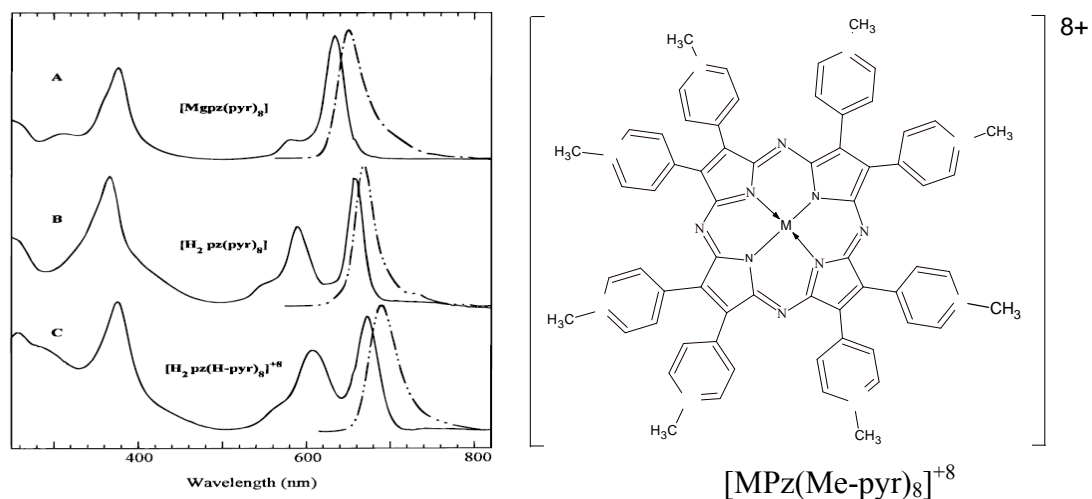


Figure 4.6 Absorption (—) and emission (— • —) of the octapyridylporphyrazines: (A) $[\text{MgPz}(\text{pyr})_8]$ in 20% MeOH in CHCl_3 , emission excitation at 378 nm; (B) $[\text{H}_2\text{Pz}(\text{pyr})_8]$ in 20% MeOH in CHCl_3 , emission excitation at 367 nm; (C) $[\text{H}_2\text{Pz}(\text{H-pyr})_8]^{8+}$ in aqueous HCl (~ 1.2 M), emission excitation at 607 nm [156].

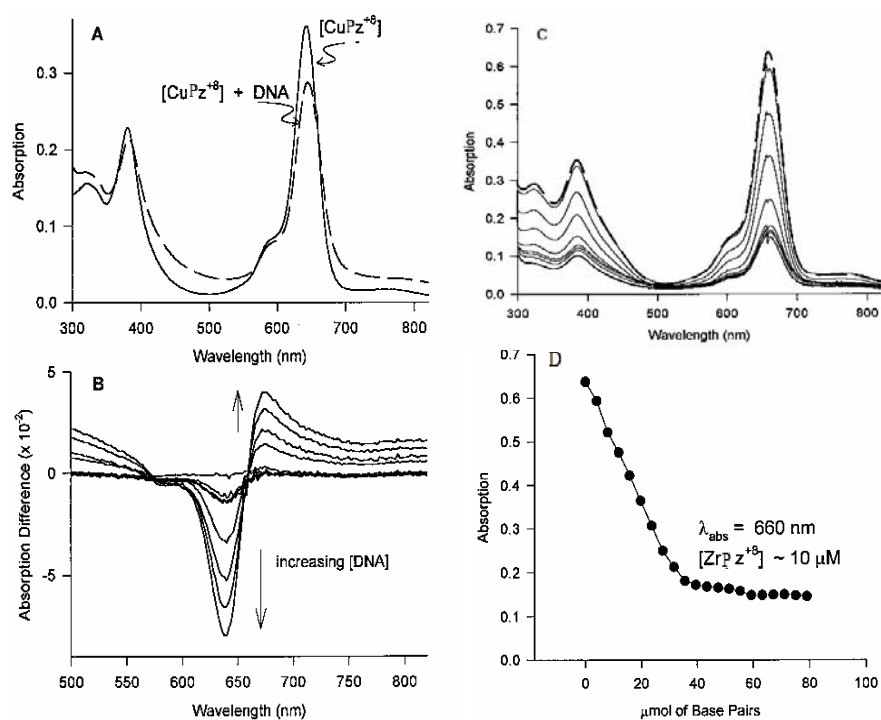


Figure 4.7 A- Electronic absorption spectra of CuPz^{+8} alone (solid line) and in the presence of CT DNA (dashed line). B- Difference absorption spectra in the Q-band region for CuPz^{+8} titrated with CT DNA. C- Electronic absorption spectra for the titration of ZnPz^{+8} with DNA at pH 7.00 in 0.1 M NaCl and 0.01 M phosphate buffer D- Plot of the absorbance at 660 nm of ZnPz^{+8} versus the concentration of CT DNA base pairs [157].

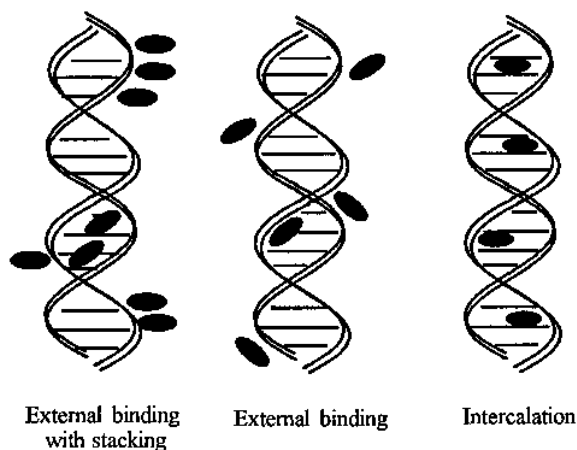


Figure 4.8 Cartoon of three possible binding modes of tetra-*N*-methyl pyridyl porphyrins with DNA [157].

The measurements show that the two octacationic porphyrazines, CuPz^{+8} and ZnPz^{+8} , strongly interact with the anionic phosphates of CT DNA. Cationic pyridyl porphyrins have been shown to exhibit three types of binding modes: external binding through interactions with the phosphates, as on the left in Figure 4.8; external binding with stacking; and intercalation. In the case of CuPz^{+8} , the shift in the absorbance maxima upon complexation to DNA indicates the occurrence of some form of π stacking interaction. By comparison with results from the pyridyl porphyrins, the shifts are not large enough to indicate that intercalation has occurred, but instead likely reflect some external stacking of the porphyrazines along the DNA phosphate backbone; there is no evidence as to whether this might occur in the minor grooves, or both. Proof of this interpretation could, in principle, be obtained by circular dichroism measurements. Attempts to see induced circular dichroism failed to show an effect; while this might be significant, it also may be because of the rather low concentrations needed to prevent precipitation. In the case of ZnPz^{+8} , the lack of a shift in the band maxima is consistent with simple electrostatic surface binding between the positive macrocycle and the negative phosphate backbone as the major mode of interaction. This difference presumably reflects the fact that ZnPz^{+8} binds an axial ligand, most likely 1120 in aqueous media, that inhibits closer stacking, whereas CuPz^{+8} does not. The existence of residual ZnPz^{+8} that remains in bound to DNA which does not precipitate even past the ‘neutralization point’, presumably reflects the fact that CT DNA is heterogeneous in length, and some strands remain soluble even with complexed macrocycle. Metallo-

octacationic porphyrazines are currently being investigated as staining agents for electrophoretic mobility gels. The observed interactions between DNA and octacationic porphyrazines suggests additional experiments with well-defined DNA and encourages to pursue ‘unsymmetrical’ porphyrazines which maintain n -2, 4 or 6 methyl-pyridyl groups for DNA binding and utilize the other 8- n 13-pyrrole sites for optional functional groups, such as phenanthroline [157].

4.1.4 Generation of Singlet Oxygen with Anionic Aluminum Phthalocyanines in Water

Kuznetsova et al. [158] synthesized Aluminum octakis(diethoxyphosphinyl-methyl)phthalocyanine **III** from the precursors which were triethyl phosphite and chloro-aluminum octachloromethylphthalocyanine by mixing at 150°C. By analogy with the resulting dye should contain the OP(O)(OEt)(Et) group as the ligand at Al. Yield of VI is 0.92 g (67.3%).

Bromoaluminum octakis(dihydroxyphosphinyl-methyl)phthalocyanine **I** was prepared by Kuznetsova et al. by treatment of aluminumoctakis(diethoxyphosphinyl-methyl)phthalocyanine VI with concentrated HBr at 110°C (λ_{max} 646 and 716 nm.)

Hydroxyaluminum octakis(hydroxyisopropoxyphosphinylmethyl)phthalocyanine **II** was synthesized from chloroaluminum octachloromethylphthalocyanine and triisopropyl phosphite at 170°C and 1 h at 190°C.

It was found that, with respect to the quantum yields of the $^1\text{O}_2$ generation, phosphonates **I-III**, depending on the structure and medium. The maxima of the long-wave Q bands of **I-III** are listed in the Table 4.1. It was found that the Q band of the phosphonates at pH 7.4 is broadened as compared to the narrow bands of monomeric phthalocyanines, and, as the phosphonate groups are esterified, the band width regularly decreases and the intensity grows, so that the band parameters become similar to those of the monomer (spectra of **I**, its partial ester **II**, and full ester **III**, Figure 4.9).

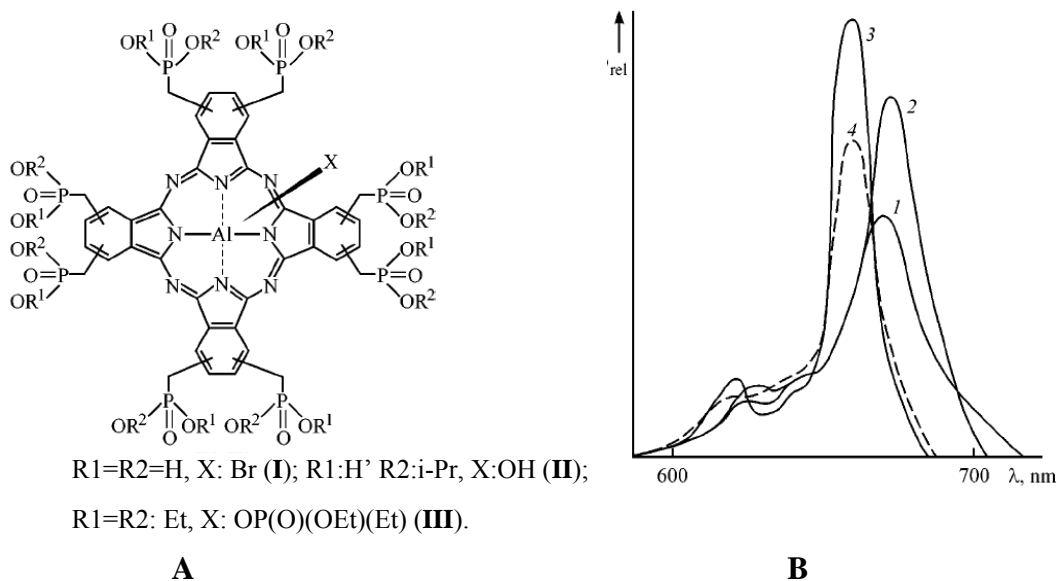


Figure 4.9 (A) Phosphonate substituted aluminum phthalocyanines. (B) Electronic absorption spectra of **I**, **II**, and **III** in aqueous buffer solution (pH 7.4) and (4) of **III** in the same solution with addition of 1 wt % Triton X-100 [158].

Table 4.1 Quantum yields of singlet oxygen generation by phthalocyanines **I-III** in aqueous solutions*

Comp. No	λ_{\max} , nm (phosphate buffer)	η_{Δ}		Macro-ring charge
		Phosphate buffer	Phosphate buffer +1% Triton X-100	
I	705	0.11 ± 0.03	0.09 ± 0.03	-16
II	715	0.12 ± 0.04	0.12 ± 0.04	-8
III	695	0.25 ± 0.04	0.30 ± 0.04	0

*Revised from Reference [158].

Phthalocyanines with free hydroxy groups in phosphonate substituents form associates that, in contrast to common associates, give no new bands in the electronic spectrum. Moreover, the associates of compounds **I** and **II** containing a large number of free acidic phosphonate groups in the concentration range 10^{-4} - 5×10^{-6} M obeyed the Bouguer-Lambert-Beer law, and addition of Triton X-100 did not alter the shape and intensity of the long-wave absorption bands. Such a behavior shows that the associates formed by these compounds in aqueous solution are very stable. The quantum yields of $^1\text{O}_2$ generation by the associates are low: about 0.1 for **I** and **II** (see Table 4.1) [159].

4.1.5 Photodynamic Activity of Some Tetraazoporphyrin Derivatives

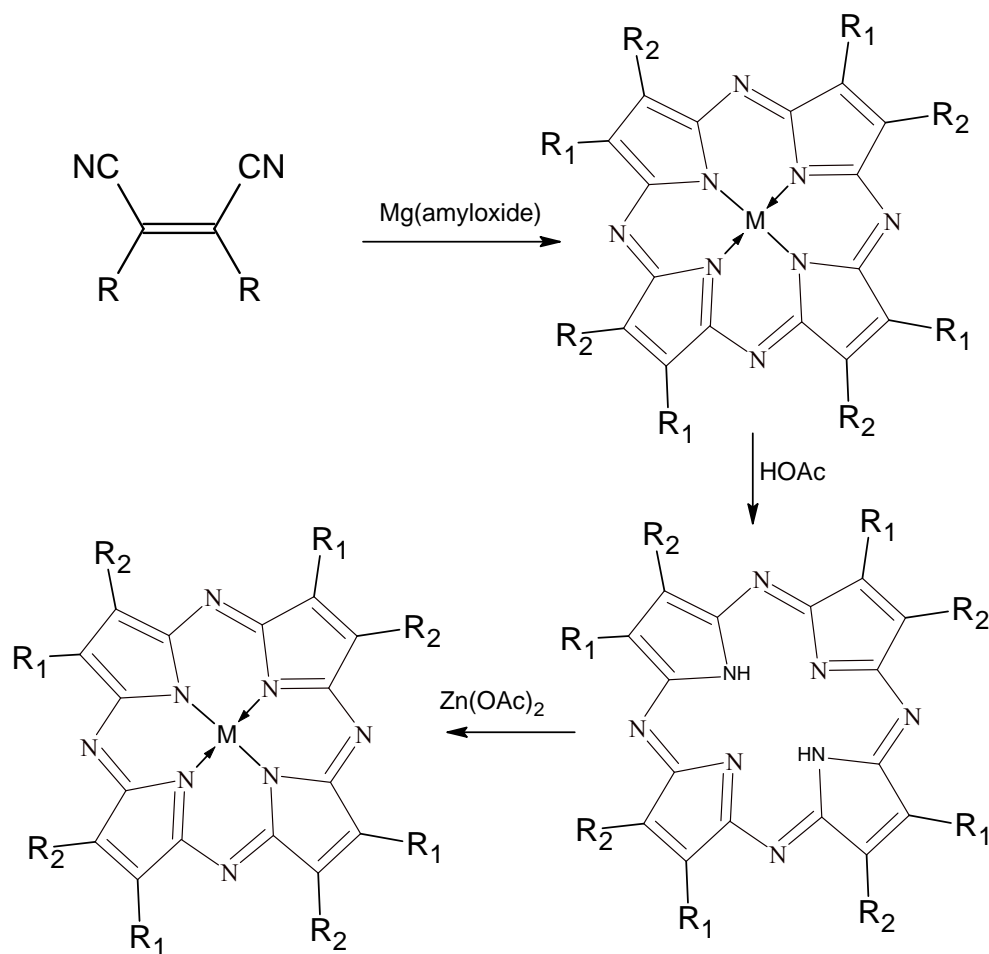


Figure 4.10 Synthesis of cyano and cyano free, and metallo porphyrazines ($R_1 = \text{CN}, \text{H}$, $R_2 = \text{diethylamino}$) [159].

The drug preparation most widely used in current clinical trials is photofrin, a composition which shows a number of well-documented disadvantages such as chemical purity and prolonged skin photosensitivity in patients receiving therapy. However, photofrin has also produced results which suggest that PDT is a very promising treatment modality for the treatment of selected neoplasms. For example, it has been reported by Kato et al that 84% of early stage lung cancers are curable by PDT if the peripheral tumor is less than 2 cm in size and it has not metastasized. For early stage, central type lung cancer, curability increases to 100%. Photofrin is a mixture of monomers and oligomers of ester- or ether-linked hematoporphyrins. The composition of photofrin seems to change with time (specifically the ratio of ester/ether). It thus has to be kept at low temperature and be protected from sunlight. Also its low absorption

(600 nm, $E = 6000$) limits its use to the treatment of superficial tumors, since light at 600 nm does not have sufficient energy to penetrate tissue. There is thus need for compounds which strongly absorb red light (700-800 nm), which would be of greater effectiveness in PDT. Tetraazaporphyrins or porphyrazines (Pzs) mimic porphyrins and phthalocyanines (Figure 1.1), have an important absorption maximum between 250 and 350 nm (Soret), like photofrin in many respects, but in addition they also exhibit strong absorption bands between 710 and 800 nm. Porphyrazines are heterocyclic compounds consisting of four pyrrole nuclei fused via nitrogen bridges and form stable chelates with metal cations. The first tetraazaporphyrin was prepared as the product of the bromination of 3-ethyl-4-methylpyrrole in the presence of ammonia. Tetraazaporphyrin itself was synthesized using a method analogous to that used in the synthesis of phthalocyanines, i.e., treatment of maleonitrile with magnesium n-propyloxide to afford the magnesium tetraazaporphyrin complex in up to 15% yield. Conversion to the free base was achieved by treatment of the metal complex with glacial acetic acid, Magnesium tetraazaporphyrin was also formed in low yield from succinimidine by heating with magnesium formate [160].

4.1.6 Tetracationic Phthalocyanines

In the last few years, phthalocyanines have been intensively studied as photosensitizers for photodynamic cancer therapy [5a, 151]. For this application the most important property of these tetrapyrroles is their solubility in water over a wide pH range. Especially, cationic water-soluble phthalocyanines have some advantages over porphyrins in PDT because of their strong absorbance at long wavelengths of the visible spectrum as well as their high yield triplet states with long lifetimes. Cationic phthalocyanines also represent a large and expanding class of compounds which have applications in biology, catalysis and materials. Novel phthalocyanine compounds which carry 4-pyridylmethoxy groups or N-methyl-4-pyridylmethoxy substituents on the periphery were synthesized by Gül A. and co-workers [161].

The synthetic procedure, started with the synthesis the phthalonitrile derivative, namely 4-(4-pyridylmethoxy)phthalonitrile. It was obtained by base-catalyzed nucleophilic aromatic nitro displacement of 4-nitrophthalonitrile (1) with the -OH function of 4-hydroxymethylpyridine Figure 4.11. Cyclotetramerization of 4-(4-pyridylmethoxy)-

phthalonitrile with anhydrous metal salts (CoCl_2 , $\text{Zn}(\text{CH}_3\text{COO})_2$) and a N-donor base (pyridine or DBU) at $160\text{ }^\circ\text{C}$ in 1-hexanol led to the formation of metallo phthalocyanines Figure 4.12. The synthesis of metal-free phthalocyanine was accomplished in hexanol in the presence of a strong base (DBU) at reflux temperature (Figure 4.12 B). Methylation of the pyridyl groups on the periphery of the zinc phthalocyanine resulted in the tetracationic derivative phthalocyanine (Figure 4.12).

All new compounds were characterized by spectral data and their elemental analyses.

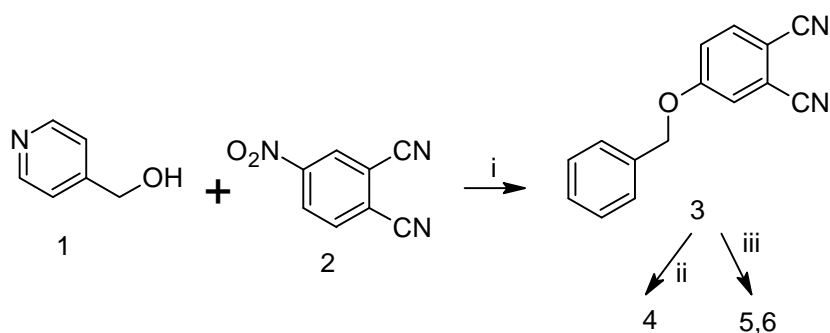


Figure 4.11 Synthesis of Pcs. (i) K_2CO_3 , DMF, $30\text{ }^\circ\text{C}$; (ii) DBU, 1-hexanol, 24 h; (iii) metal salts, 24 h [161].

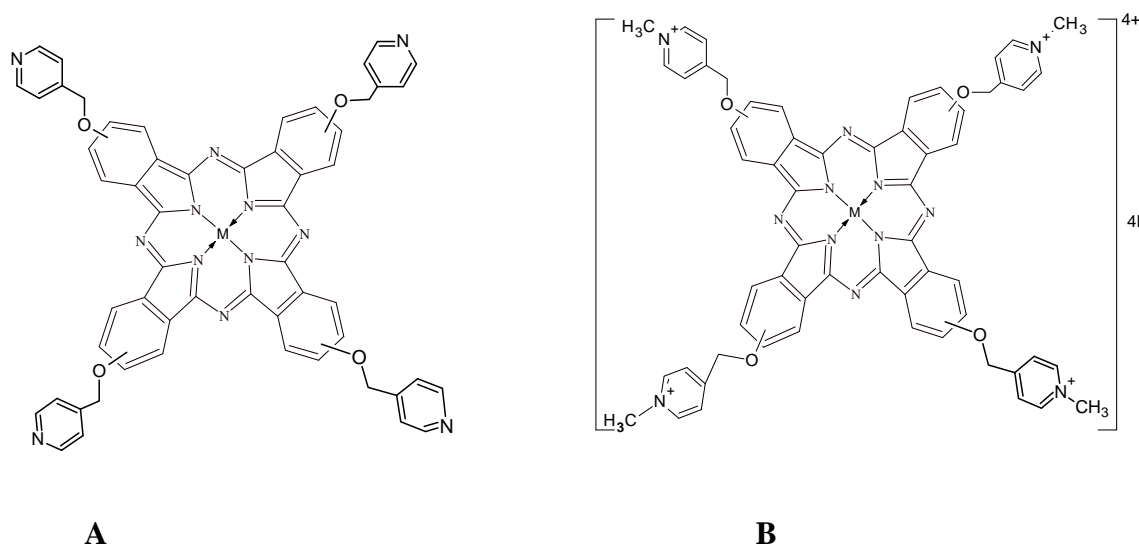


Figure 4.12 A: Phthalocyanines (3-5), **B:** Quaternized Pc (6) [162].

Metal-free and metallophthalocyanines containing four 4-(4-pyridylmethoxy) groups on the periphery have been synthesized and characterized by Karaoglu, H.R.P. et.

al. Pyridyl groups on the periphery of the zinc phthalocyanine have been quaternized to prepare tetracationic derivative. By extension from the interest in the pyridyl phthalocyanines, the new macrocycles are liable to find many applications, as is the case with interactions of similar tetracationic or octacationic tetrapyrrol rings with DNA [161].

4.1.7 Nonanuclear Supramolecular Structures from Simple Modular Units

Octakis(2-hydroxyethylthio)porphyrzinatomagnesium was synthesized as previously reported [162]. Complete esterification of all the –OH groups in **1** with pyridine-4-carboxylic acid (isonicotinic acid) to give octakis(4-pyridoxyethylthio)porphyrzinato magnesium was accomplished in pyridine in the presence of dicyclohexylcarbodiimide and 4-toluenesulfonic acid as catalysts. The coordination of VO(acac)₂ with pyridine donors, [163] the interaction of this reagent with **2** was performed in chloroform. Nonanuclear dark green solid supramolecular product, [VO(acac)₂(4-pyCOOCH₂CH₂S)]₈MgPz (Figure 4.13) was obtained by Öztürk, R. and Gül, A. in high yield (76%) [164]. The proposed structures of the octakis(pyridyl) derivative and the supramolecule [VO(acac)₂(4-pyCOOCH₂CH₂S)]₈MgPz (Figure 4.13) are consistent with their spectral characterization; the vanadium content of [VO(acac)₂(4-pyCOOCH₂CH₂S)]₈MgPz was determined by ICP after decomposition of the product with concentrated HNO₃ and the result closely followed the octa coordination. The visible absorption spectra of octakis(4-pyridoxyethylthio)porphyrzinato magnesium and [VO(acac)₂(4-pyCOOCH₂CH₂S)]₈MgPz in chloroform are similar (Figure 4.13). Since VO(acac)₂ complexes are not expected to have intense absorptions comparable with the B and Q bands of porphyrzines, this result is meaningful. Although the Q bands are known to be extremely sensitive to aggregation of the tetrapyrrole cores, complexation of pyridine units on the periphery has negligible effect in this sense. Coordination of the VO(acac)₂ groups to the pyridine donors on the periphery of diamagnetic octakis(4-pyridoxyethylthio)porphyrzinato magnesium resulted in the paramagnetic supramolecular structure of [VO(acac)₂(4-pyCOOCH₂CH₂S)]₈MgPz. This phenomenon has been followed by the EPR technique. The EPR spectra of **3** in powder form or as a chloroform solution clearly indicated the presence of paramagnetic centers (Figure 4.14) [162].

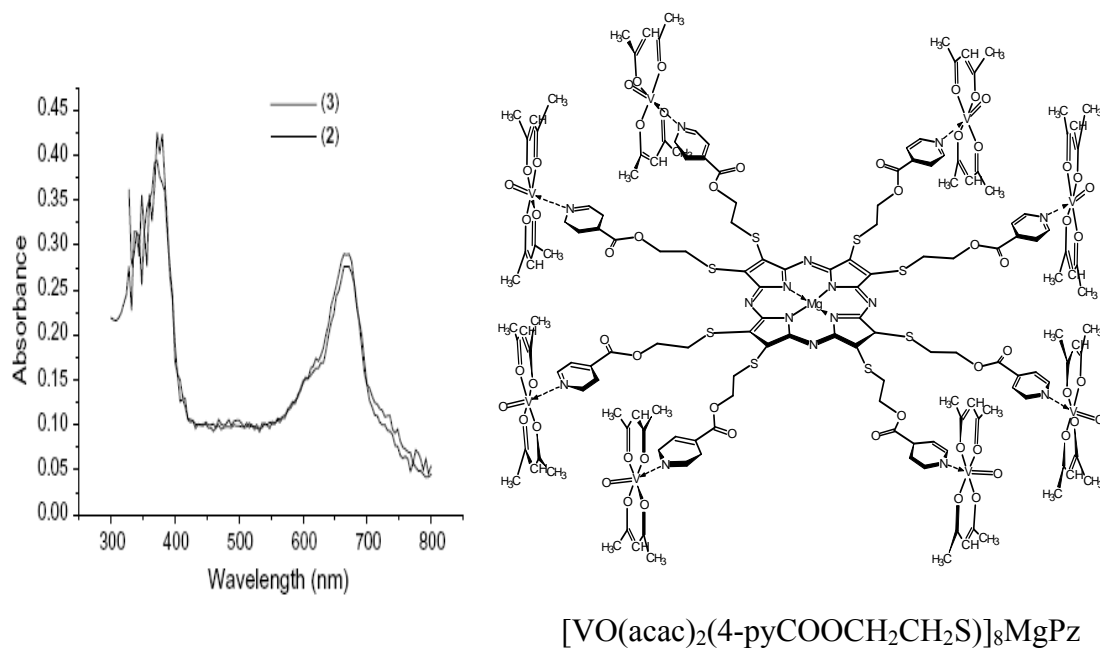


Figure 4.13 Electronic absorption spectra of octakis(4- pyridoxyethylthio)porphyrinato magnesium octakis(4- pyridoxyethylthio)porphyrinato magnesium and $[\text{VO}(\text{acac})_2(4\text{-pyCOOCH}_2\text{CH}_2\text{S})]_8\text{MgPz}$ [164].

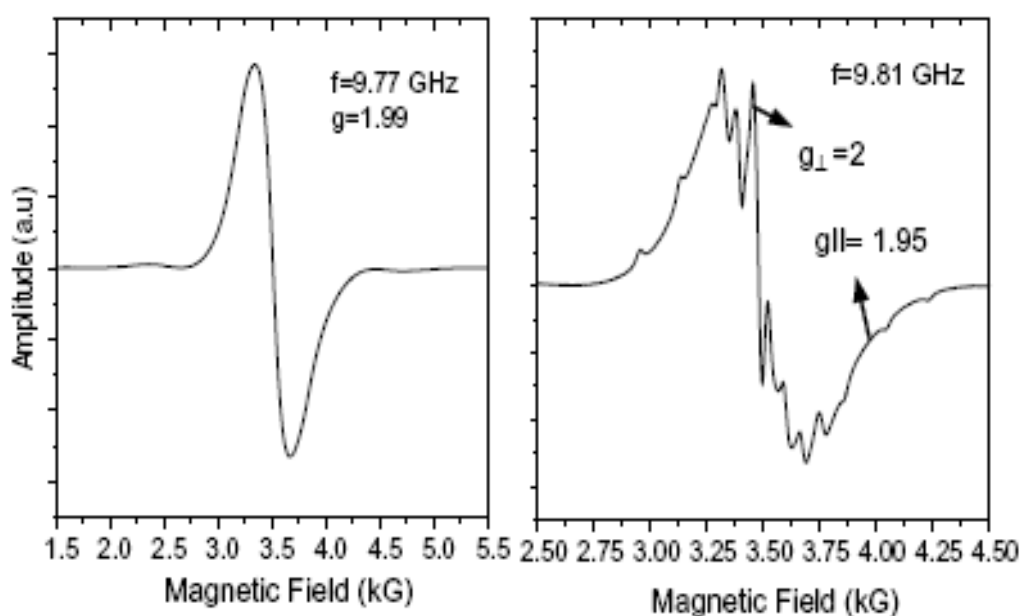


Figure 4.14 X-band EPR spectra of (a) $\text{VO}(\text{acac})_2$ and (b) $[\text{VO}(\text{acac})_2(4\text{-py-COOCH}_2\text{CH}_2\text{S})]_8\text{MgPz}$ in powder form at 300 K [164].

4.1.8 Porphyrazines with Tertiary or Quaternized Aminoethyl Substituents

The addition of bulky substituents on the periphery position of the porphyrazine molecules increases the solubility in apolar solvents, while sulphonium or quaternary ammonium groups lead to water -or polar solvent- soluble derivatives. Novel soluble porphyrazine structures which carry eight 2-dimethyl or 2-trimethylaminoethylthio-substituents on the periphery was prepared by Gül, A and Polat, M. [165]. It is expected that the latter compound will be soluble in water in a wide pH range.

The preparation scheme of Octakis(2-dimethylaminoethylthio)porphyrazinato magnesium (MgPz) and [Octakis(2-trimethylammoniumethylthio)porphyrazinato-magnesium] octaiodide (MgPz) were drawn as in Figure 4.15.

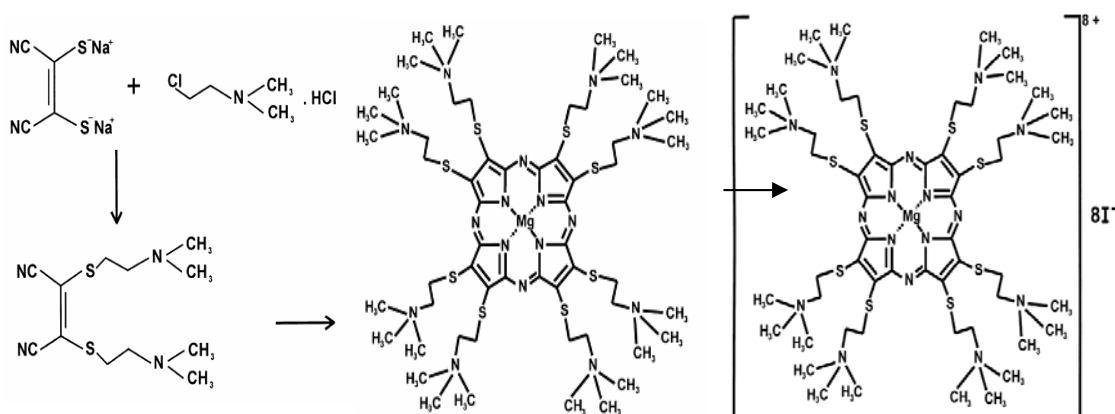


Figure 4.15 Octakis(2-dimethylaminoethylthio)porphyrazinatomagnesium (MgPz) and Octakis(2-trimethylammoniumethylthio)porphyrazinatomagnesium] octaiodide (MgPz) [165].

There is a single Q band absorption in the low energy region and a single B band. These absorptions correspond to $\pi \rightarrow \pi^*$ transition and are observed around 664 ± 675 and 374 ± 379 nm depending on the polarity and donor properties of the solvents (e.g. acetone, ethanol, methanol, DMF, chloroform and pyridine) at concentrations of approximately 10^{-4} M. When water-soluble tetrapyrrole derivatives are required, sulphonium or quaternary ammonium groups are introduced on the periphery.

Peripheral dimethylaminoethyl substituents of MgPz, which lead to solubility in common organic solvents, are extremely suitable for conversion into quaternary ammonium groups by alkylation with alkyl halides such as CH₃I [166]. When MgPz was treated with methyl iodide the hygroscopic porphyrazine with eight quaternary ammonium groups [(MgPz)₈⁺.8I⁻] was obtained (Figure 4.15). There are no major changes in the IR spectrum after quaternization. The electronic spectrum in water exhibits absorption maxima at 660 and 358 nm. In polar organic solvents, there is a slight bathochromic shift, but the extinction coefficients are about twice as high. These changes can be explained by the higher tendency of porphyrazine molecules to aggregate in aqueous solution [167].

4.2 PRINCIPLES OF PHOTO DYNAMIC THERAPY

4.2.1 Photochemotherapy

Photochemotherapy involves the use of visible light or ultraviolet light in clinical medicine. In direct photo chemotherapy, light is used alone, whereas in indirect photochemotherapy, light is used in conjunction with a photosensitisers. Photoradiation therapy (PRT) or photodynamic therapy (PDT) is some of the alternative names used to describe photochemotherapy [168-170]. In this approach visible light is used in combination with light sensitive agents in an oxygen-rich environment. The source of the photons may be an ordinary tungsten lamp, an argon lamp or a laser. A tunable dye laser has the advantage that monochromatic light of a predetermined wavelength can be effectively channeled by way of a fiber optic device into a deeply located tumor [168].

Photodynamic therapy is the indirect treatment of cancer which involves the selective uptake of the photosensitisers in a much higher concentration in tumor tissues than in normal tissues. It is worth noting that, unlike with X-rays, in the absence of photosensitisers the visible light is essentially harmless. Basic photochemical properties of porphyrins which have to do with detecting the tumor cell by fluorescence and destroying them by the photodynamic effect, have been reported [168a].

Photochemotherapy was first reported by a Dane, Niels Finsen, in the 1880s when he showed that a tubercular condition of the skin called *lupus vulgaris* could be treated

by direct photochemotherapy. It was also observed in the early years of the 20th century that certain substances called photodynamic agents could photosensitize mammals which in turn results from the excitation of the electronic ground state (S_0) of the sensitizer when it absorbs light of suitable wavelength, ($S_0 \rightarrow {}^1S^*$). The singlet excited state sensitizer can decay back to the ground state with the release of energy in the form of fluorescence and enable identification of tumor tissue [171-175].

The singlet excited state is short lived (generally less than 1 μ s) and under suitable conditions it undergoes conversion to a longer-lived triplet excited state (${}^3S^*$). This process is known as intersystem crossing, which involves the unpairing of paired electrons in the excited state. Another emission, usually in the near infra-red region, comes from the longer lived excited triplet state of the sensitizer. In fluid solution this emission is usually not observed in organic molecules because the triplet excited state is de-activated in other ways. In the presence of oxygen (3O_2), which is found in most cells, one of these ways involves the transfer of excitation energy from the photosensitiser triplet species to the dioxygen molecule. [172-175]. The electronic energy in the singlet electronic excited state can undergo fast conversion into vibrational energy in the excited singlet state of the sensitizer before intersystem crossing to the triplet excited state [176].

The dioxygen molecule is excited from its triplet ground state to the singlet state dioxygen (1O_2), provided the energy of the triplet excited state of the photosensitiser is higher than that of the singlet excited state dioxygen [168, 177]. There are two types of mechanisms which are thought to be the main path under which singlet excited state oxygen is produced, referred to as Type I and Type II mechanisms [171]. The Type I mechanism involves an hydrogen-atom abstraction or electron-transfer between the excited triplet state of the photosensitiser and a substrate that is either a solvent, another sensitizer or biological substrate to afford free radicals or radical ions that are highly reactive. Free radicals so formed interact with oxygen to generate reactive oxygen species such as superoxide anions or hydroxyl radicals which produce oxidative damage, expressed as biological lesions [173, 178].

The Type II mechanism involves an interaction between the triplet state photosensitiser (${}^3S^*$) and an oxygen molecule to form electronically excited state

singlet state oxygen ($^1\text{O}_2$) which is highly reactive and is responsible for oxidative damage of many biological systems. It is generally accepted that the Type II mechanism predominates during PDT with singlet oxygen responsible in cell damage, while the Type I mechanism becomes more important at low oxygen concentrations or in more polar environments. Figure 4.16 illustrates Type II mechanism [174, 178].

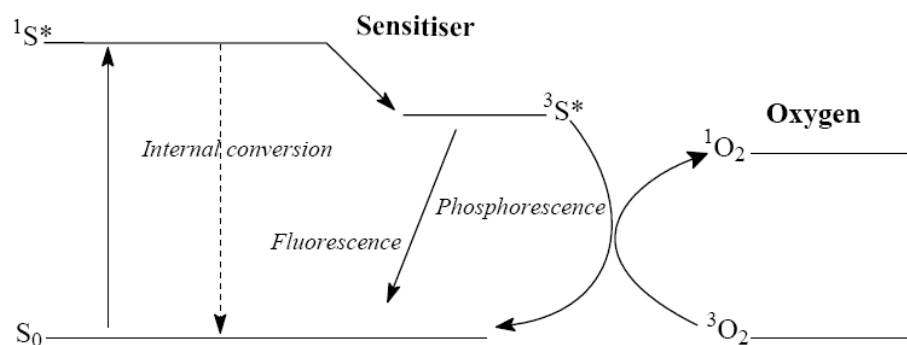


Figure 4.16 Photosensitisation of oxygen via type II mechanism [4].

S_0 - Sensitiser in singlet electronic ground state. $^1S^*$ - Sensitiser in singlet electronic excited state. $^3S^*$ - Sensitiser in triplet electronic excited state. $^3\text{O}_2$ -Oxygen in triplet electronic ground state. $^1\text{O}_2$ - Oxygen in singlet electronic excited state.

The excited singlet state dioxygen is much more toxic and reactive than triplet ground state oxygen, and is known to react with membrane components such as unsaturated lipids, cholesterol and proteins.⁸¹ Therefore just as chlorophyll in plants utilises energy from the sunlight to produce sugars, porphyrins utilizes energy from light to produce toxic oxygen species. In photosensitized tissue such a reaction would be expected to lead to membrane damage and eventually to cell death. It is most important to note that when the excited triplet state photosensitisers transfer electronic energy to ground state $^3\text{O}_2$ it returns back to its singlet ground state. Singlet oxygen formed in this way is generally thought to be the main pathway leading to photonecrosis in sensitized tissue. Thus, there is no chemical transformation of the sensitiser when the singlet state oxygen is generated and the cycle may be repeated upon absorption of another photon. For a single photosensitisers molecule, generation of many times its own concentration of singlet oxygen is possible, which is a very efficient way of photosensitizations, provided there is sufficient oxygen supply. The transfer of energy from the triplet state

of the sensitiser to the triplet oxygen may be so efficient that the yield of the singlet state oxygen may approach the photosensitisers triplet state yield [179, 180].

4.2.2 How to Perform PDT

In a typical treatment of cancer with PDT, the photosensitisers is dissolved in a suitable solvent and intravenously injected to the patient (Figure 4.17) [181].

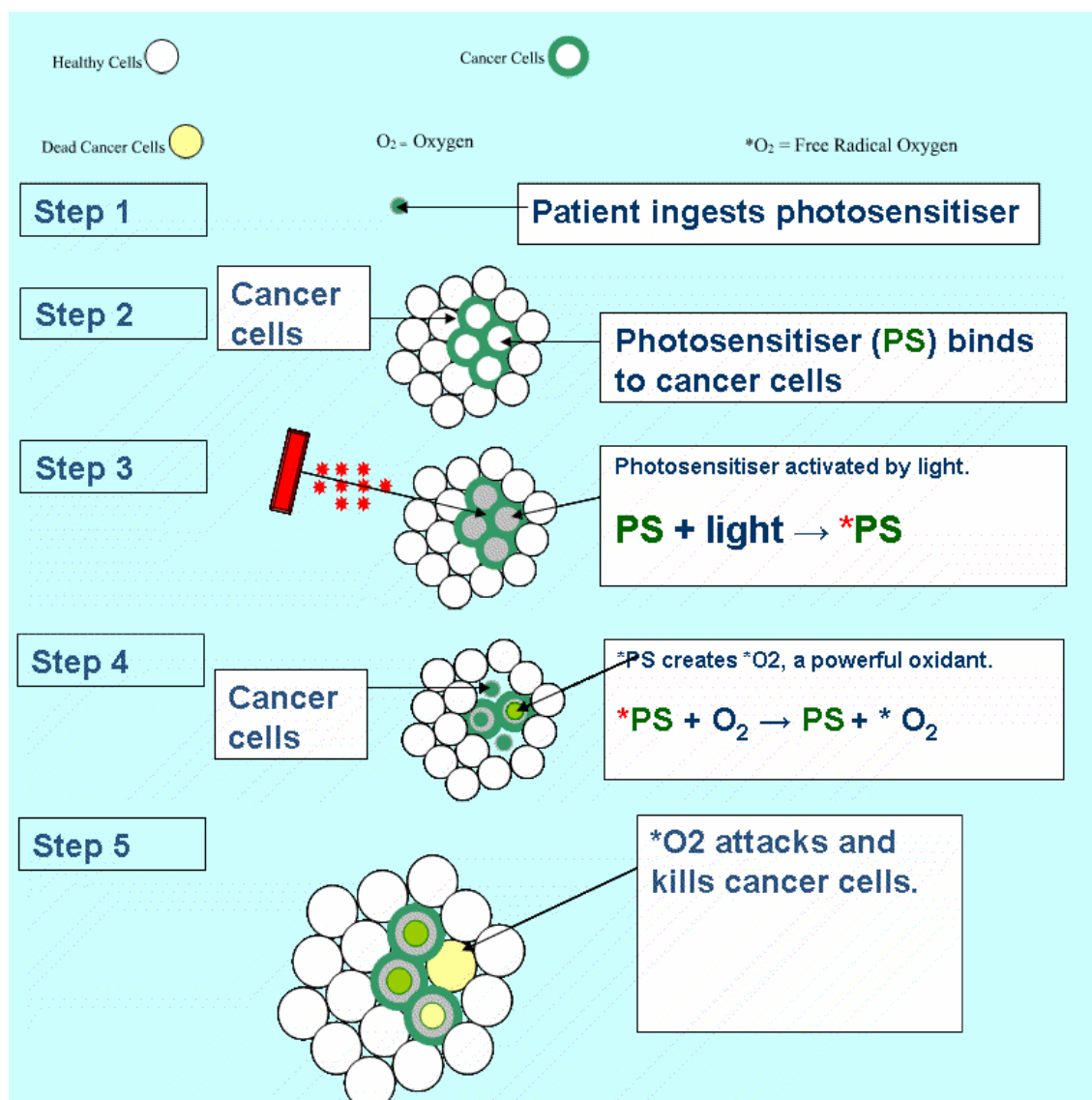


Figure 4.17 How PDT works [182].

The patient is then confined to the dark to allow the photosensitisers to equilibrate (24-72 hours), during which most of the photosensitisers accumulates preferentially in the tumor tissue. The patient is then confined to the dark to allow the photosensitisers to

equilibrate (24-72 hours), during which most of the photosensitisers accumulates preferentially in the tumor tissue. The patient is anaesthetized, and a dose of light is administered using an appropriate light delivery technique, such as an optic fiber from a laser source. Tumor cell destruction begins immediately and a period of time is allowed for the photosensitisers and its metabolites to be eliminated from the body, before the patient is allowed back into the light [181].

4.2.3 Photosensitisers Amphiphilicity in PDT

Below is a schematic representation of the membrane bilayer depicting the two layers (Figure 4.18). The aliphatic portion of the membrane is hydrophobic while the polar portion is hydrophilic. All cellular organelles such as the nucleus, mitochondria, and cytoplasmic reticulum are surrounded by a cell membrane. Entry of extra cellular substances into the cell and into all intracellular organelles is controlled by such membranes.

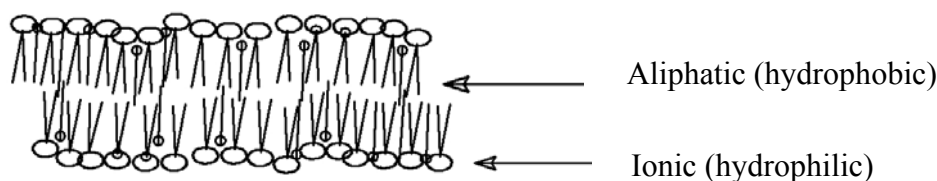


Figure 4.18 Schematic representation of membrane layer [4].

The dissolved photosensitisers are transported by the blood or plasma fluid to the tumor cells. Before reaching the target cells, it passes through the different cell environments, a hydrophobic environment in the cell membrane and a hydrophilic environment in the cytoplasm. Blood is mostly composed of water, so for the photosensitisers to be transported by the blood it must be hydrophilic. However, for the photosensitisers to reach the affected cells, it must also be hydrophobic so that it can pass easily through the various cell membranes. Hence good photosensitisers must possess sufficient hydrophilicity to be transported easily through the blood and enough hydrophobicity to cross the various membranes.

If the photosensitisers are too hydrophobic, it will not be excreted from the body and will persist in the tissues. For excretion and elimination, it must be hydrophilic.

Studies have shown that hydrophobic photosensitisers take a long time to be excreted out of the body. Consequently, there is a high risk for the patient since a long period is needed for the patient to be in the dark so as to prevent general photosensitivity, while the drug is being cleared from the body. Ideally the photosensitisers needs to possess equal hydrophilicity and hydrophobicity since it needs to pass through both hydrophilic and hydrophobic environments before and after reaching the target cells [4].

If the photosensitisers are too hydrophilic, much of it will not reach the tumor cells leaving many affected cells having no photosensitisers or with only very low concentrations thereof. This leads to incomplete death of tumor cells since most of the photosensitisers passes out of the body before reaching the target cells, resulting in a small amount of the drug that accumulates in tumor tissue. Much more of the photosensitisers will accumulate in tumor tissue if it is hydrophobic.

This is the guiding principle that provides chemists with the most difficult problem since they need to ensure that the drug chromophore has the desired long-wavelength of absorption. A red shift or bathochromic effect is a shift of an absorption maximum towards longer wavelength. It may be produced by the change in the medium or by a substituent in the chromophore which leads to the red shift.⁹¹ Hydrophilic environments tend to cause red shifts [4].

Red shift has been achieved either by expanding the macrocycle to produce phthalocyanines, texaphyrins, peripherally chromophore functionalised porphyrines, porphyrin vinylogues etc; or by reducing one or more of the porphyrin's pyrrole rings to give chlorins. Another way of red-shifting and intensifying the long wavelength absorption band of the photosensitisers is to extend the macrocycle conjugation, e.g. with ethynyl groups. The net effect is to give these compounds a green color, compared to the usual purple-red color [4].

These strategies cause a red shift and an increase in the intensity of the long wavelength absorption of the chromophore. In the red region there is the deepest tissue penetration of light, enabling the light to reach even the deepest cells. Since the tumors can be quite deep, red absorption of the photosensitisers is therefore needed for the light to effect maximum damage to cancerous tissue [4].

4.2.4 Singlet Oxygen Yields

Since singlet oxygen is important in cell destruction by PDT, substantial amounts are needed to maximize tumor cell destruction. The more singlet oxygen produced, the more tumor cells will be destroyed. If the photosensitiser is hydrophilic, much of it will reach the tumor cells resulting in increased production of singlet oxygen. Furthermore, the higher the hydrophilicity of the photosensitiser, the more it will be absorbed in hydroxylic environments where there is a higher concentration of triplet oxygen. Thus there will be an increase in the contact between the photosensitiser and triplet ground oxygen.

Singlet oxygen yield is related to triplet quantum yield of the sensitiser, the lifetime of the triplet quantum yield, the efficiency of energy transfer from the excited triplet state to the ground state oxygen and the ability of the substituents to quench singlet oxygen. It is expected that the higher the triplet quantum yield with efficient energy transfer, the higher the singlet oxygen yield. If there is inefficient quenching of the triplet state by the ground state oxygen, less singlet excited oxygen is formed. Also the longer the lifetime of the triplet state, the higher the amount of singlet oxygen that might be produced since there will be less of the triplet excited state which might be converted back to the ground state. The ground state oxygen to be excited must be sufficient enough in order to have large amount of singlet oxygen produced [183-185].

4.2.5 Development of Photosensitisers

Haematoporphyrin derivative and photofrin, both complex mixtures of compounds represent the first-generation of photosensitisers. Second-generation photosensitisers on the other hand are pure single compounds that exhibit photosensitization properties and they include a number of porphyrins and phthalocyanines derivatives. During the early years in the development of photosensitisers for PDT, certain design criteria for a good photosensitiser became apparent [168, 171]. These can be summarized as follows:

- Lack of toxicity in the dark.
- Selective uptake by tumor tissue.
- Short-term retention to avoid the persistence of photosensitivity.
- Triplet energy greater than 94 kJ/mol.
- Intermediate lipid water partition coefficient.

-Single substance.

-Light absorption in the red or far red range of the visible spectrum.

The substances that meet these criteria include suitably modified porphyrins, chlorins, porphyrazines [186-191] and phthalocyanines. So far, many photosensitisers have been synthesized and tested; some of them show little or no activity in photo necrosis, sometimes poisonous. But these efforts have not been wasted, for they have provided the basis for the above design criteria and will continue to do so.

4.2.6 Porphyrin, Porphyrazine and Phthalocyanines as Photosynthesizers

Porphyrins were among the first group of compounds to be used as photodynamic therapy agents. Many of the second generation porphyrins are now in clinical trials for different tumor lesions in different locations. They have improved tumor cell concentration compared to normal cells and also have improved fluid solubility and deep tissue penetration.

Porphyrazine derivatives are showing to be potential candidates as photosensitisers in photodynamic therapy. Recent photophysical studies of some zinc metalated peripherally substituted porphyrazines have shown high triplet quantum yields which are coupled with high oxygen quantum yields. They also absorb strongly in the red region which also makes them capable of deep tissue penetration and their biomedical application will soon be elaborated [187-191].

Phthalocyanines and their derivatives have shown great promise in PDT. They are porphyrin-like second-generation sensitizers for photodynamic therapy [187, 191]. The most important attribute that makes phthalocyanines suitable for PDT is the intense absorption in the far red and long-lived excited triplet state [4].

During the past few years, a large number of new sensitizers have been suggested for clinical use, on the basis of experimental studies in animal or in cell cultures. There are several uncertainties and considerable expense related to bringing new agents to the clinic, and these account for the slow incorporation of new sensitizers into medical practice. While adverse reactions are often considered to be of less than major importance in conventional drug therapy of life-threatening disease, PDT will be applied generally to early lesions with curative intent. The occurrence of unexpected

toxicity could seriously impair future trials. A major stumbling block to the use of PDT in the removal of tumor cells is the lack of suitable photosensitisers that can accumulate selectively to the tumor cells and destroy them leaving normal cells unaffected after illumination with light. Although photosensitisers that can accumulate selectively to the tumor cells have been discovered, their major limitation is that they are activated with wavelengths of light that are not capable of penetrating deeply through tissues or blood. Other important limitations of current photosensitisers include the difficulty in the functionalisation and purification of the functionalized compounds. Photosensitisers are generally water insoluble, but they can be made to be water-soluble by functionalisation with hydrophilic groups. Excretion from the body is also one of the most important limitations in the use of photosensitisers. Many that have been synthesized are removed very slowly from the body and therefore cause skin phototoxicity when the patient comes in contact with light. Delayed excretion results, in the patient being forced to stay in the dark for long periods of time to give a sufficient period for the photosensitisers to remove from the normal tissue.

PDT is advantageous over standard therapy since it is not painful and is noninvasive. PDT also has the ability to treat multiple lesions at one sitting, good patient acceptance, excellent cosmetic results and apparent lack of major side effects. Acute effects caused by singlet oxygen include severe damage to various cell membranes including plasma, mitochondrial, lysosomal, endoplasmic reticulum, and nuclear membranes; inhibition of enzymes, including mitochondrial, DNA repair and lysosomal enzymes; and inactivation of membrane transport systems. The diseased tissue in which the photosensitisers is localized should preferably be destroyed with either little or no damage to surrounding normal tissue.

Cancer consists of large group of diseases resulting from uncontrolled proliferation of cells. These diseases can originate in almost any tissue of the body. Symptoms and signs of cancer depend on many factors including the location of the tumors, rate of growth, tendency to invade and divide, and some other individual conditions of patients. The most common cancers originate and spread within the chest, abdomen, or pelvis. These sites are difficult to treat because of the close positioning of many overlapping organs. Continued cell division leads to the formation of tumors that invade normal tissues and organs. In many cases, the cancer cells become dislodged and

spread to other locations within the body where they then take up residence and grow, forming secondary tumors. In these situations, the cancer is frequently advanced and not curable by current approaches.

Several new second-generation photosensitisers are now in clinical trials and are showing promising results since their treatment times, typical light and drug doses are smaller than for HpD. Viewed against photofrin, the new second-generation sensitiser, plus ALA-PDT, are beginning to prove their worth. An important factor with new sensitiser is their ability to enhance selectivity of tumor damage at lower doses of the sensitiser. Whether photosensitivity is an important issue depends on the treatment. In treatment of lethal tumors, it doesn't matter how photosensitive patients become: the priority is to ensure maximum tumor destruction. Today, only a purified form of hematoporphyrin derivative is in therapy, but is not efficient enough for tumor treatment, however, it can be used to treat tumor cells at an early stage. The main disadvantage of Photofrin is its unknown composition for it is still composed of a mixture of porphyrins. Therefore, the synthesis of photosensitisers in which there is certainly regarding the structure and purity thereof is of great importance for the development of new photosensitisers [4].

One of the requirements of new photosensitisers is water solubility, while selective uptake of the photosensitisers by the tumor cells versus healthy tissue is also important. This requires that photosensitisers should be soluble in body fluid and be more concentrated in tumor cells [171]. Although some second generation photosensitisers are water soluble and are less toxic, there is still some problem with selective uptake of the photosensitisers by the tumor cells compared to normal cells.

As a potential solution, synthesis of phosphonic acid substituted porphyrazines is of great interest for cellular recognition and water solubility. A specific objective of this study was to synthesize porphyrazines with phosphonic acid as peripheral substituents. This will be addressed by the development of technology in which phosphonic acid-functionalized porphyrazines will be produced from the corresponding phosphonate ester-substituted maleonitriles.

CHAPTER 5

EXPERIMENTAL PART

5.1 CHEMICALS AND APPARATUS

Sodium cyanide (NaCN), magnesium granules, Copper(II) acetate ($\text{Cu}(\text{OAc})_2$), cobalt (II) acetate ($\text{Co}(\text{OAc})_2$), Vanadyl sulphate pentahydrate ($\text{VOSO}_4 \cdot 5\text{H}_2\text{O}$), Carbon disulfide (CS_2), dimethylformamide (DMF), dimethylsulfoxide (DMSO), diethyl 2-bromoethylphosphonate ($\text{BrCH}_2\text{CH}_2\text{P}(\text{OCH}_2\text{CH}_3)_2$), trifluoroacetic acid (TFA), chloroform (CHCl_3), n-hexane ($\text{CH}_3(\text{CH}_2)_4\text{CH}_3$), dichloromethane (CH_2Cl_2), diethyl ether ($\text{CH}_3\text{CH}_2\text{OCH}_2\text{CH}_3$), Sodium sulphate (Na_2SO_4), ammonia (NH_3), methanol (CH_3OH), Ethanol ($\text{CH}_3\text{CH}_2\text{OH}$), Propanol ($\text{CH}_3\text{CH}_2\text{CH}_2\text{OH}$)

5.2 INSTRUMENTATIONS

^1H NMR and ^{13}C NMR spectra were recorded on a NMR using an Inova 500 MHz Varian system spectrometer for solutions in CDCl_3 . Multiplicities were described using the following abbreviations: s=singlet, d=doublet, t=triplet, q=quartet, m=multiplet and br=broad. FT-IR spectra were recorded on Mattson Satellite spectrophotometer in the range of $400\text{-}4000\text{ cm}^{-1}$ (abbreviations: m, s, br and w). UV-visible spectra were recorded by UNICAM between the 300-800 nm in the related solvents. FAB-MS spectra were recorded by the laboratory FAB-MS spectrophotometer of KATU (Blacksea Technical University). Elemental analyses were done by laboratory of Research & Development-Training Center of Middle East Technical University (METU) Central Laboratory.

5.3 SYNTHESIS OF PORPHYRAZINE

5.3.1 Synthesis of Dithiomaleonitrile Disodium Salt (1)

11 g (0.234mol) dry and powder NaCN was stirred in 70 mL of DMF around 10 minutes. 14.11 mL (0.234 mol) CS₂ was added into that solution drop wise with stirring in ice bath for 10 minutes. Dark brown solution was stirred for extra 10 minutes and diluted to 200 mL with isobutanol and heated until all of the contents were dissolved in solvent. The solution was filtered with vacuum filtration to remove unreacted NaCN while solution was hot. Then solution was left to cool and crystallize. Needle type brown crystals was formed and filtered by vacuum filtration. The crystals were washed with diethyl ether and dried in hood.

The obtained needle type brown crystals were dissolved in 100 ml of chloroform and the dark brown solution was filtered. The solution was left to stand for 4-5 days and precipitation occurred. The precipitate having the product and sulphur was filtered and dried. Then it was dissolved in minimum methanol that can only dissolve the product and diethyl ether was added for crystallization of the product. Yellowish crystals were filtered and washed with ether and left to dry. The product was soluble in methanol, ethanol and water and insoluble in diethyl ether, chloroform and benzene. The disodium dithiomaleonitrile salt was characterized with FT-IR (Appendix A).

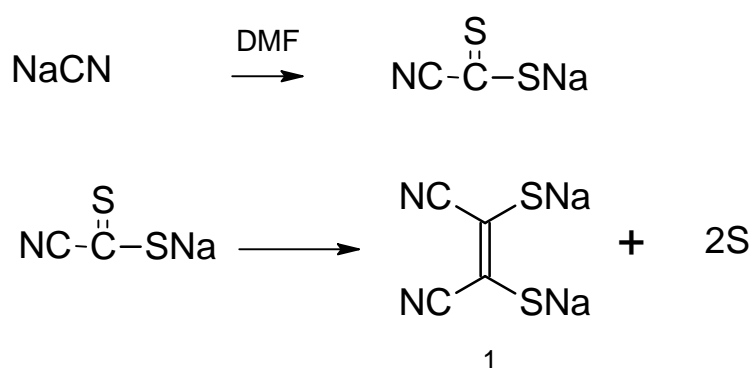


Figure 5.1 Synthesis of dithiomaleonitrile disodium salt.

5.3.2 Synthesis of 1,2-Bis{2-(diethyl phosphonate)ethylthio} Maleonitrile (2)

2 g (0.07mol) dry dithiomaleonitrile disodium salt **1** and 5 g (0.0204mol) diethyl 2-bromoethylphosphonate were stirred for 5 days at room temperature in ethanol. The reaction was monitored by TLC. After the evaporation of solvent, the NaBr crystals and oily product of 1,2-Bis{2-(diethyl phosphonate) ethylthio} maleonitrile **2** was synthesized. The 1,2-Bis{2-(diethyl phosphonate) ethylthio} maleonitrile was extracted from NaBr salt with chloroform. Chloroform was evaporated with rotary evaporator. And the product was washed with diethyl ether. After diethyl ether was removed, 3.785 g product was obtained. The product was soluble in chloroform, ethanol, diethyl ether and in common organic solvents but insoluble in water. The yield was 77%. FT-IR (KBr): 2983 cm^{-1} , 2910 cm^{-1} , 2208 cm^{-1} , 1641 cm^{-1} , 1392 cm^{-1} , 1300 cm^{-1} , 1240 cm^{-1} , 1024 cm^{-1} , 968 cm^{-1} . ^1H NMR (CDCl_3 , δ , ppm) 1.3 (t, 12H), δ 4.082 (q, 8H), δ 3.284 (t, 4H), δ 2.373 (t, 4H). ^{13}C NMR (CDCl_3 , δ , ppm) 16.638 (CCH₃), 62.32 (OCH₂), 24.01 (SCH₂), 30.419 (PCH₂). ^{31}P NMR (CDCl_3 , δ , ppm) 26.5 and 26.8 (P). UV-visible (CHCl_3): 368, 668 nm; FAB-MS for $\text{C}_{16}\text{H}_{28}\text{N}_2\text{O}_6\text{P}_2\text{S}_2$; (M+1) 471. Elemental analysis: C 35.2, H 5.62, N 3.96, S 9.23; Calculated: C 40.85, H 5.96, N 5.96, S 6.80. FT-IR, ^1H NMR, ^{13}C NMR, ^{31}P NMR and FAB-MS spectra were given in Appendices B, C, D, E and F, respectively.

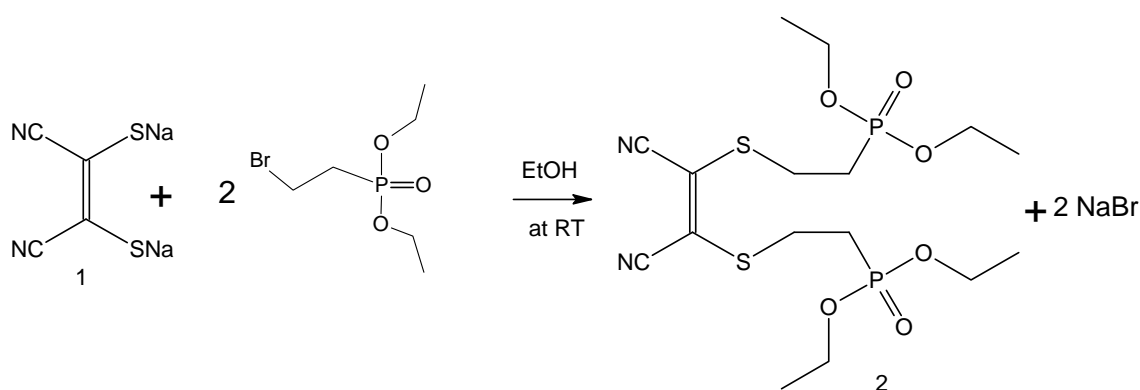


Figure 5.2 Synthesis of 1,2-Bis{2-(diethylphosphonate)ethylthio} maleonitrile ligand 2.

5.3.3 Synthesis of Magnesium Octakis(2-(diethylphosphonate)ethylthio(3a) or Magnesium Octakis(2-(dpropylphosphonate)ethylthio (3b) Porphyrazines

102 mg (0.5 mmol) magnesium and a small crystal of iodine were refluxed in 20 ml n-propanol for overnight. The cloudy solution of magnesium propanolate was prepared.

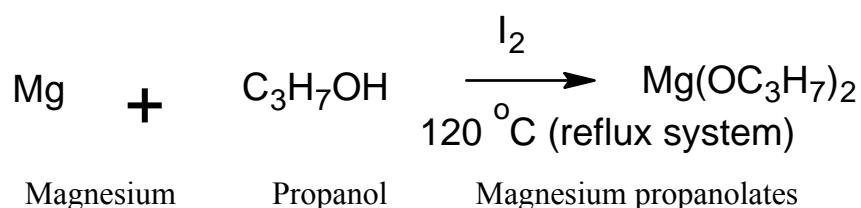


Figure 5.3 Preparation of magnesium propanolates.

500 mg (1.063 mmol) of 1,2-Bis{2-(diethyl phosphonate) ethylthio} maleonitrile **2** was added into boiling while magnesium propanolate. When 1,2-Bis{2-(diethyl phosphonate) ethylthio} maleonitrile **2** was added; the color of solution turn yellowish to brown and after several hours the color change from brownish to dark blue. To be completed the reaction; reaction was continued overnight. Then the solution was taken and filtered immediately while it was hot with vacuum filtration. After vacuum evaporation the solvent, the viscous dark blue porphyrazine was obtained. The resultant product was taken into chloroform phase. After removing the solvent the crude porphyrazine was extracted with hexane. Finally, two porphyrazines, one with hexane soluble, the other with hexane insoluble were obtained. Both porphyrazines were good soluble in chloroform, ethanol, dichloromethane and methanol. FT-IR (KBr, cm^{-1}): 2965, 2877, 1635, 1461, 1248, 1067, 997, ^1H NMR (CDCl_3 , δ , ppm): 0,873 (t, 48H), 1.59(m, 32H), 1.59 (t, 16H), 3.3 (t, 16H), 3.85 (t, 32H). ^{13}C NMR (CDCl_3 , δ , ppm): 9.09 (CH_3), 14.67 (SCH_2), 21.81 (CH_2), 22.87 (PCH_2), 71.6 (OCH_2), ^{31}P NMR (CDCl_3 , δ , ppm): 29.82; UV-visible (CHCl_3 , λ_{max}): 368 and 668 nm; FAB-MS: $\text{C}_{80}\text{H}_{144}\text{MgN}_8\text{O}_{24}\text{P}_8\text{S}_8$: (M+1) 2133; Elemental analysis: found; C 50.36, H 8.65, N 1.33, S 3.3, calculated; C 40.5, H 18, N 5.25, S 12.0. FAB-MS: $\text{C}_{64}\text{H}_{112}\text{MgN}_8\text{O}_{24}\text{P}_8\text{S}_8$; (M+1) 1908. UV-visible, FT-IR, ^1H NMR, ^{13}C NMR, ^{31}P NMR and FAB-MS spectra were given in Appendices G, H, L I, J, K, and N respectively for propyl ester of

porphyrazine (3b). UV-visible, FT-IR and FAB-MS spectra were given in Appendices L and M for ethyl ester of porphyrazine (3a).

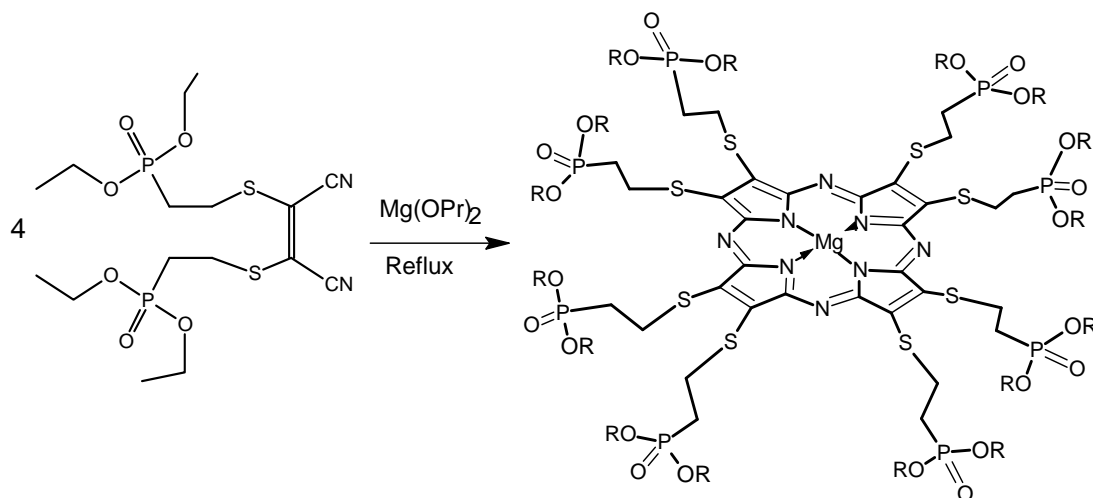


Figure 5.4 The synthesis of magnesium octakis(2-(diethylphosphonate)ethylthio porphyrazine (MgPzs) R: C_2H_5 (3a), C_3H_7 (3b).

5.3.4 Synthesis of Metal Free Octakis(2-(dpropylphosphonate)ethylthio Porphyrazine (4)

150 mg (0.07 mmol) MgPz **3b** (propyl ester) was stirred in 2 mL TFA (trifluoroacetic acid) at room temperature for 4-5 hours in a closed tube. Then, it was dropped on ice and neutralized with 6 M NH_3 solution. Then the product was washed with several times with water, and it was taken into chloroform phase. The chloroform was evaporated. Purple colored porphyrazine was obtained.

The same procedure was applied to the ethyl ester of porphyrazine. The purple colored metal free porphyrazine was obtained. The yield was 50%. FT-IR (KBr, cm^{-1}): 3292, 2955, 2925, 2867, 1722, 1456, 1296, 1228, 1136, 997, 740. ^1H NMR (CDCl_3 , δ , ppm): 0.981 (t, 48H), 1.708 (m, 32H), 4.13 (t, 32H), 2.88 (t, 32H) 2. (t, 16H). ^{13}C NMR (CDCl_3 , δ , ppm): 10.26 (CH_3), 23.7 (CH_2), 67.3 (OCH_2), 15.9 (SCH_2), 26.7 (PCH_2). ^{31}P NMR (CDCl_3 , δ , ppm): UV-visible (CHCl_3 , λ_{max}): 352, 632 and 708 nm. UV-visible,

FT-IR, ^1H NMR, and ^{13}C NMR, spectra were given in Appendices O, P, Q, and R respectively.

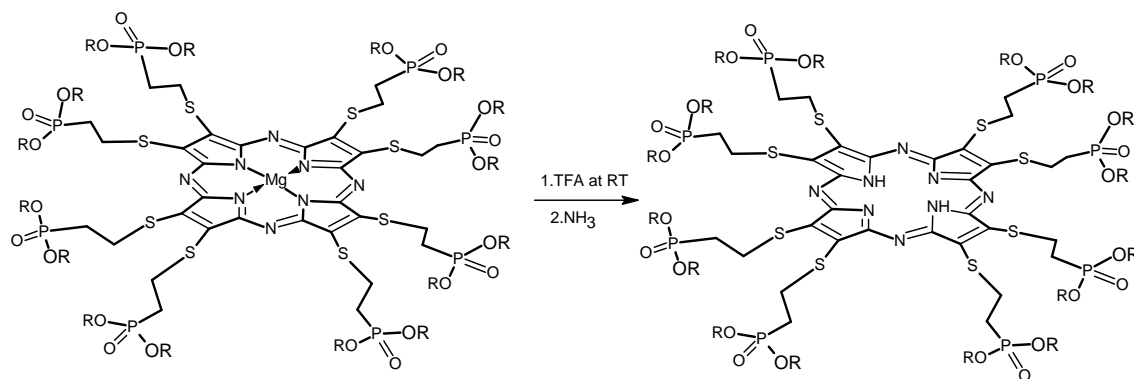


Figure 5.5 Synthesis of metal free porphyrazine (H_2Pz) **4**, R: C_2H_5 or C_3H_7 .

5.3.5 Dealkylation of Phosphonate Esters of MgPz with TMSBr (5)

135 mg (0.06 mmol) porphyrazine 3b was dissolved in 15 mL dichloromethane and 122.4 mg (0.8 mmol) bromotrimethyl silane (TMSBr) was added on porphyrazine solution. The solution was mixed at 40°C for 6 hours. Then dichloromethane was evaporated with rotary evaporator and then methanol- water mixture (90:10) was added and stirred for 2 hours at room temperature. Methanol was evaporated at rotary evaporator. Water insoluble product was washed several times with water and extracted with dichloromethane. The color of the product was purple. The yield was 40%. FT-IR (KBr , cm^{-1}): 2965-2875, 1642, 1521, 1186, 1067, 846. UV-visible (CHCl_3 , λ_{max}): 362, 638 and 706 nm; ^1H NMR (CDCl_3 , δ , ppm): 1.6 (t, 16H), 3.5 (t, 16H); ^{13}C NMR (CDCl_3 , δ , ppm): δ 14-16 (PCH_2), 30-32 (SCH_2), 141 ($\text{C}=\text{C}$). UV-visible, FT-IR, ^1H NMR, and ^{13}C NMR, spectra were given in Appendices S, T, U, and W respectively.

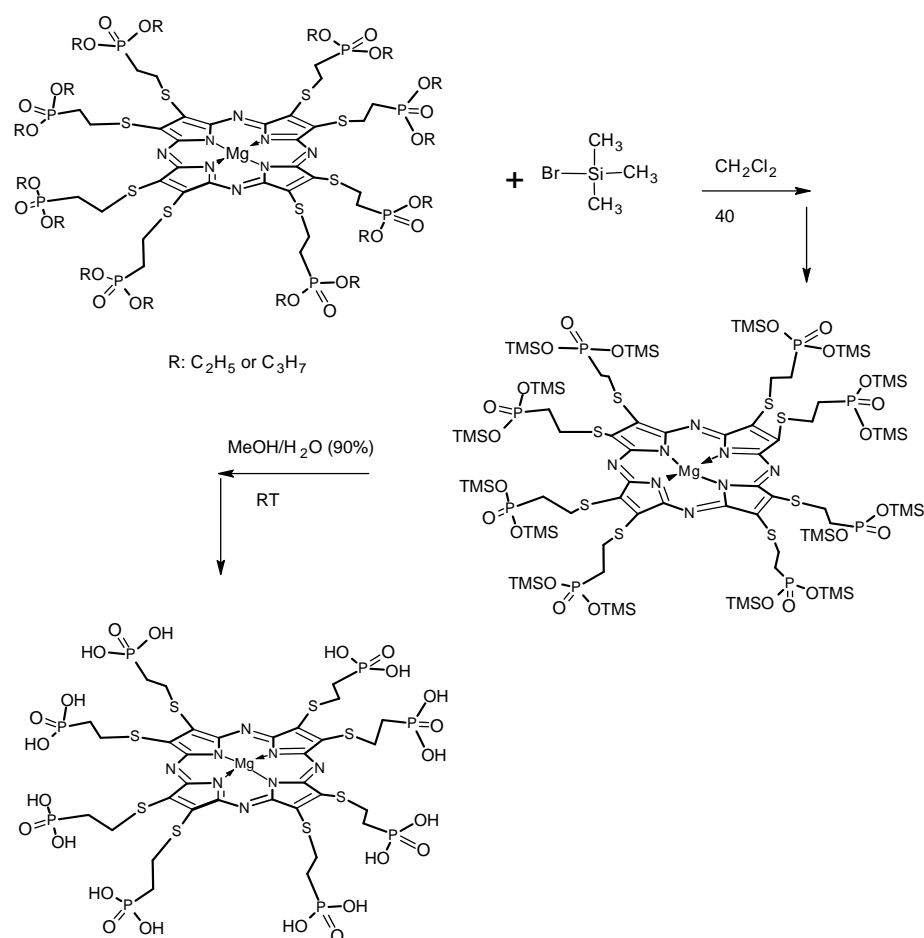


Figure 5.6 Synthesis of phosphonic acid substituted porphyrazine **5**.

5.3.6 Synthesis of Metal Complexes of Octakis(2-(diethylphosphonate)ethylthio) Porphyrazines

5.3.6.1 Synthesis of Co (II) Porphyrazine

40 (0,021 mmol) mg metal free porphyrazine is dissolved in 15 mL chloroform and (0.084mmol) 20 mg Co(OAc)₂.H₂O was dissolved in 1 mL ethanol and added porphyrazine solution and refluxed under nitrogen for overnight. The color of metal free porphyrazine solution changed from purple to green. The solvent was evaporated and product was characterized with UV-visible and FT-IR. The yield was around 40%. FT-IR (KBr, cm⁻¹): 2925-2852, 1722, 1457, 1236, 1060, 1004, 752. UV-visible (CHCl₃, λ_{max}): 336, 640 nm. The UV- visible and FT-IR spectra were given Appendix X and Y, respectively.

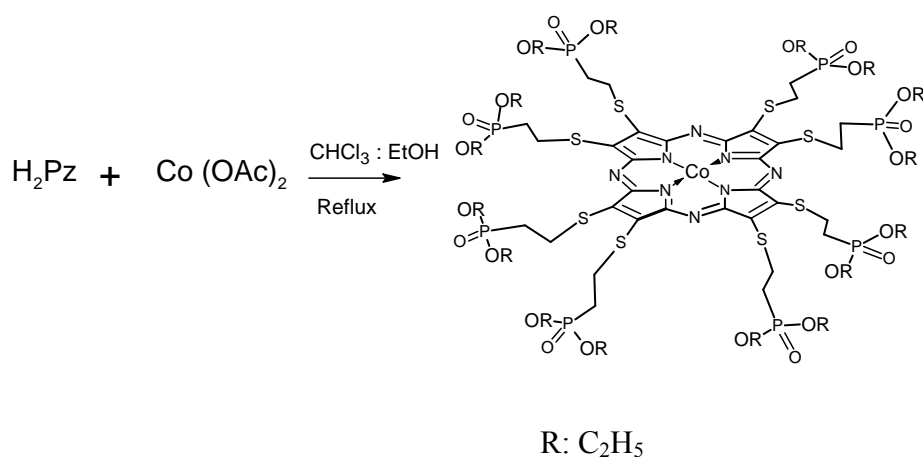


Figure 5.7 Synthesis of Co(II)Pz.

5.3.6.2 Synthesis of Cu (II) Porphyrazine

40 (0,021 mmol) mg metal free porphyrazine is dissolved in chloroform and (0.084 mmol) 17 mg Cu(OAc)₂.H₂O was dissolved in chloroform by heating and added porphyrazine solution and reaction was left at reflux under nitrogen overnight. The color of metal free porphyrazine solution changed from purple to dark blue. The solvent was evaporated and product was characterized with UV-visible and FT-IR. The yield was around 40%. FT-IR (KBr, cm⁻¹): 2966-2856, 1722, 1459, 1240, 1112, 1000, 755. UV-visible (CHCl₃, λ_{max}): 336 and 664 nm. The UV- visible and FT-IR spectra were given Appendix X and Y respectively.

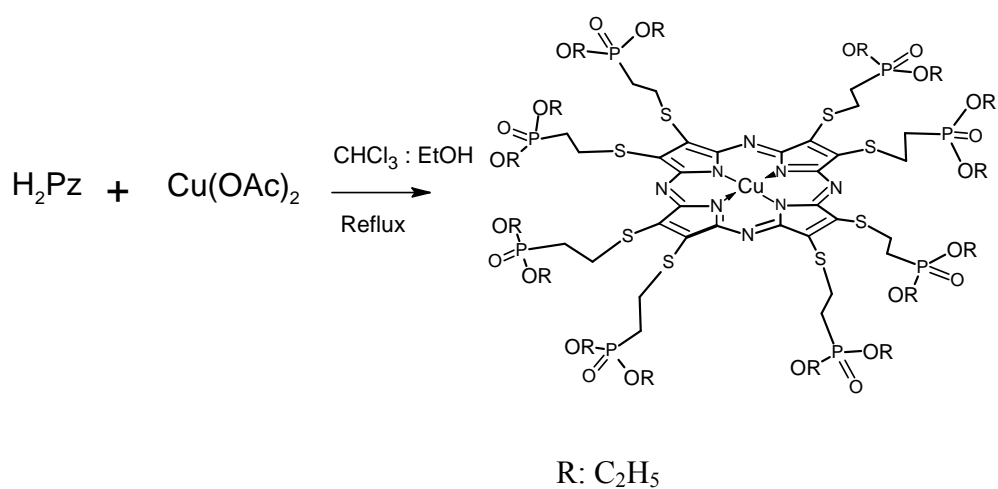


Figure 5.8 Synthesis of Cu(II)Pz.

5.3.6.3 Synthesis of (VO)²⁺ Porphyrazine

40 mg (0,019 mmol) metal free porphyrazine was dissolved in 15 mL chloroform and 20 mg (0.084mmol) VOSO₄.5H₂O is dissolved in 1 mL ethanol and added porphyrazine solution and refluxed under nitrogen for overnight. The color of metal free porphyrazine solution changed from purple to green. The solvent was evaporated and product was characterized with UV-visible and FT-IR. The yield was around 40%. FT-IR (KBr, cm⁻¹): 2923, 2852, 1740, 1464, 1263, 1115-1012, 750. UV-visible (CHCl₃, λ_{max}): 336 and 664 nm. The UV- visible and FT-IR spectra were given Appendix Z.

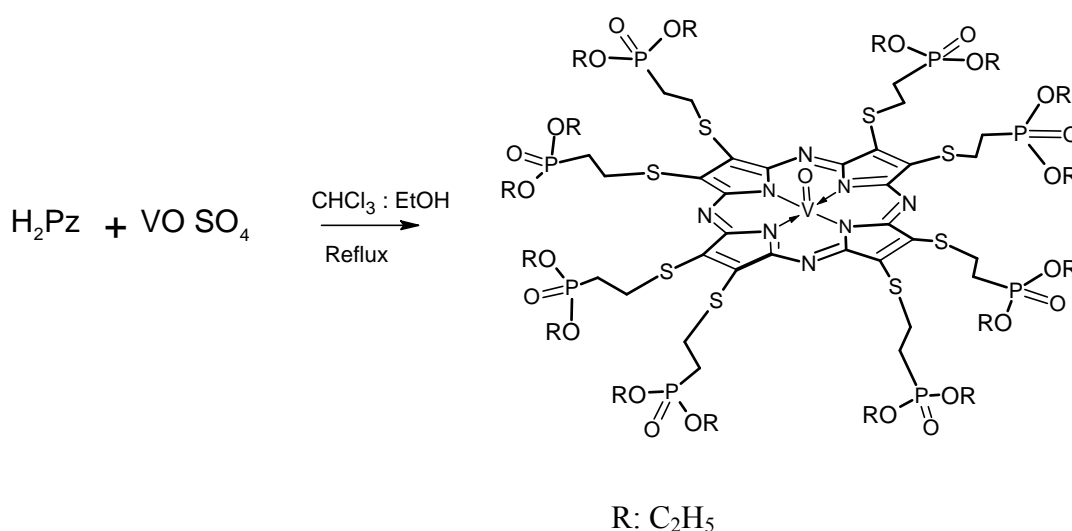


Figure 5.9 Synthesis of VO-Pz.

5.3.7 Na and Ca Salts of Phosphonate Substituted Porphyrazines

The sodium salt phosphonic acid substituted of propyhrazine **5** was accomplished by adding solution of (>0.5 M) NaOH solution on the porphyrazine **5**. Purple colored solution was obtained. The UV-visible spectrum was recorded. When the solution was treated with (C₄H₉)₄NI, the resultant product extracted with CHCl₃ where the sodium salt was not.

The calcium salt of phosphonic acid substituted of propyhrazine **5** was synthesized by adding CaCl_2 solution onto the sodium solution of porphyrazine. The dark blue colored precipitate of Ca_8MgPz was obtained. The solution was heated to remove the $\text{Ca}(\text{OH})_2$ precipitate and dark blue precipitate was filtered. The resultant product was insoluble in organic solvents while it was soluble in DMF. The UV-visible spectrum was recorded in DMF. FT-IR (KBr, cm^{-1}): 2915, 2512, 1793, 1735-1419-1190, 1078, 873, 707. UV-visible (DMF, λ_{max}): 368 and 660 nm. The UV- visible and FT-IR spectra were given Appendix A1 and B1 respectively.

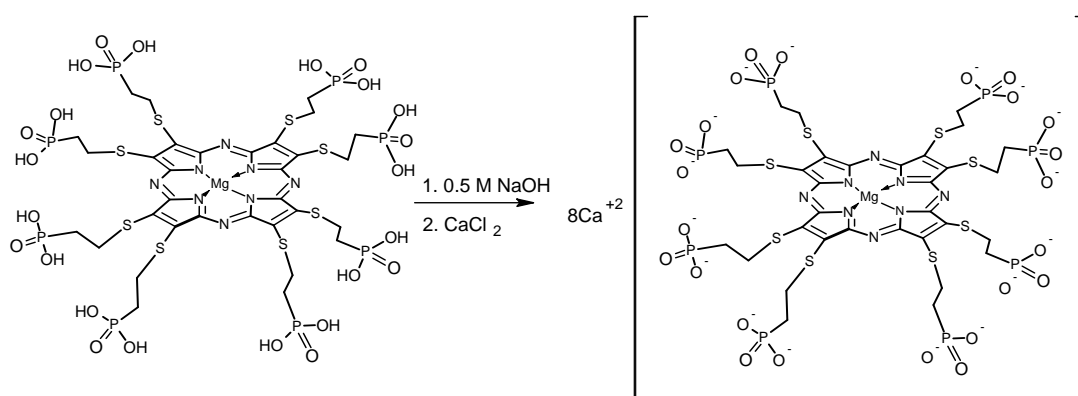


Figure 5.10 Synthesis of Ca_8MgPz .

indicates the existence of C≡N bonds of proposed ligand. The peaks at 967, 1037, 1248, 1279 cm^{-1} on FT-IR spectrum belong to ligand's phosphonate groups. The compound has been monitored with TLC chromatography (the eluent was 1:3 CHCl_3 : MeOH). In the ^1H NMR spectrum, the chemical shifts and their groups are as follows; (CDCl_3): δ 1.3(t, 12H, $-\text{CH}_3$), δ 4.082 (q, 8H, $-\text{OCH}_2$), δ 3.284 (t, 4H, SCH_2), δ 2.373 (t, 4H, $-\text{PCH}_2$). In the ^{13}C NMR (CDCl_3): δ 16.638 (CCH_3), 62.32 (OCH_2), 24.01 (SCH_2), 30.419 (PCH_2) peaks indicate the presence of ligand **2**. ^{31}P NMR (δ 26.5 ppm) confirms the existence of P atoms on the ligand **2**. The second peak around δ 26.8 may come from the trans isomer (fumaronitrile) of the dithiomaleonitrile ethyl phosphonate ligand. Mass spectrum of ligand **2** indicates the proposed ligand's **2**. The peak at 471.24 (M⁺) confirms the molecular mass of proposed ligand where calculated molecular mass is 470 g/mol.

The UV-visible, ^1H , ^{13}C , and ^{31}P NMR, and FAB-MS spectra of ligand **2** were in the Appendices B, C, D, E, and F; FT-IR, with respectively.

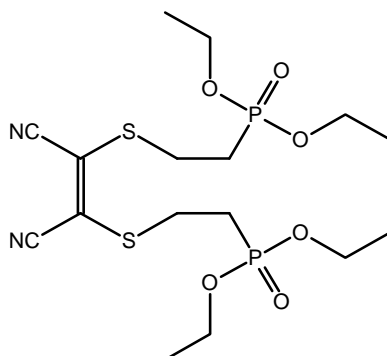
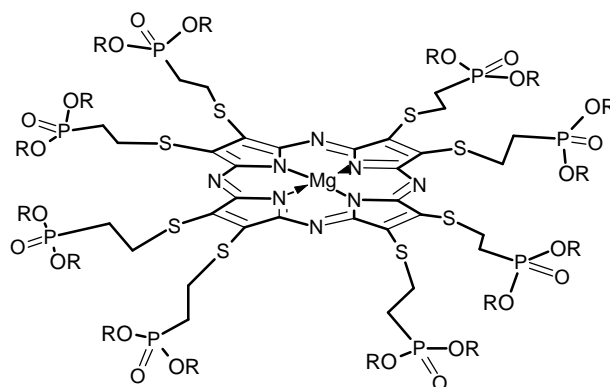


Figure 6.1 The structure of 1,2-Bis{2-(diethyl phosphonate) ethylthio} maleonitrile ligand **2**.

6.3 MAGNESIUM OCTAKIS (2-(DIETHYLPHOSPHONATE) ETHYLTHIO) PORPHYRAZINES

The porphyrazine compound has been prepared by the macrocyclization of the ligand **2** in the presence of magnesium propanolates. When ligand **2** and $\text{Mg}(\text{OPr})_2$ were refluxed, the color of the compound turned from brown to dark blue. After the solvent was removed the dark blue viscous compound obtained in good yield. Two

porphyrazine molecules (**3a** and **3b**) formed during macrocyclization have been isolated by the hexane extraction. The propyl ester **3b** is hexane soluble whereas the ethyl ester **3a** is hexane insoluble. The former has formed due to the trans-esterification reaction between **3a** and the propanolates ions in the reaction media (Figure 6.2). The formation of **3b** has been proved by the FAB-MS analysis (Appendix M). Both porphyrazines were good soluble in chloroform, ethanol, dichloromethane and methanol. FAB-MS for $C_{80}H_{144}MgN_8O_{24}P_8S_8$ (propyl ester) (M+1) 2133; and for $C_{64}H_{112}MgN_8O_{24}P_8S_8$ (ethyl ester); (M+1) 1908 support the trans esterification during macrocyclization. The related spectra were given in Appendices M and N, respectively. Replacement of propyl with ethyl group on phosphonate affect the solubility of porphyrazines in nonpolar solvents especially n-hexane. In the UV-visible spectrum (Figure 6.3), the peaks have been seen at the 364 and 668 nm which are the characteristic porphyrazine peaks when the compared with literature. This indicates that both **3a** and **3b** substances are porphyrazine with different aryl group on phosphorous. The UV-visible spectra of **3a** and **3b** were given Appendix G.



R: Ethyl (**3a**) or Propyl (**3b**).

Figure 6.2 The structure of magnesium octakis(2-(diethylphosphonate)ethylthio) porphyrazine.

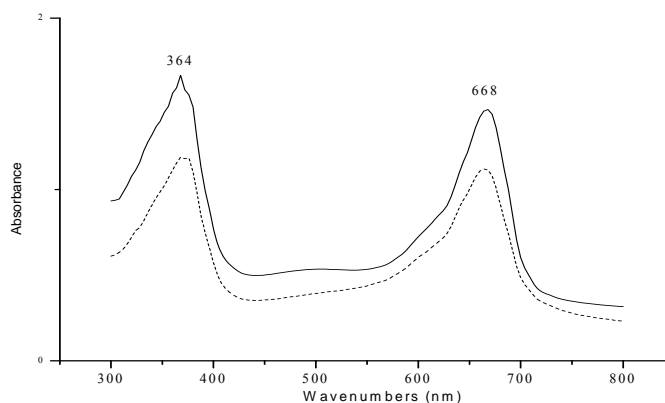


Figure 6.3 UV-visible spectrum of with lines __ **3a** (ethyl) and**3b** (propyl) esters of Pzs in chloroform.

In the FT-IR spectrum, the disappearance of $\text{C}\equiv\text{N}$ peak at 2200 cm^{-1} is the most important clue for the macrocyclization of ligand **2** to form porphyrazine molecules. Also the existence peak at 997 cm^{-1} , 1067 cm^{-1} P-OR esters (str) 1248 cm^{-1} P=O (str) which belong to phosphonate groups and 2877 cm^{-1} C-H (str) support the proposed porphyrazines molecules. The FT-IR spectra **3a** and **3b** were given Appendix L and H respectively. ^1H , ^{13}C , and ^{31}P NMR also indicates the proton, carbon and phosphorus peaks of porphyrazine molecules. ^1H , ^{13}C , and ^{31}P NMR were given for **3b** in Appendices I and J.

6.4 METAL FREE PORPHYRAZINES

Metal free porphyrazine was prepared by treatment of metalated porphyrazine with trifluoroacetic acid (TFA) at room temperature. Then it was neutralized with ammonia solution by controlling pH paper. When solution was neutralized, the precipitate of H_2Pz was extracted with chloroform. When magnesium metal is removed from center of porphyrazine cycle, two N atoms of pyrrole groups are protonated. In the IR spectrum, the existence of peak at 3289 cm^{-1} indicates the N-H bond stretching of H_2Pz . The FT-IR spectrum of compound **4** was given in the Appendix P.

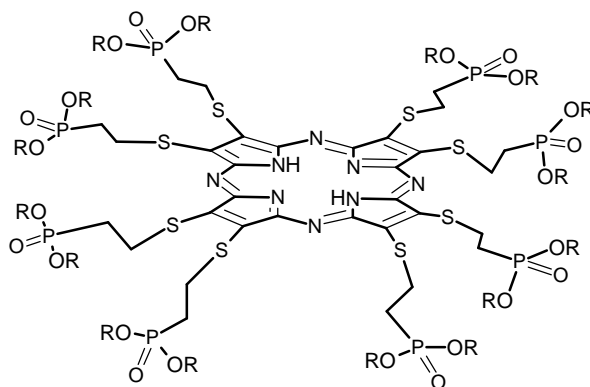


Figure 6.4 The structure of metal free octakis(2-(diethylphosphonate)ethylthio)porphyrazine **4**.

The splitting of the Q band absorption at 632 and 708 nm on the UV-visible spectrum (Appendix O) confirms the changes in symmetry from D_{4h} to D_{2h} of metal free porphyrazine. The intense peak around 362 nm can be attributed to B band absorption, and the existence of absorption peak around 500 nm, can be due to aggregation of porphyrazine core. In the ^1H NMR spectrum of metal free porphyrazine, the peak around -1.39 ppm indicates the N-H protons at the centre of porphyrazine molecules. The ^1H and ^{13}C NMR spectra of H_2Pz **4** were given in the Appendix Q and R.

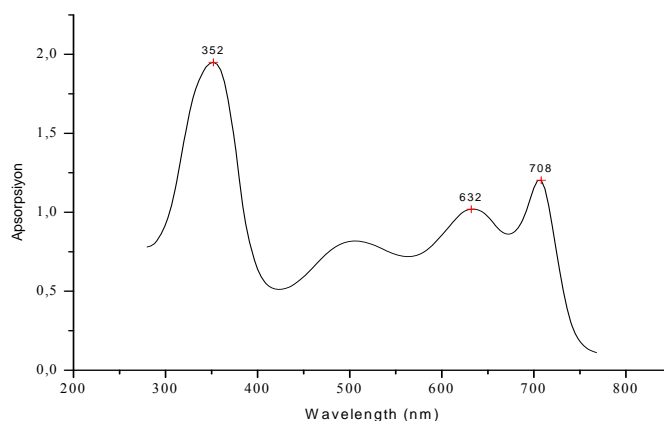


Figure 6.5 The UV-visible spectrum of metal free octakis(2-(diethylphosphonate)ethylthio)porphyrazine **4**.

6.5 PHOSPHONIC ACID SUBSTITUTED PORPHYRAZINES

The porphyrazine 3b was treated with 16 equivalent of TMSBr in CH₂Cl₂ in a sealed tube for 4 hours, followed by 95% methanol- water mixture [192, 193]. During the dealkylation process, the color of the compound turned from dark blue to purple. When the solvent was removed, the highly viscous product **5** was obtained in good yield (65 %). The resultant product is insoluble in water, but soluble in common organic solvents, such as chloroform, ethanol and DMF. TMSBr cleaves the P=O(OR)₂ dialkyl esters selectively producing P=O disilyl esters intermediates which is hydrolyzed with water or methanol to the acid. The cleavage of the disilyl ester units has produced the phosphonic acid groups on the peripheral positions (Figure 6.6). Those acidic protons may produce intermolecular H bonding with meso-nitrogen atoms of the ring which decreases the symmetry from D_{4h} to D_{2h} and results in splitting of the Q band absorption. (Appendix S).

In the ¹H NMR of the Mg(PO(OH)₂), the peak around 5 ppm indicates OH peak and absence of ester carbon peaks on ¹³C MNR at 69 ppm indicates the cleavage of phosphonate esters to phosphonic acid. ¹H, and ¹³C NMR were given in the Appendix U, V and W respectively.

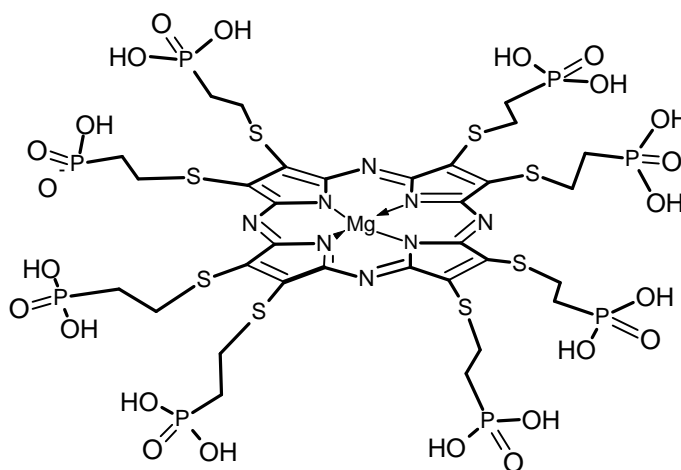


Figure 6.6 The structure phosphonic acid substituted porphyrazine MgPzOH **5**.

6.6 METALATION OF METAL FREE PORPHYRAZINES

Metalation of porphyrazine were prepared by the reaction of metal salts ($\text{Co}(\text{OAc})_2$, $\text{Cu}(\text{OAc})_2$, and VOSO_4) with metal free porphyrazine in ethanol. The UV-visible spectra indicate that the metalated porphyrazine absorption peak as B band at Q bands were common $\text{M}(\text{II})\text{Pzs}$ peaks. The absorbances at 334, 664 nm are for $\text{Cu}(\text{II})\text{Pz}$, 336, 644 nm are for $\text{Co}(\text{II})\text{Pz}$, and 336, 660 nm are for $(\text{VO})^{2+}\text{Pz}$ molecules. The absence of N-H stretching peak around 3296 cm^{-1} shows the metal coordination into the center of metal free porphyrazine. The UV-visible and FT-IR spectra for and $\text{Co}(\text{II})\text{Pz}$ $\text{Cu}(\text{II})\text{Pz}$ were given Appendix X and Y, respectively. The UV- visible and FT-IR spectra for $(\text{VO})^{2+}\text{Pz}$ were given Appendix Z.

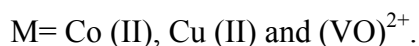
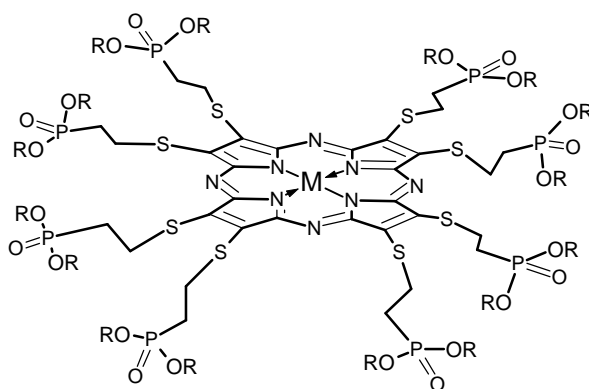


Figure 6.7 The structure metalated porphyrazines.

6.7 SODIUM AND CALCIUM SALT OF PORPHYRAZINES

The phosphonic acid substituted porphyrazine was treated with diluted NaOH solution. The neutralization with NaOH cleaved the H-bonding and gave anionic porphyrazine. This has been proved by the treatment of water soluble porphyrazine with the $(\text{C}_4\text{H}_9)\text{NI}$ which gives the organic solubility.

The calcium salt of phosphonic acid substituted of propyhrazine **5** was prepared by adding CaCl_2 solution onto the sodium salt solution of porphyrazine **5**. The dark blue colored Ca_8MgPz was insoluble in common organic solvents. It was soluble only in

DMF. The formation of Ca_8MgPz was supported by FT-IR (Appendix B1) and UV-visible spectra (Appendix A1). In the FT-IR spectrum, the broad peak at 1190- 1735 cm^{-1} could be ionic $\text{Ca}-(\text{O}=\text{PO}_2^{2-})$ bonds. In the UV-visible spectrum the, the peaks at 368 and 660 nm proves the metalated porphyrazine spectrum. The disappearance of splitting of the Q band in the UV-visible spectrum of phosphonic acid substituted porphyrazine indicates that magnesium ions remains at the center of porphyrazines. The absorption spectrum of the compound shows the D_{4h} symmetry of the common metalated porphyrazine.

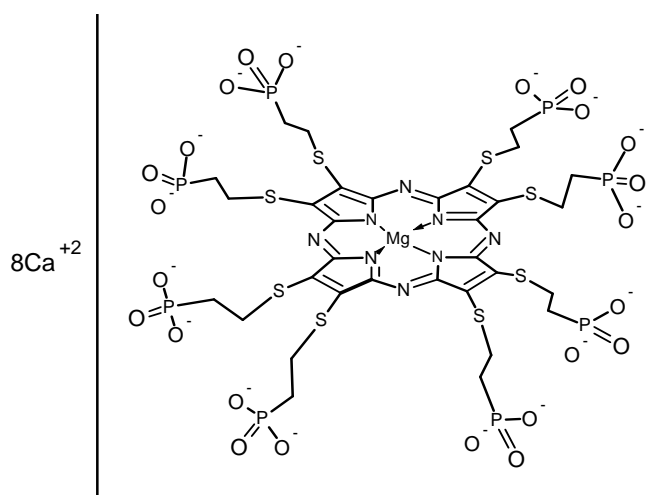


Figure 6.8 The structure Ca_8MgPz .

CHAPTER 7

CONCLUSION

Macrocyclic tetrapyrroles (porphyrin, phthalocyanine and porphyrazine) are the subject of great interest in areas such as catalysis, photodynamic therapy (PDT) and supramolecular chemistry. Although, porphyrazines attract significantly less attention compared to porphyrins and phthalocyanines, they have, recently, been of great interest due to their photophysical properties with peripherally ionic groups and interesting area of supramolecular chemistry by having macrocyclic, stable and planar structures. While the ionic groups provide binding of porphyrazines to some biomacromolecules such as DNA and proteins, the symmetrical octakis functionalisation also promotes several supramolecular interactions.

In this work, we have synthesized phosphonate substituted maleonitrile from the dithiomaleonitrile disodium salt and 2-bromoethyldiethylphosphonate. The phosphonate substituted porphyrazines have been prepared by macrocyclization of 1,2-bis{2-(diethylphosphonate)ethylthio}maleonitrile with the template of freshly prepared $\text{Mg}(\text{OPr})_2$.

The cleavage of phosphonate esters of porphyrazines were accomplished by treatment with TMSBr (Bromotrimethyl silane). The cleavage of the ester units has produced the phosphonic acid groups on the peripheral positions. The treatment of phosphonic acidic porphyrazine with alkaline solution in the presence of Ca^{2+} ions gives the Ca_8MgPz .

In summary; porphyrazines with phosphonic acid substituents are potentials for PDT treatment. In this work we have synthesized soluble (in organic solvents such as chloroform, acetone, ethanol and in alkaline solutions) porphyrazines phosphonic acid substituents on the peripheral positions. For further investigations, we will study the supramolecular interactions with several metals and the cationic proteins (i.e. histone proteins) through the phosphonate groups as well as the photosensitizing properties

REFERENCES

1. Guo L., Ellis D.E., Hoffman B.M., Ishikawa Y., *Inorg. Chem.*, Vol. 35, 1996, pp.5304-5312.
2. Baerends E.J., Ricciardi G., Rosa A., Gisbergen S.J.A., *Coordination Chemistry Reviews*, Vol. 230, 2002, pp. 5-27.
3. Kobayashi N., *Coordination Chemistry Reviews*, Vol. 227, 2002, pp.129-152.
4. Mbatha B.G., PhD. Thesis in UNIVERSITY OF JOHANNESBURG 2006.
5. a) Ali H., and Lier J .E., *Chem. Rev.*, Vol. 99, 1999, pp.2379-2450. b) Crossley M.J., Santic P.J., Walton R. and Reimers J.R., *Org. Biomol. Chem.*Vol.1, 2003, pp. 2777.
6. Mack J., Stillman M.J., Kobayashi N., *Coordination Chem. Reviews*, Vol. 251, 2007, pp.429.
7. Infante I. and Lej F., *Chemical Physics Letters*, Vol. 367, 2003, pp. 308-318.
8. Mbatha B.G., *Solubilisation of Porphyrins used in Photodynamic Therapy of Cancer* M.S. Thesis, University of Transkei, 1999.
9. Leznoff C.C., Lever A.B.P., Eds. *Phthalocyanines: Properties and Applications*, Vol. 1-4 VCH Publishers New York, 1990-1996.
10. Weiss C., Kobayashi H., Gouterman M.J., *Mol.Spectrosc.* Vol.16, 1965, pp.415.
11. Stuzhin P.A., Bauer E.M. and Ercolani C., *Inorg. Chem.*, Vol. 37, 1998, pp.1533.
12. Sibert J.W., Baumann T.F., Williams D.J., White A.J.P., Barrett A.G.M. and Hoffman B.M., *J. Am .Chem. Soc.*, Vol.118, 1996, pp.10487.
13. Baumann T.F., Barrett A.G.M., and Hoffman B.M., *Inorg. Chem.*, Vol. 36, 1997, pp.5661.
14. Lam H., Marcuccio S.M., Svirskaya P.I., Greenberg S., Lever A.B.P. and Leznoff C.C., *Can. J. Chem.*, Vol. 67, 1989, pp.1087.
15. Cook M.J., and Jafari-Fini A., *Tetrahedron*, Vol. 56, 2000, pp.4085.
16. Linßen T.G., and Hanack M., *Chem. Ber.*, Vol.127, 1994, pp.2051.

17. Kukhar, V. P.; Hudson, V. R., *Aminophosphonic and Aminophosphinic Acids: Chemistry and Biological Activity*, Eds.; John Wiley: New York, 2000.
18. Drag M., Latajka R., Gumienna-Kontecka, E., Kozlowski H., and Kafarski P., *Tetrahedron: Asymmetry*, Vol.14, 2003, pp.1837.
19. H. Fleish, in: J.P. Bilezikian, L.G. Raisz, G.A. Rodan (Eds.), *Principles of Bone Biology*, Academic Press, San Diego, 1996, CA., pp.1037–1052
20. Sharmana W.M., Liera J.E., Allenb C.M., *Advanced Drug Delivery Reviews*, 56, 2004, pp. 53–76.
21. Kobayashi N., , In: Smith K., Guilard R., Kadish K.M., editors, *Porphyrin handbook*, Vol. 2,3, New York: Academic Press, 1999, pp.318.
22. Fitzgerald J., Taylor W. and Owen H., *Synthesis*, No.9, 1991, pp.686-688.
23. Forsyth T.P., Williams D.B.G., Montalban A.G., .Stern C.L., Barret A.G.M. and Hoffman B.M., *J.Org.Chem.*, 1 Vol.63, 1998, pp. 331.
24. Baumann T.F., Nasir M.S., Sibert J.W., White A.J.P., Olmstead M.M., Williams D.J., Barret A.G.M., and Hoffman B.M., *J. Am. Chem. Soc.*, Vol. 118, 1996, pp. 10479.
25. Lange S.J., Nie H., Stern C.L., Barret A.G.M., and Hoffman B.M., *Inorg. Chem.*, Vol.37, 1998, pp. 6435.
26. Beall L.S., Mani N.S., White A.J.P., Williams D.J., Barrett A.G.M. and Hoffman B.M., *J. Org. Chem.*, Vol. 63, 1998, pp. 5806.
27. a) Kadish K.M., Smith K.M., and Guilard R., Phthalocyanines 15, 2003, pp. 97. b) Bottomley L.A., *J. Electroanal. Chem.*, 1986, pp. 331-346.
28. Goldberg D.P., Montalban A.G., White A.J.P., Williams D.J., Barrett A.G.M. and Hoffman B.M., *Inorg. Chem.*, Vol.37, 1998, pp. 2873.
29. Faust R. and Weber C., *J. Org. Chem.*, Vol. 64, 1999, pp. 2571.
30. Kobayashi N., Ashida T., Osa T. and Konami H., *Inorg.Chem.*, Vol. 33, 1994, pp. 1735.
31. Milgrom L., and Robert S.M., *Chemistry in Britain* May 1998.
32. Choi C., Tsang P., Huang J., Chan E.Y.M., Ko W., Fong W. and Ng D.K.P., *Chem. Commun.*, Issue 19, 2004, pp. 2236-227
33. Giuntini F., Nistri D., Chiti G., Fantetti L., Jori G. and Roncucci G., *Tetrahedron Lett.*, Vol.44, 2003, pp. 515-517.
34. Todd W.J., Bailly F., Pavez J., Faguy P.W., Baldwin R.P. and Buchanam R.M., *J.Chem.Soc.*, Vol.120, 1998, pp. 4887.

35. Montalban A.G., Lange S.J.L.S.Beall Mani N.S., D.J.Williams A.J.P.White Barrett A.G.M.,and Hoffman B.M., *J.Org.Chem.*, Vol.62, 1997, pp. 9284.
36. Cammidge A.N., Cook M.J., Harrison K.J., and McKeown N.B., *J.Chem. Soc. Perk.Trans.*, 1991, pp.3053.
37. Goldberg D.P., Montalban A.G., White A.J.P., Williams D.J., Barrett A.G.M.,and Hoffmann B.M., *Inorg.Chem.*, Vol.37, 1998, pp. 2873.
38. Lange S.J., Nie H., Stern C.L., Barrett A.G.M.,and Hoffman B.M., *Inorg.Chem.*, Vol.37, 1998, pp. 6435.
39. Antipas A., Dolphin D., Gouterman M. and Johnson E.C., *J. Am. Chem. Soc.*, Vol. 100, 1978, pp. 7705.
40. Nevin W.A., Liu W., Greenberg S., Hempstead M.R., Marcuccio S.M., Melník M., Leznoff C.C.and Lever A.B.P., *Inorg. Chem.*, Vol. 26, 1987, pp. 891.
41. Leznoff C.C., Marcuccio S.M., Greenberg S. and Lever A.B.P., *Can. J. Chem.*, Vol. 63, 1985, pp. 623.
42. Chen Y., Huang L., Ranade M.A., and Zhang X.P., *J. Org. Chem.*, Vol. 68, 2003, pp. 3714.
43. Ogunsipe A., Chen J., and Nyokong T., *New J. Chem.*, Vol. 28, 2004, pp.1.
44. Uchida H., Reddy P., Nakamura S. and Toru T., *J.Org. Chem.*, Vol.68, 2003, pp. 8736.
45. Mani N.S., Beall L.S., Miller T., Anderson O.P., Hope H., Parkin S.R., Williams D.J., Barrett A.G.M., and Hoffman B.M., *J. Chem. Soc. Chem. Commun.*, 1994, pp. 2095.
46. Velázquez C.S., Baumann T.F., Olmstead M.M., Hope H., Barrett A.G.M., and Hoffman B.M., *J. Am. Chem. Soc.*, Vol.115, 1993, pp. 9997.
47. Mani N.S., Beall L.S., White A.J.P., Williams D.J., Marrett A.G.M. and Hoffman B.M., *J. Chem. Soc., Chem. Commun.*, 1994, pp.1943.
48. Sakellariou E.G., Montalban A.G., Meunier H.G., Ostler R.B., Rumbles G., Barrett A.M. and Hoffman B.M., *J. Photochem. Photobiol. A: Chem.*, Vol.136, 2000, pp. 185.
49. Giribabu L., Chandrasekharam M S., Mohan M., Rao C., Kantam S.M.L., Reddy M.R., Reddy P.Y., Toru T., *Synlett*, Vol.48, 2006, pp. 1604.
50. a) Uchida H., Tanaka H., Yoshiyama H., Reddy P.Y., Nakamura S., Toru T., *Synlett*, 2002, pp. 1649. b) Uchida H., Reddy P.Y., Nakamura S., Toru T., *J. Org. Chem.*, Vol. 68, 2003, pp. 8736. c) Uchida H., Yoshiyama H., Reddy P.Y., Nakamura S., Toru T., *Bull. Chem., Soc., Jpn.*, Vol.77, 2004, pp. 1401.
51. Chandrasekharam M., Rao C.S., Singh S.P., Kantam M.L., Reddy M.R., Reddy P.,

- and Toru Y., T. *Tetrahedron Letters*, Vol. 48, 2007, pp. 2627.
52. Kopranev V.N., Luk'yanets E.A., *Russian Chemical Bulletin*, Vol. 44, 1995, pp. 2216.
53. Hambright P., *Coord. Chem., Rev.*, Vol. 6, 1971, pp. 247.
54. Berezin B.D., and Enikolopyan N.S., *Metalloporfiriny Metalloporfirins*, Nauka Moscow, 1988.
55. Stuzhin P.A. and Khelevina O.G., *Coord. Chemistry Reviews*, Vol.147, 1996, pp. 41-86.
56. Berezin B.D., *Coordination Compounds of Porphyrins and Phthalocyanine*, Wiley, New York, 1981.
57. Chen B., and Tulinsky A., *J. Am. Chem. Soc.*, Vol. 94, 1972, pp.4144.
58. Silvers S.J., and Tulinsky A., *J. Am. Chem. Soc.*, Vol. 89, pp.1967.
59. Tulinsky A., *Ann. N.Y. Acad. Sci.*, Vol. 206, 1973, pp. 47.
60. Laucher J.W. and Ibers J.A., *J. Am. Chem. Soc.*, Vol. 95, 1973, pp. 5148.
61. Webb L.E. and Fleischer E.B., *J. Chem. Phys.*, Vol. 43, 1965, pp. 3100.
62. Hamor M.J., Hamor T.A., and Hoard J.L., *J. Am. Chem. Soc.* Vol. 86, 1964, pp. 1938.
63. Robertson J.M., *J. Chem. Soc.*, 1936, pp. 1195.
64. Hoskins B.F., Mason S.A., and White J.C.B., *J. Chem. Soc., Chem. Commun*, 1969, pp. 554.
65. Woodward I., *J. Chem. Soc.*, 1940, pp. 601.
66. Robertson J.M., *J. Chem. Soc.*, 1939, pp.1809.
67. Das I.M., and Chandhuri B., *Acta Crystall. Sect., B*, Vol. 28, 1972, pp. 579.
68. Balch A.L., Olmstead M.M., and Safari N., *Inorg. Chem.*, Vol.32, 1993, pp. 291.
69. Velazques C.B., Fox G.A., Broderick W.E., Andersen K.A., Anderson O.P., Barret A.G.M., and Hoffman B.M.J., *Am. Chem. Soc.*, Vol.114, 1992, pp. 7416.
70. Masuda H., Taya T., Osaki K., Sugimoto H., Yoshida Z.-I., and Ogoshi H., *Inorg. Chem.*, Vol.19, 1980, pp. 950.
71. Martinsen J., Pace L.X., Phillips T.E., Hoffman B.M., and *J. Am. Chem. Soc.*, Vol.104, 1982, pp. 83.
72. Schramm C.J., Scaringe R.P., Stojakovic D.R., Hoffman B.M., Ibers X.A., and Mark TX., *J. Am. Chem. Soc.*, Vol. 102, 1980, pp. 6702.

73. Weiss C., Kobayashi H., and Gouterman M., *J. Mol. Spectrosc.*, Vol. 16, 1965, pp. 415.
74. Schaffer A.M., and Gouterman M., *Theor. Chim. Acta*, Vol. 25, 1972, pp. 62.
75. Mamaev V.M., Gloriov L.P., and Boyko L.G., *Zh. Strukt. Khim.*, Vol. 20, 1979, pp. 332.
76. Dvornikov S.S., Knyukshto V.N., Kuz'mitsky V.A., Shul'ga A.M., and Solovyov K.N., *J. Lumin.*, Vol. 23, 1981, pp. 373
77. Stuzhin P.A., Thesis, *Institute of Chemical Technology, Ivanovo*, 1985.
78. Solovyov K.N., *Institute of Physics, Akademii Nauk Belorusskoi SSR, Minsk*, 1969.
79. Kopranchikov V.N., Vorotnikov A.M., Ivanova T.M., and Luk'yanets E.A., *Khim. Geterotsikl. Soedin*, 1988, 1351.
80. Badger G.M., Harris R.L., Jones R.A., and Sasse J.M., *X Chem. Soc*, 1962, pp. 4329.
81. Kuz'mitsky V.A. and Solovyov K.N., *J. Mol. Spect.*, Vol. 65, 1980, pp. 219.
82. Solovyov K.N., Mashenkov V.A., and Gradyushko A.T., *Zh. Prikl. Spektrosk.*, Vol. 13, 1970, pp. 339.
83. Mamaev V.M., Ishtchenko S.Y., and Gloriov L.P., *Izv.Vyssh. Uchebn. Zaved Khim. Khim.Tekhnol.*, Vol. 321, 1989, pp. 3.
84. Berezin B.D., *Izv. Vyssh. Uchebn. Zaved Khim. Khim.Tekhnol* 2, 1959, pp.165.
85. Fleischer E.B., *Acc. Chem. Res.*, Vol. 3, 1970, pp.105.
86. Sharp J.N., and Lardon M., *J. Phys. Chem.*, Vol. 72, 1968, pp. 3230.
87. Orti E., Piqueras M.C., Crespo R., and Bredas J.L., *Chem. Mater.*, Vol. 2, 1990, pp.110.
88. Berkovitch Z.-Y., and Ellis D.E., *X Am. Chem. Soc.*, Vol. 103, 1981, 6066.
89. Mamaev V.M., Gloriov L.P., and Orlov V.V., *Izv.Vyssh. Uchebn. Zaved., Khim. Khim.Tekhnol.* Vol. 32, 1989, pp. 3.
90. Mamaev V.M., and Gloriov L.P., *Ivanovo*, 1981, pp.17.
91. Dudreva B., and Grande S., *J. Phys. Paris Colloq.C2*, Vol. 33, 1972, pp. 183.
92. Meyer B.H., Storm C.B., and Earl W.L., *J. Am. Chem. Soc.*, Vol. 108, 1986, 6072.
93. Kendrick R.D., Fridrich S., Wehrle B., Limbach H.-H., and Yannoni C.S., *J. Magn. Reson.*, Vol. 65, 1985, pp. 159.
94. Wehrle B., Limbach H.-H., Kocher M., Ermer O., and Vogel E., *Angew. Chem.*,

- Vol. 99, 1987, pp. 914.
95. Andronova N.A., and Luk'yanets E.A., *Zh. Prikl. Spektrosk.*, Vol. 20, 1974, pp. 312.
 96. Hanack M., Metz J., and Pawlowsk G., *Chem. Ber.*, Vol. 115, 1982, 2836.
 97. Marcuccio S.M., Svirskaya P.I., Greenberg S., Lever A.B.P., Leznoff C.C., and Tomer K.B., *Can. J. Chem.*, Vol. 63, 1985, pp.3057.
 98. Vysotsky Y.B., Kuzmitsky V.A., and Solovyov K.N., *Theor. Chim. Acta*, Vol. 59, 1981, pp. 467.
 99. Borovkov N.Y., and Akopov A.S., *Zh. Strukt. Khim.*, Vol. 28, 1987, 175.
 100. Kopranenkov V.N., Tarkhanova E.A., and Luk'yanets E.A., *Zh. Org. Khim*, Vol. 15, 1979, pp. 642.
 101. Niwa Y., Kobayashi H., and Tsuchiya T., *Inorg. Chem.*, Vol. 13, 1974, pp. 2891.
 102. (a) Grishin Y.K., Subbotin O.A., Ustynyuk Y.A., Kopranenkov V.N., Goncharova L.S., and Luk'yanets E.A., *Zh. Strukt. Khim*, Vol. 20, 1979, pp. 352.
(b) Kopranenkov V.N., Askerov D.B., Shul'ga A.M., and Luk'yanets E.A., *Khim. Geterotsikl. Soedin*, 1988, pp. 1261.
 103. (a) Khelevina O.G., Chizhova N.V., and Berezin B.D., *Zh. Org. Khim.*, Vol. 27, 1991, pp. 805, (b) Khelevina O.G., Chizhova N.V., and Berezin B.D., *Khim. Geterotsikl. Soedin.*, Vol. 1992, pp. 619.
 104. Sheinin V.B., Andrianov V.G., and Berezin B.D., *Zh. Org. Khim*. Vol. 20, 1984, pp. 2192.
 105. Berezin B.D. and Khelevina O.G., *Porphyryns: Structure Properties and Synthesis* Moscow: Nauka, 1985.
 106. Khelevina O.G., and Rumyantseva S.V., *Advances in Porphyrin Chemistry* , Golubchikov O.A., Ed., St. Petersburg: NII Khimii SPbGU Vol. 4, 2004, pp. 128.
 107. Stuzhin P.A., Khelevina O.G., and Berezin B.D., *Phthalocyanines: Properties and Applications*, Leznoff C.C., and Lever A.B.P.N., Eds., New York: VCH, Vol. 4, 1996, pp.19.
 108. Stuzhin P.A. and Khelevina O.G., *Koord. Khim.*, Vol. 24, 1998, pp. 782.
 109. Stuzhin P.A., *J. Porphyrins Phthalocyanines*, Vol. 3, 1999, pp. 500.
 110. Khelevine O.G., Romanenko Y.V., and Islyaikin M.K., *Russian Journal of Coordination Chemistry*, Vol. 33, 2007, pp. 155–160
 111. Petrov O. A., *Russian Journal of Coordination Chemistry*, Vol. 27, 2001, pp. 449.
 112. Clarke J.A., Dawson P.J., Grigg R., and Rochester C.N., *Chem. Soc. Perkin*, Vol. 77, 1973, pp. 414.

113. Sheinin V.B., Berezin B.D., Khelevine O.G., Stuzhin P.A., and Telegin F.Y., *Zh. Org. Khim.*, Vol. 21, 1985, pp. 1571.
114. Weiss C., Kobayashi H., and Gouterman M., *J. Mol. Spectr.*, Vol.16, 1965, pp. 415.
115. Gouterman M., G Wagnier R., and Snyder L.C., *J. Mol. Spectr.*, Vol. 11, 1963, pp. 108.
116. Dvomikov S.S., Knyukshto V.N., Kuzmitsky V.A., Shul'ga A.M., and Solovyov K.N.J., *Luminescence*, Vol. 23, 1981, pp. 372.
117. Solovyov K.N., Mashenkov V.A., and Kachura T.F., *Opt. Spekt.*, Vol. 27, 1969, pp. 50.
118. Tsvetkova I.V., Andrianov V.G., and Berezin B.D., *Izv.Vyssh. Uchehn. Zaved Khim. Khim. Tekhnoi*, Vol. 37, 1994, pp. 72.
119. Tsvetkova I.V., *Thesis Institute of Chemical Technology Ivanovo*, 1994.
120. McEwen W., *J. Am. Chem. Soc.*, Vol. 58, 1936, 1124: 68, 1946, pp. 711.
121. Andrianov V.G., *Thesis Institute of Chemical Technology Ivanovo*, 1972.
122. Berezin B.D., *Coor. Comp. of Porphyrins and Phalocyanines*, Wiley, New York, 1981.
123. Sheinin B., Andrianov V.G., Berezin B.D., and Koroleva T.A., *Zh. Org. Khim.*, Vol. 2, 1985, pp. 1564.
124. Tsvetkova I.V., Andrianov V.G., and Berezin B.D., *Izv. Vyssh. Uchehn. Zaved., Khim. Khim. Tekhnoi.*, Vol. 36, 1993, pp. 32.
125. Sheinin V.B., *Thesis Institute of Chemical Technology, Ivanovo*, 1981.
126. Sheinin V.B., Andrianov V.G., and Berezin B.D., *Zh. Org. Khim.*, Vol. 20, 1984, pp. 2192.
127. Bordwell F.G., Drucker G.E., and Fried H.E., *Org. Chem.*, Vol. 46, 1981, pp. 632.
128. Smimov V.I., V'yugin A.I., and Krestov A.G., *Zh.Viz. Khim.*, Vol. 63, 1989, pp. 2245.
129. Trofimenko G.M., and Berezin B.D., *Russ. J.,Inorg.,Chem.*, Vol. 38, 1993, pp. 971.
130. Khelevine O.G., Chizhova N.V., and Berezin B.D., *Koord. Khim*, Vol. 17, 1991, pp.400.
131. Stuzhin P.A. and Khelevine O.G., *Coord. Chem. Rev.*, 1995 .
132. Whalley M., *J. Chem. Soc.*, 1961, pp. 866.
133. Vul'fson S.V., Lebedev O.A., and Luk'yanets E.A., *Zh. Prikl. Spektrosk.*, Vol. 17,

- 1972, pp. 902.
134. Berezin B.D., Khelevine O.G., Gerasimova N.D., and Stuzhin P.A., *Russ. J. Phys. Chem.*, Vol. 56, 1982, pp. 1699.
 135. Jiang H., Iftimia N.V., Xu Y., Eggert J.A., Fajardo L.L., Klove K.L., *Acad. Radiol.* Vol.9, 2002, pp. 186.
 136. Weissleder R., Ntziachristos V., *Nat. Med.*, Vol. 9, 2003, pp. 123.
 137. Kessel D., Dougherty T.J., *Rev. Contemp. Pharmacother.* Vol.10, 1999, 19.
 138. Bonnett R., *Rev. Contemp. Pharmacother.*, Vol.10, 1999, pp. 1.
 139. Pandey R.K., W. Horspool F.Lenci Eds., *CRC Handbook of Organic Photochemistry and Photobiology* second ed., CRC Press Boca Raton 2004, pp. 144.
 140. Wohrle D., Hirth A., Bogdahn-Rai T., Schnurpfeil G., Shopova M., *Russ. Chem. Bull.*, Vol.47, 1998, pp. 807.
 141. Little F.M., Gomer C.J., Hyman S., M.L.J., *J. Neuro-Oncol.*, Vol. 2, 1984, pp. 361.
 142. Achilefu S., Dorshow R.B., Bugaj J.E., Rajagopalan R., *Invest. Radiol.*, Vol. 35, 2000, pp. 479.
 143. Sessler J.L., Seidel D., *Synthetic expanded porphyrin chemistry Angew. Chem. Int. Ed.*, Vol.42, 2003, pp. 5134.
 144. Hammer N.D., Lee S., Vesper B.J., Elseth K.M., Hoffman B.M., Barrett A.G.M., Radosevich J.A., *J. Med. Chem.* Vol.48, 2005, 8125 – 8133.
 145. Lee S., White A.J.P., Williams D.J., Barrett A.G.M., and Hoffman B.M., *J. Org. Chem.*, Vol. 66, 2001, pp. 461.
 146. Lukyanets E.A., *J. Porphyrins Phthalocyan.*, Vol.3, 1999, pp. 424.
 147. Choi M.T.M., Li P.P.S., Ng D.K.P., *Tetrahedron*, Vol. 56, 2000, 3 pp.881.
 148. Tai S. and Hayashi N., *J. Chem. Soc., Perkin Trans.*, Vol. 2, 1991 pp., 1275.
 149. Zimcik P., Miletin M., Ponec J., Kostka M., Fiedler Z., *J. Photochemistry and Photobiology A: Chemistry*, Vol. 155, 2003, pp. 127.
 150. Oda K., S Ogura., Okur I., *J. Phot.. Photobiol. B Biol.*, Vol. 59, 2000, pp. 20.
 151. Rosenthal I., *Photochem. Photobiol.*, Vol. 53, 1991, pp.859.
 152. Gouterman M., *In The Porphyrins Dolphin D., Ed., Ac. Press: New York*, Vol. 3, 1978, pp. 1.
 153. Jackson A.H., *In the Porphyrins Dolphin D., Ed., Academic Press: New York*,

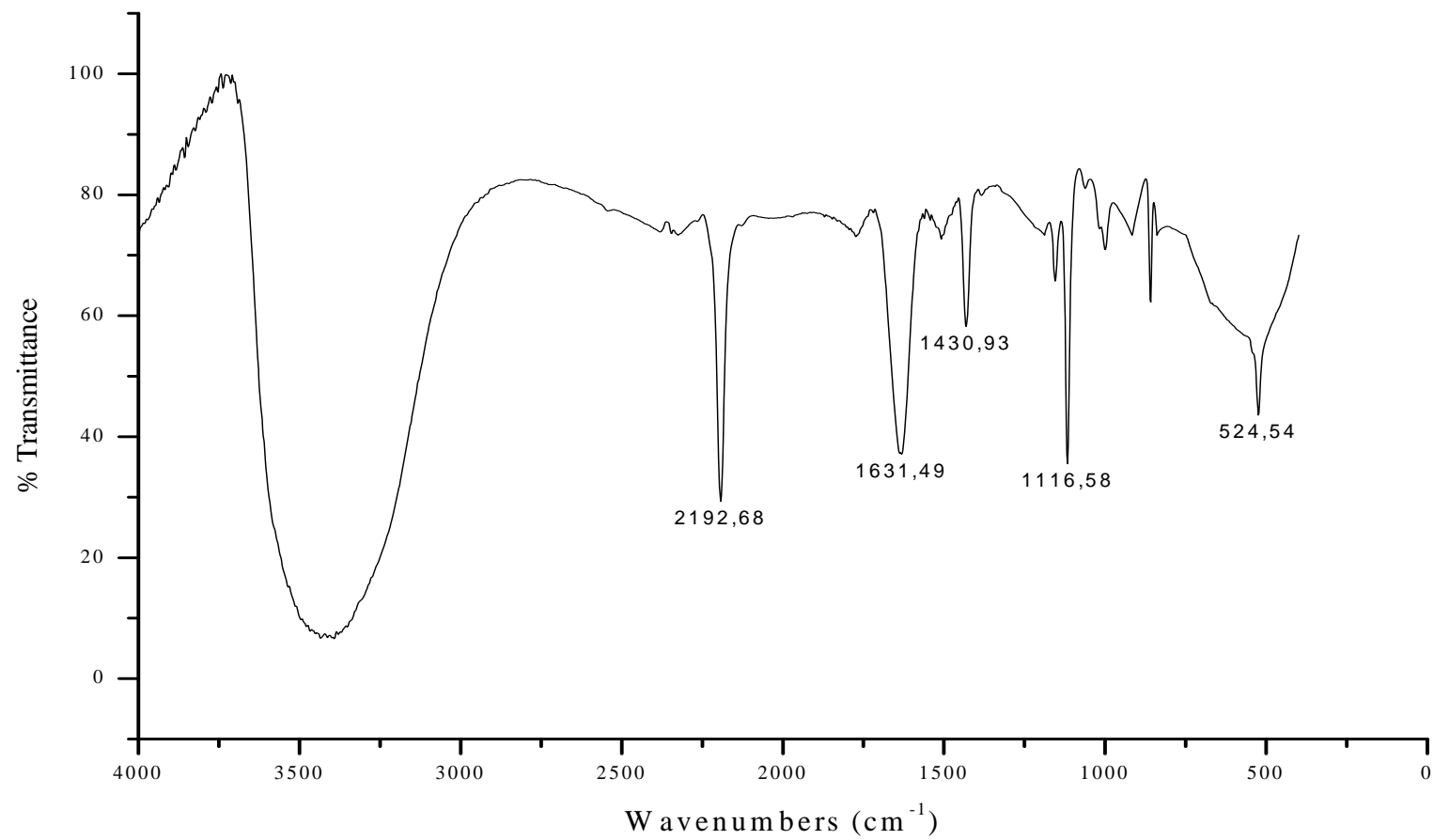
- Vol. 1, 1978, pp.365.
154. Cook A.S., Williams D.B.G., White A.J.P., Williams D.J., Lange S.J., Barrett A.G.M., Hoffman B.M., *Angew. Chem., Int. Ed. Engl.*, Vol. 36, 1997, pp.760.
 155. Forsyth T.P., Williams D.B.G., Montalban A.G., Stern C.L., Barrett A.G.M., Hoffman B.M., *J. Org. Chem.*, Vol. 63, 1998, pp.331.
 156. Anderson M.E., Barrett A.G.M. and Hoffman B.M., *Inorg. Chem.*, Vol. 38, 1999, pp. 6143.
 157. Anderson M.E., Barrett A.G.M., Hoffman B.M., *Inorganic Biochemistry*, Vol. 80, 2000, pp. 257.
 158. Kuznetsova N.A., Gretsova N.S., Derkacheva V.M., Mikhaleenko S.A., Solov'eva L.I., Yuzhakova O.A., Kaliya O.L., and Luk'yanets E.A., *Russian J. of General Chem.*, Vol.72, 2002, pp.300.
 159. Morgan A.R., Petousis N.H., and Lier J.E., *Eur. J. Med. Chem.*, Vol. 32, 1997, 21.
 160. Dent C.E., Linstead R.P., *J. Chem. Soc.*, Vol.1934, pp.1027.
 161. Karaoğlu H.R.P., Gül A., Koçak M.B., *Dyes and Pigments*, Vol.76, 2008, 231.
 162. Sağlam Ö., Gül A., *Polyhedron*, 20, 2000, pp. 269; Akkus H., Gül A., *Transition Met. Chem.*, Vol.26, 2000, 689
 163. Ebdon J.R., Guisti L., Hunt B.J., Jones M.S., *Polym. Degrad. Stab.*, Vol. 60, 1998, pp. 401.
 164. Öztürk R. and Gül A., *Tetrahedron Letters*, Vol. 45, 2004, pp. 947.
 165. Polat M., Gül A., *Dyes and Pigments*, Vol. 45, 2000, pp. 195.
 166. Dabak S., Gümüş G., Gül A., Bekaroğlu O., *J. Coord. Chem.*, Vol. 38, 1996, pp. 287.
 167. Stillman M.J., Nyokong T., In: Leznof C.C., Lever A.B.P. editors, *Phthalocyanines properties and applications*, VCH, Vol. 1989, pp. 158.
 168. (a) Bonnett R., *New Scientist* 1989, 55; (b) Saleeby C.W., *Sunlight and health 3rd ed. Nisbet and co* 1923-1926. (c) Leredde P., *Photothérapie et photobiologie Paris Naud.*, 1903. (d) Montgomery F.H., *J. Cutan. Dis.*, Vol.21, 1903, pp.529.
 169. Pandey R.K., Shiao F.Y., Sumlin A.B., Dougherty T.J., and Smith K.M., *Bioorg. Med. Chem. Lett.*, Vol.4, 1994, pp. 1263.
 170. Pandey R.K., Jagerovic N., Ryan J.M., Dougherty T.J., and Smith K.M., *Tetrahedron*, Vol. 52, 1996, pp. 5349.
 171. Bonnett R., *Chemical Soc. Rev.*, Vol. 24, 1995, pp. 19.
 172. Sharman W.M., Allen C.M., and Lier J.E., *Source: Drug Discovery Today*, Vol.

- 4, 1999, pp. 507.
173. MacRobert A.J., Brown S.G., and Phillips D., *Photosensitising Compounds : their Chemistry Biology and Clinical Use Wiley* , Vol. 146, 1989, pp. 4.
174. Castano A.P., Demidova T.N., Hamblin M.R., *Photodiag. Photodyn. Therapy*, Vol. 1, 2004, pp.279.
175. El-Khouly M.E., Ito O., Smith P.M., and D'Souza F., *J. Photochem. Photobiol.C.Photochem. Reviews* Vol. 5, 2004, pp.79.
176. Liu R.S.H., and Edman J.R., *J. Am. Chem. Soc.*, Vol. 91, 1969, pp.1492.
177. Schmidt R., and Bodesheim M., *J. Phys. Chem.*, Vol. 98, 1994, pp. 2874.
178. Ochsner M., *J. Photochem. Photobiol. B : Biol.*, Vol. 39, 1997, pp.1
179. Ferraudi G., Arguello G.A., Ali H., Lier J.E., *Photochem. Photobiol.* Vol. 47, 1988, pp.657-660.
180. Firey P.A., Jones T.W., Jori G., Rodgers M.A.J., *Photochem. Photobiol.* Vol. 48, 1988, pp. 357.
181. Songca S.P. , Bonnett R. , Maes C.M. , *S. Afr. J. Chem.*, Vol. 50, 1997, pp.40.
182. <http://www.opalclinic.com.au/PDTSDDT.html>.
183. Brown S., Bergh H., Dougherty T.J., *Int. Photodyn.*, Vol. 1, 1996, pp. 6.
184. Bishop S.M., Beeby A., Parker A.W., Foley M.S.C., and Phillips D., *J. Photochem. Photobiol. A : Chem.*, Vol. 90, 1995, pp. 39.
185. Ha J., Jung G.Y., Kim M., Lee Y.H., Shin K., and Kim Y., *Bull. Korean Chem. Soc.*, Vol. 22, 2001, pp. 63.
186. Bonnet R., Djelal B., *m-TPHC Photodyn.*, Vol. 6, 1993, pp.2.
187. Roberts W.G., Klein M.K., Loomis M., Weldy S., and Berns M.W., *J. Natl. Cancer Inst.*, Vol. 83, 1991, pp.18-23.
188. Sakellariou E.G., Montalban A.G., Beall S.L., Henderson D., Meunier H.G., Phillips D., Suhling K., Barrett A.G.M., and Hoffman B.M., *Tetrahedron* , Vol. 59, 2003, pp. 9083.
189. Sakellariou E.G., Montalban A.G., Meunier H.G., Ostler R.B., Rumbles G., Barrett A.M., and Hoffman B.M., *J. Photochem. Photobiol. A: Chem.*, Vol. 136, 2000, pp.185-187.
190. Montalban A.G., Meunier H.G., Ostler R.B., Barrett A.G.M., Hoffman B.M., and Rumbles G., *J. Phys. Chem. A.*, Vol. 103, 1999, pp.4352-4358.
191. Sakellariou E.G., Montalban A.G., Meunier H.G., Rumbles G., Phillips D., Ostler R.B., Suhling K., Barrett A.G.M., and Hoffman B.M., *Inorg. Chem.*, Vol. 41,

2000, pp.2182-2187.

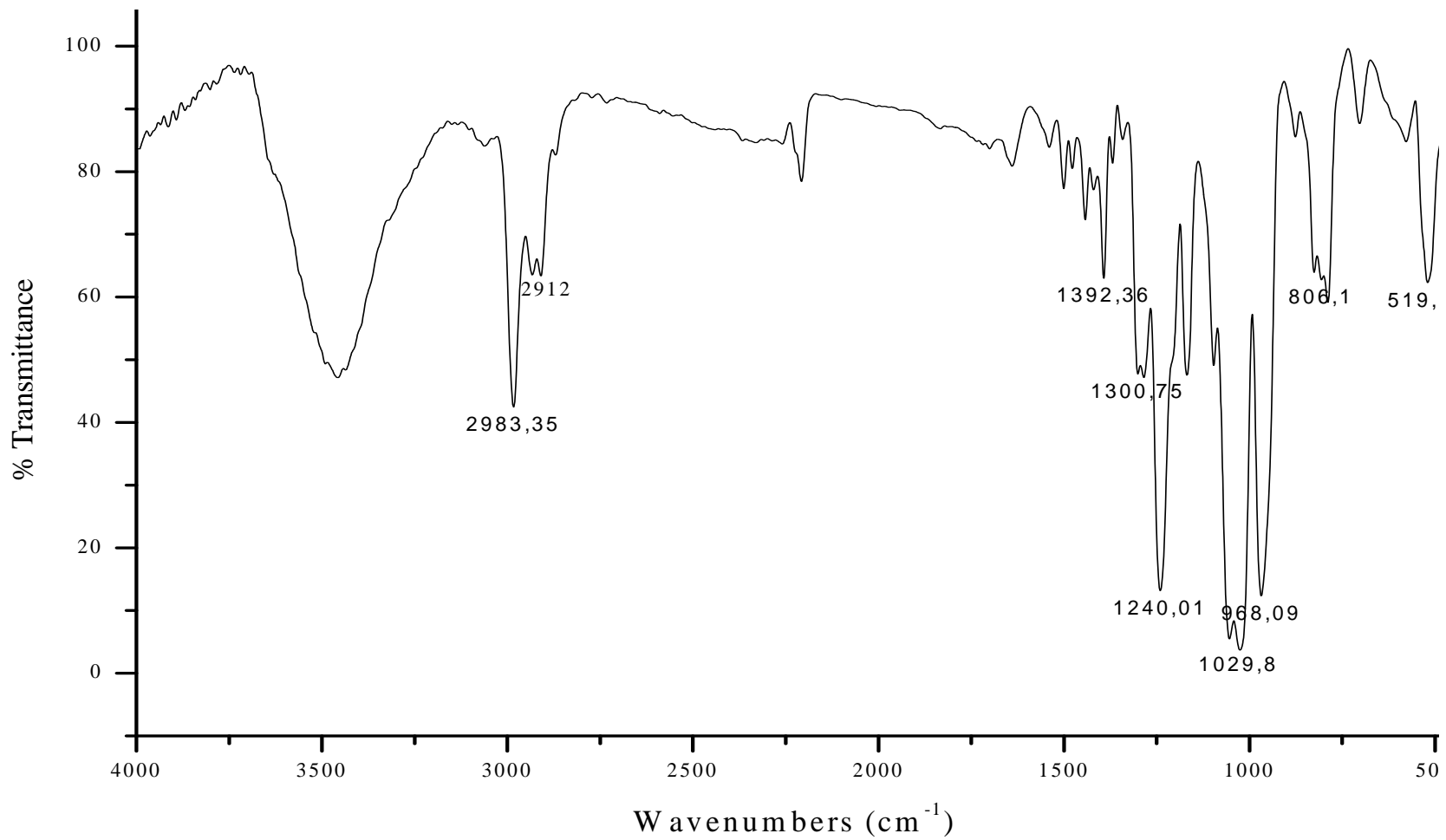
192. Bozic L.T., J. *Vibrational Spectroscopy*, Vol. 28, 2001, pp.235-241.

193. Kumar G. D. K., Saenz D., Lokesh A., Natajan G. L., *Tetrahedron Lett.*, Vol. 47, 2006, pp.6281-6284.



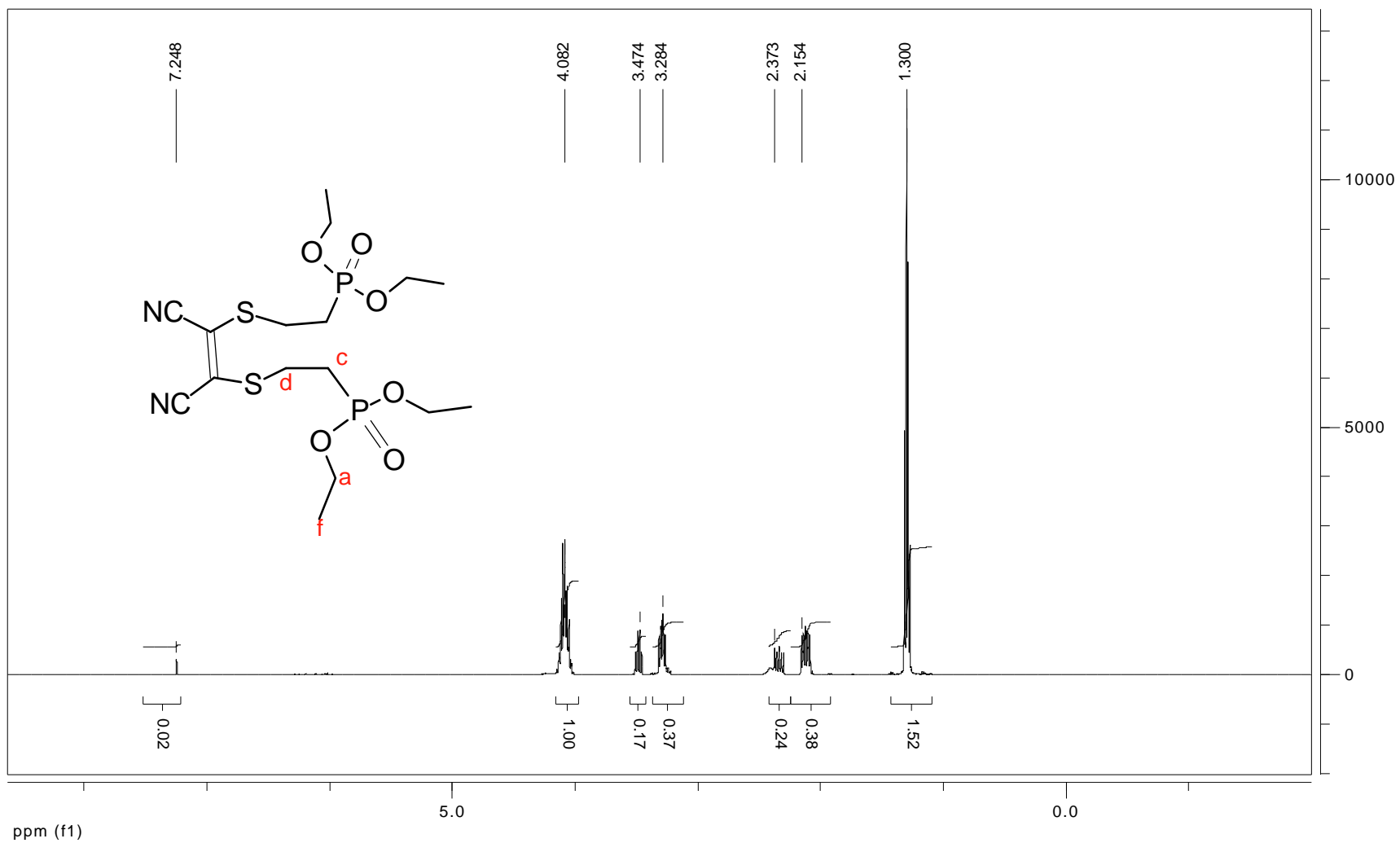
APPENDIX A

FT-IR SPECTRUM OF DISODIUM DITHIOMALEONITRILE 1

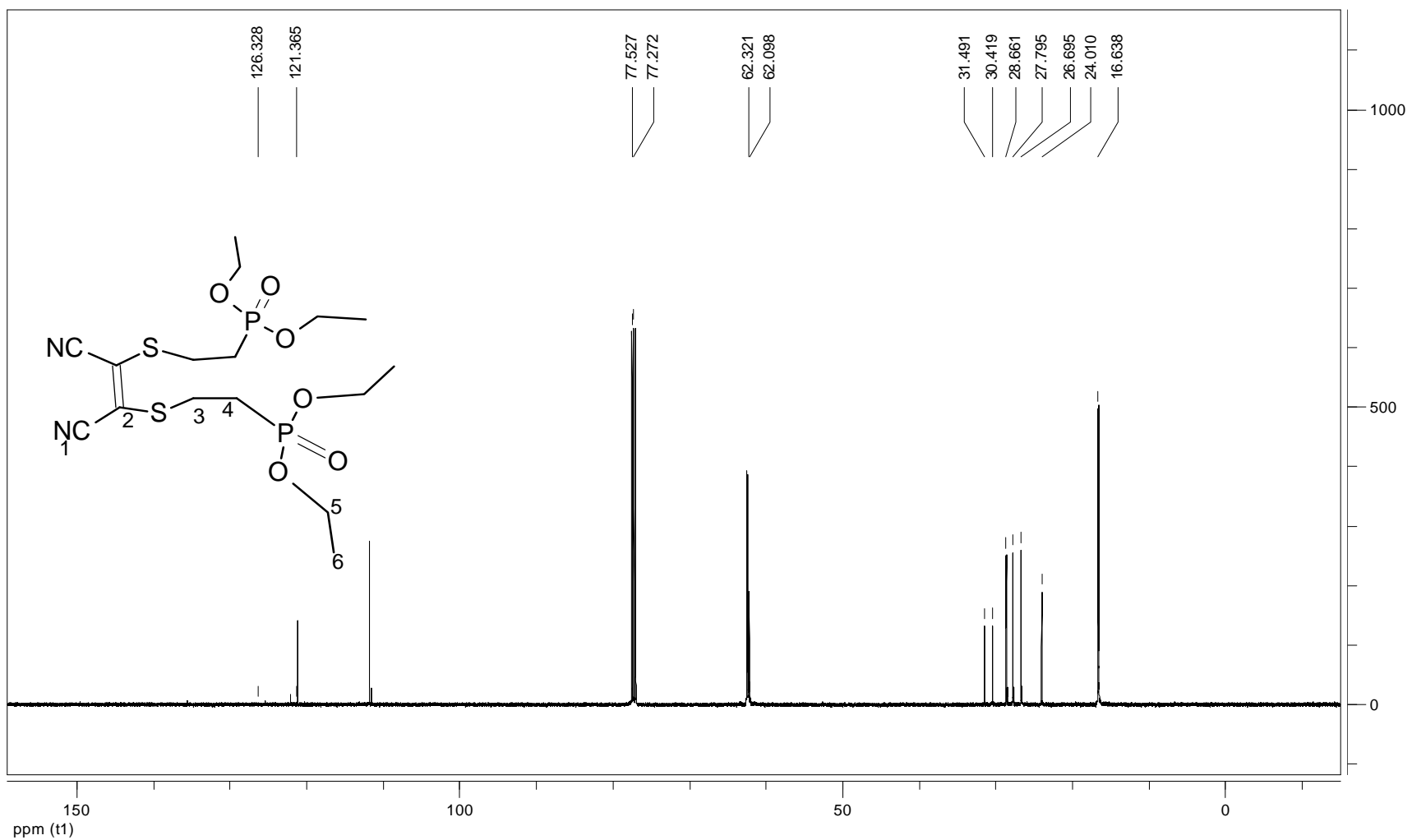


FT-IR SPECTRUM OF 1,2-BIS{2-(DIETHYLPHOSPHONATE) ETHYLTHIO}
MALEONITRILE LIGAND 2

APPENDIX C

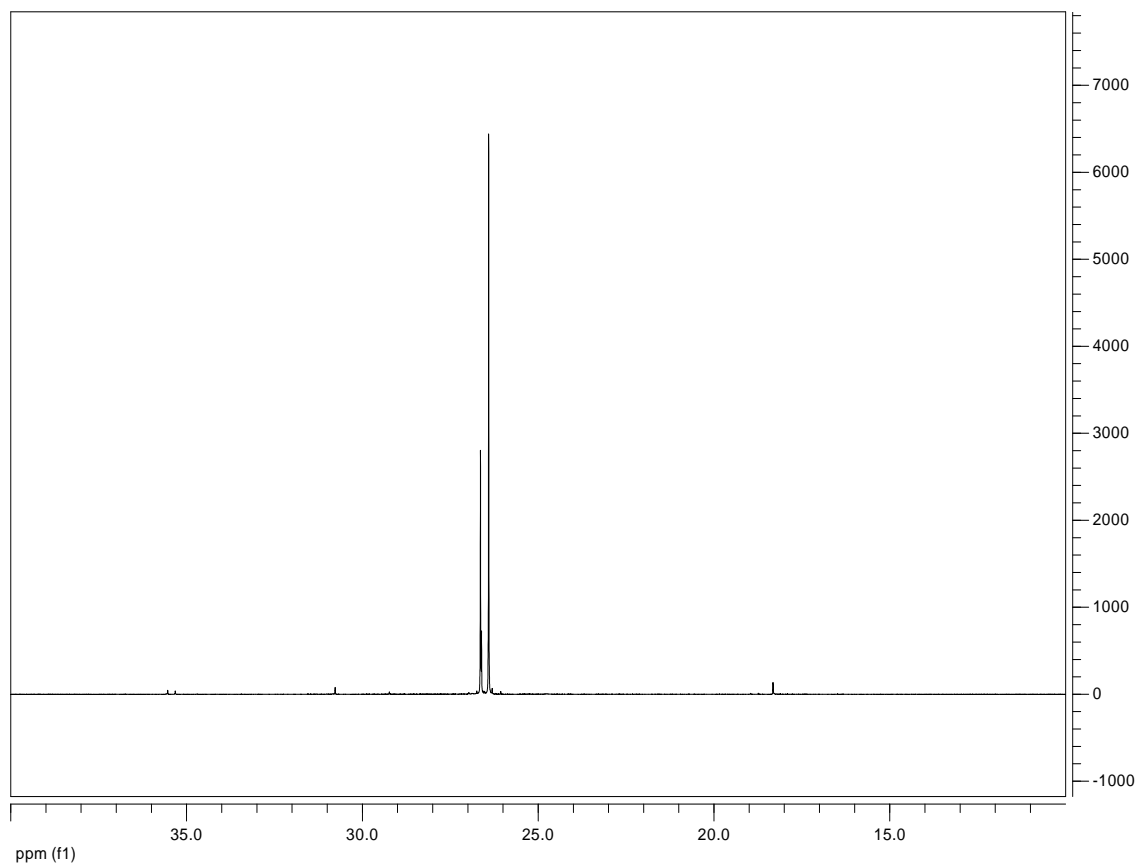


¹H NMR OF 1,2-BIS{2-(DIETHYLPHOSPHONATE) ETHYLTHIO} MALEONITRILE LIGAND 2



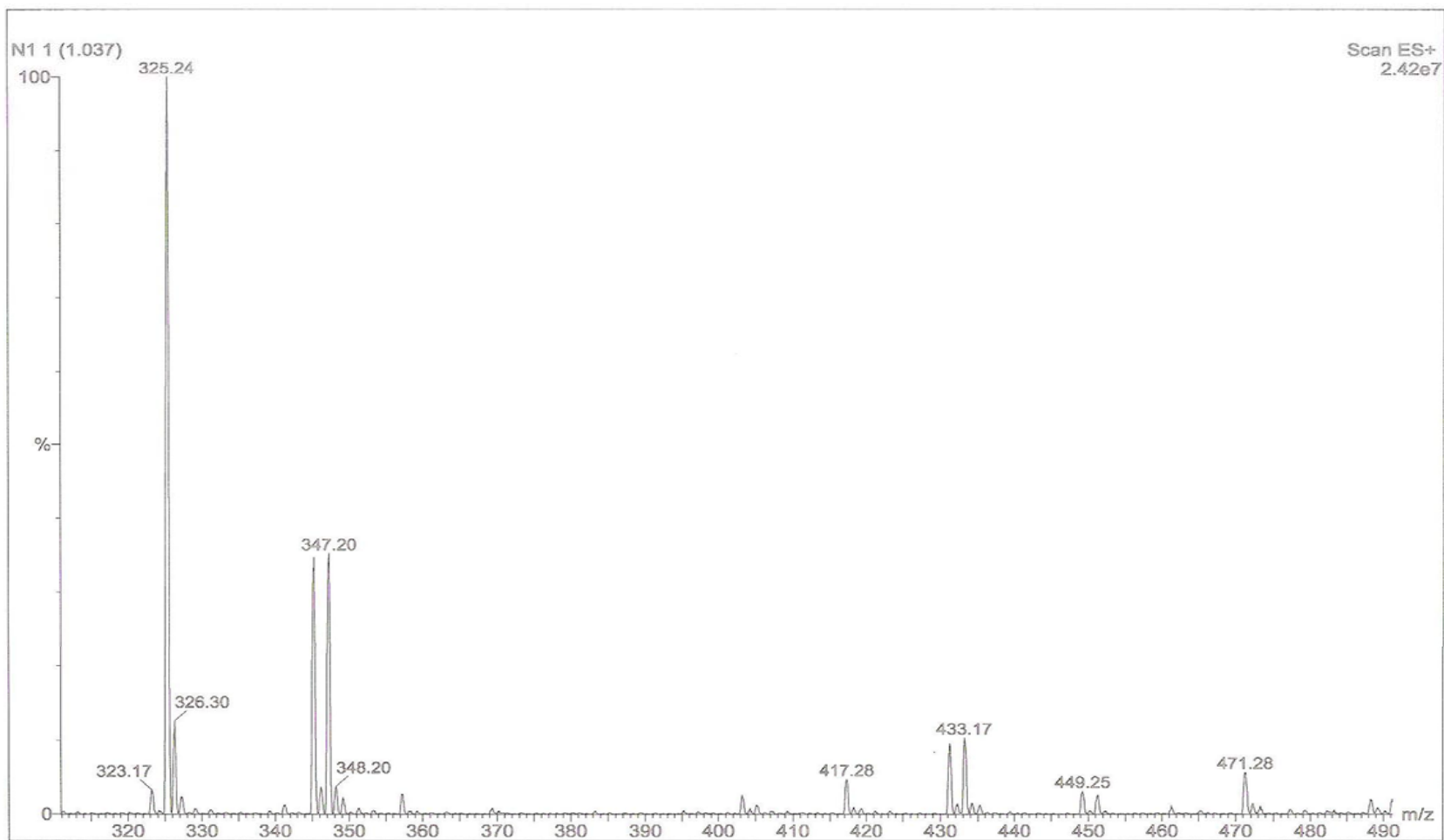
^{13}C NMR OF 1,2-BIS{2-(DIETHYLPHOSPHONATE) ETHYLTHIO} MALEONITRILE LIGAND 2
 FT-IR SPECTRUM OF **MgPz 3b**

APPENDIX E



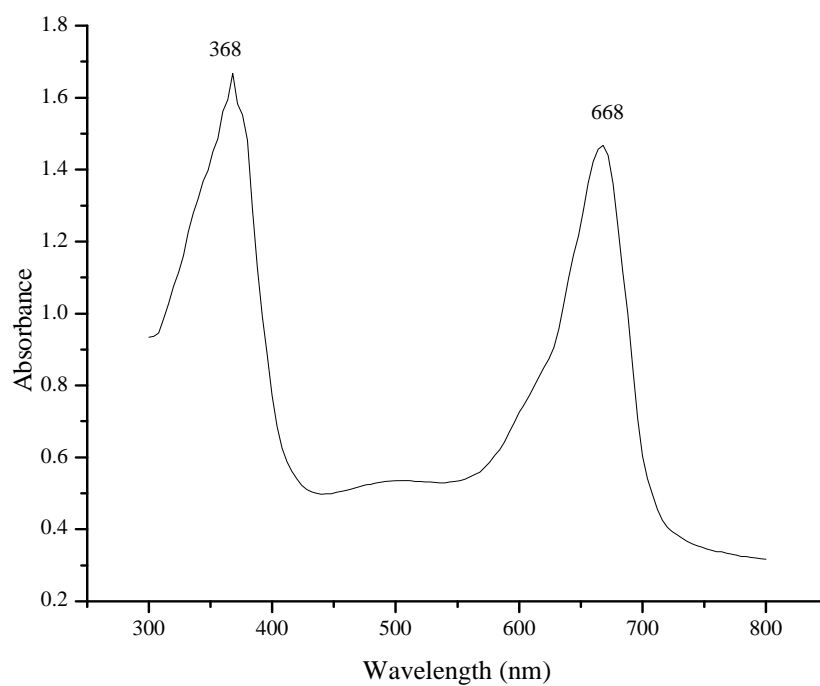
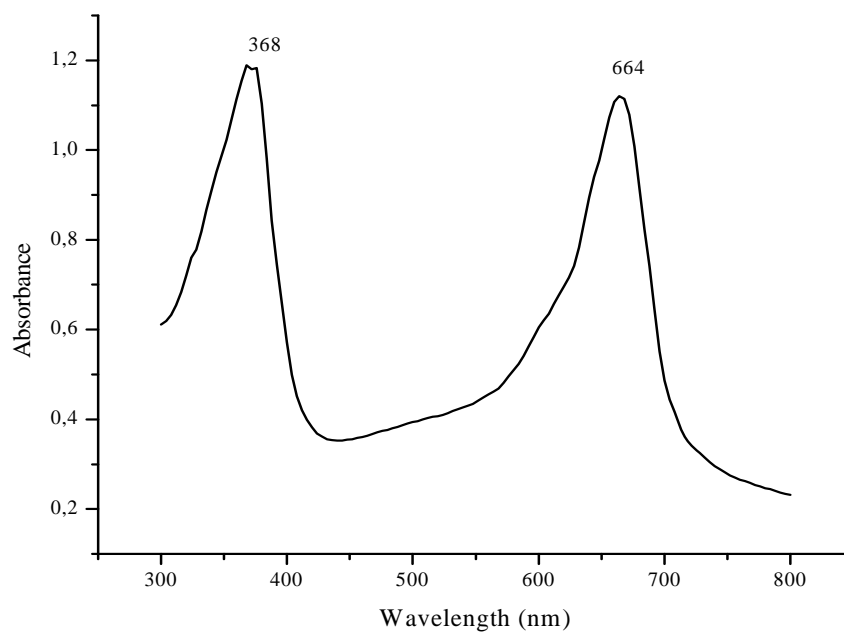
^{31}P NMR OF 1,2-BIS{2-(DIETHYLPHOSPHONATE) ETHYLTHIO}
MALEONITRILE LIGAND 2

APPENDIX F

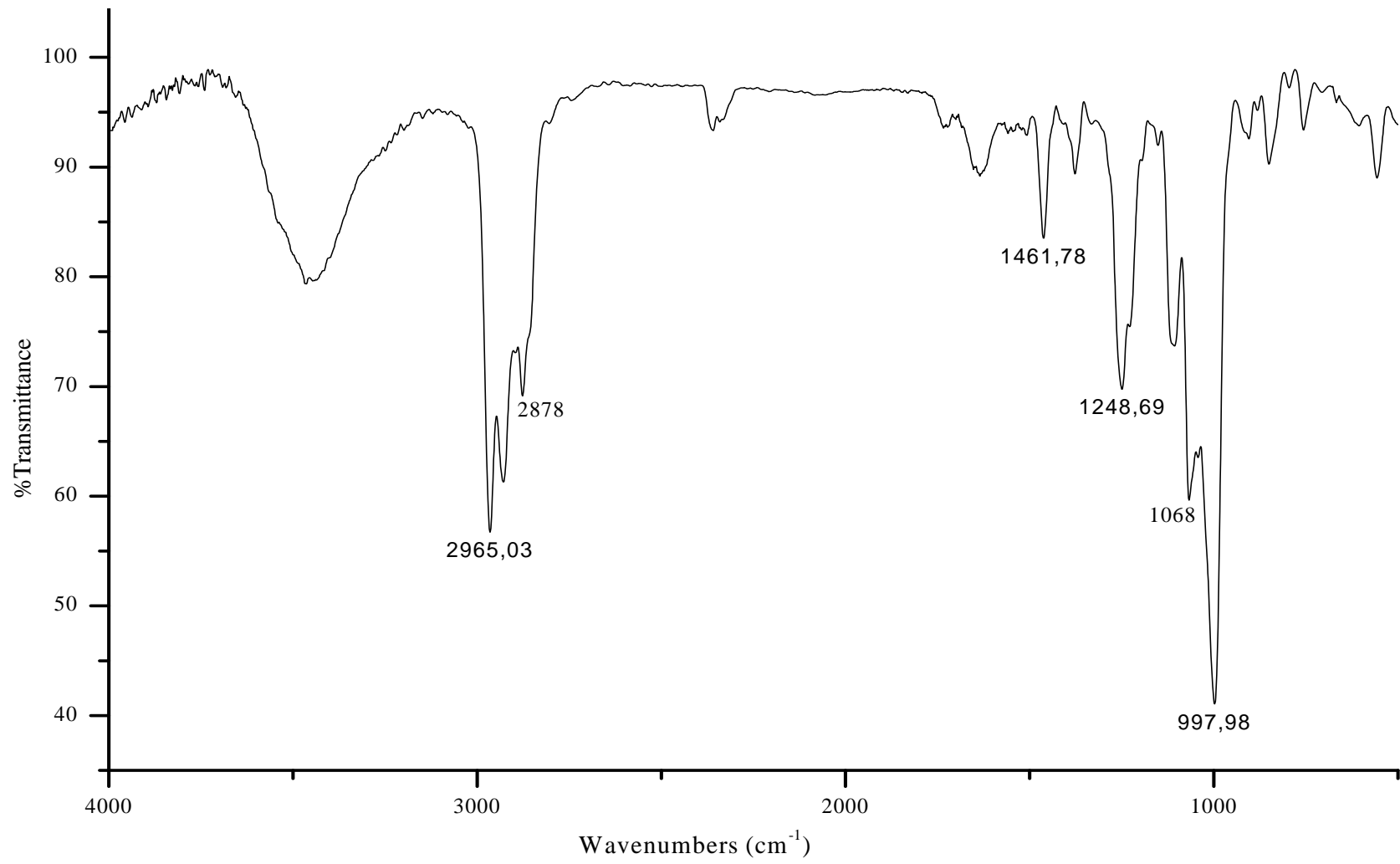


FAB-MS OF 1,2-BIS{2-(DIETHYL PHOSPHONATE) ETHYLTHIO}MALEONITRILE LIGAND 2

APPENDIX G

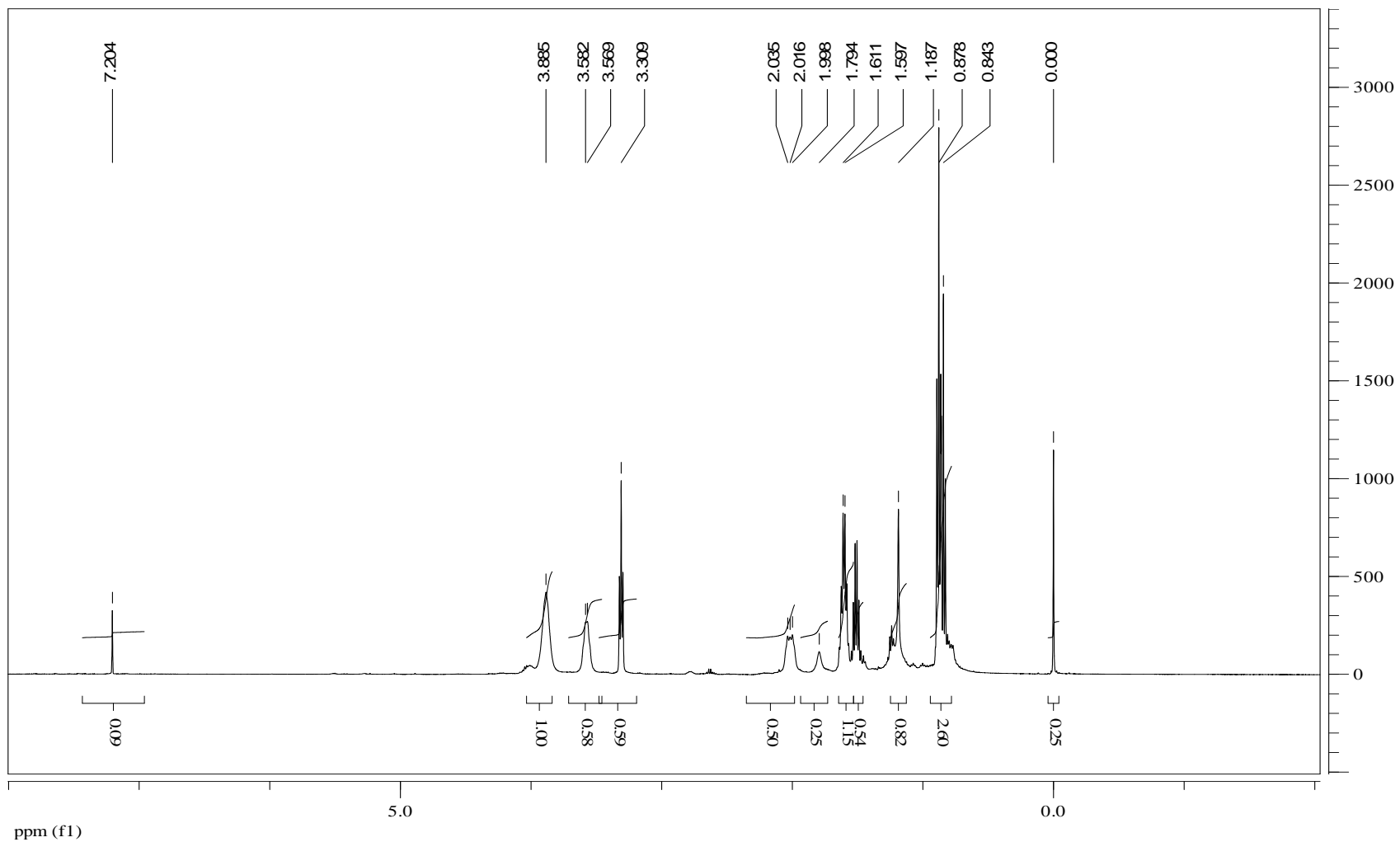
**a****b**

UV-VISIBLE SPECTRUM OF (a) ETHYL **3a** AND (b) PROPYL **3b**
PHOSPHONATE ESTERS OF Pzs



FT-IR SPECTRUM of MgPz 3b

APPENDIX H

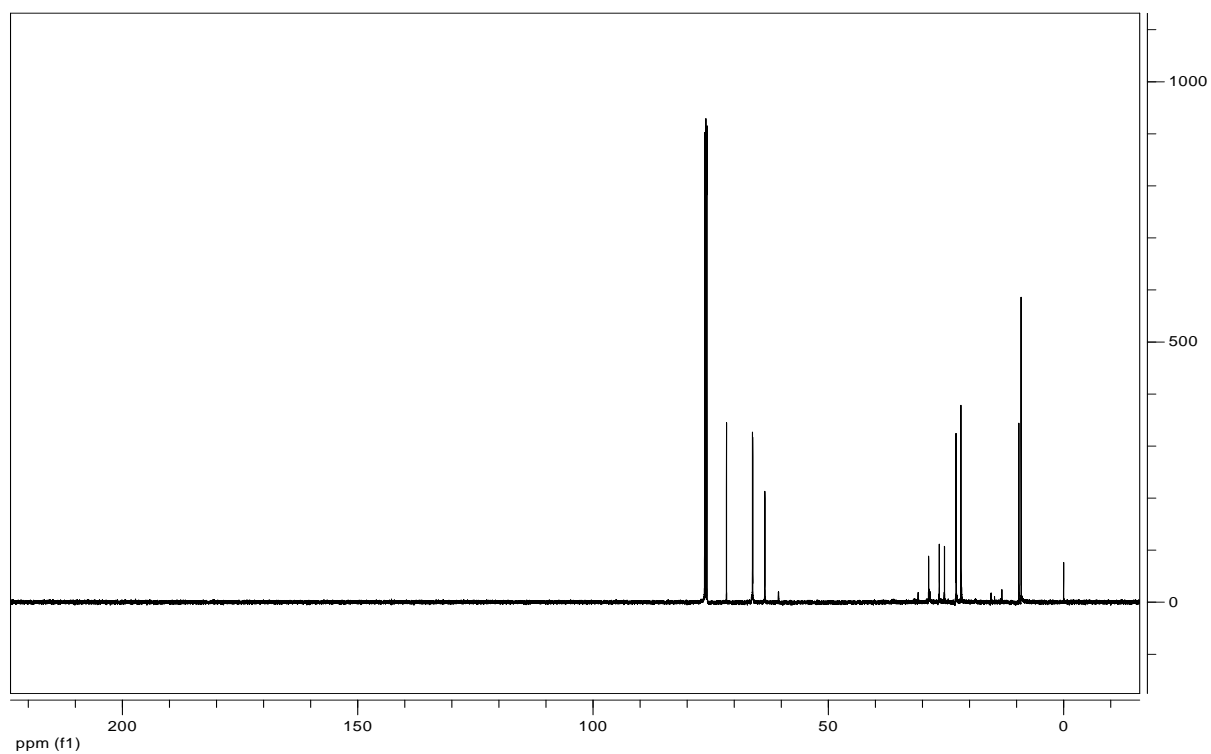
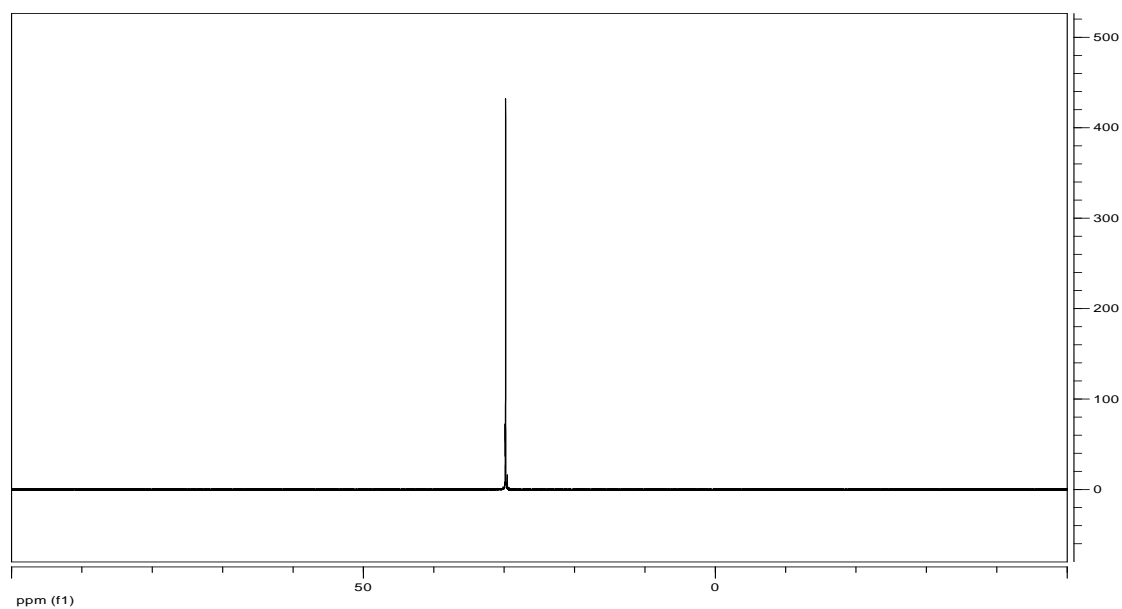


APPENDIX I

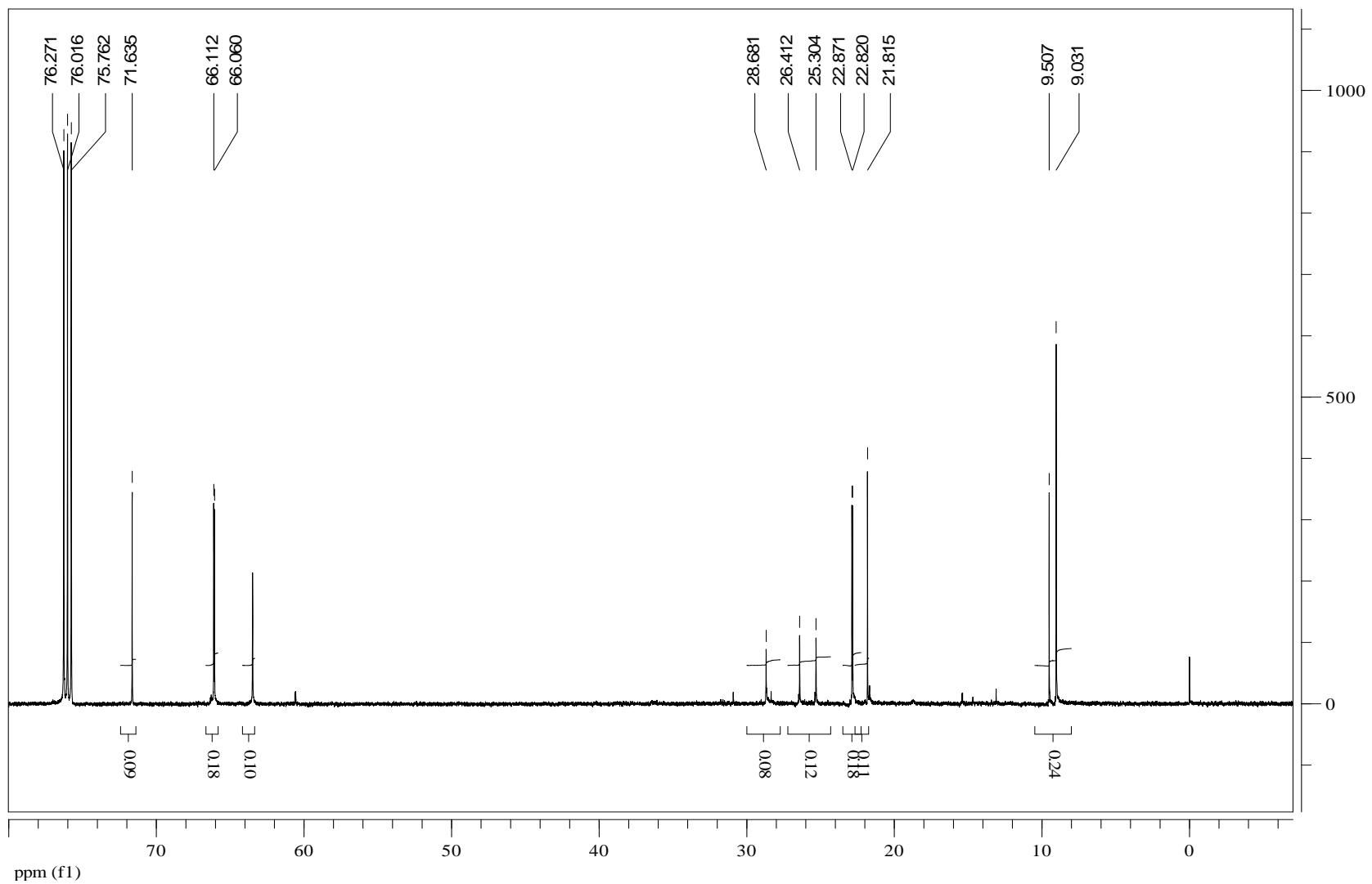
^1H NMR of MgPz **3b**

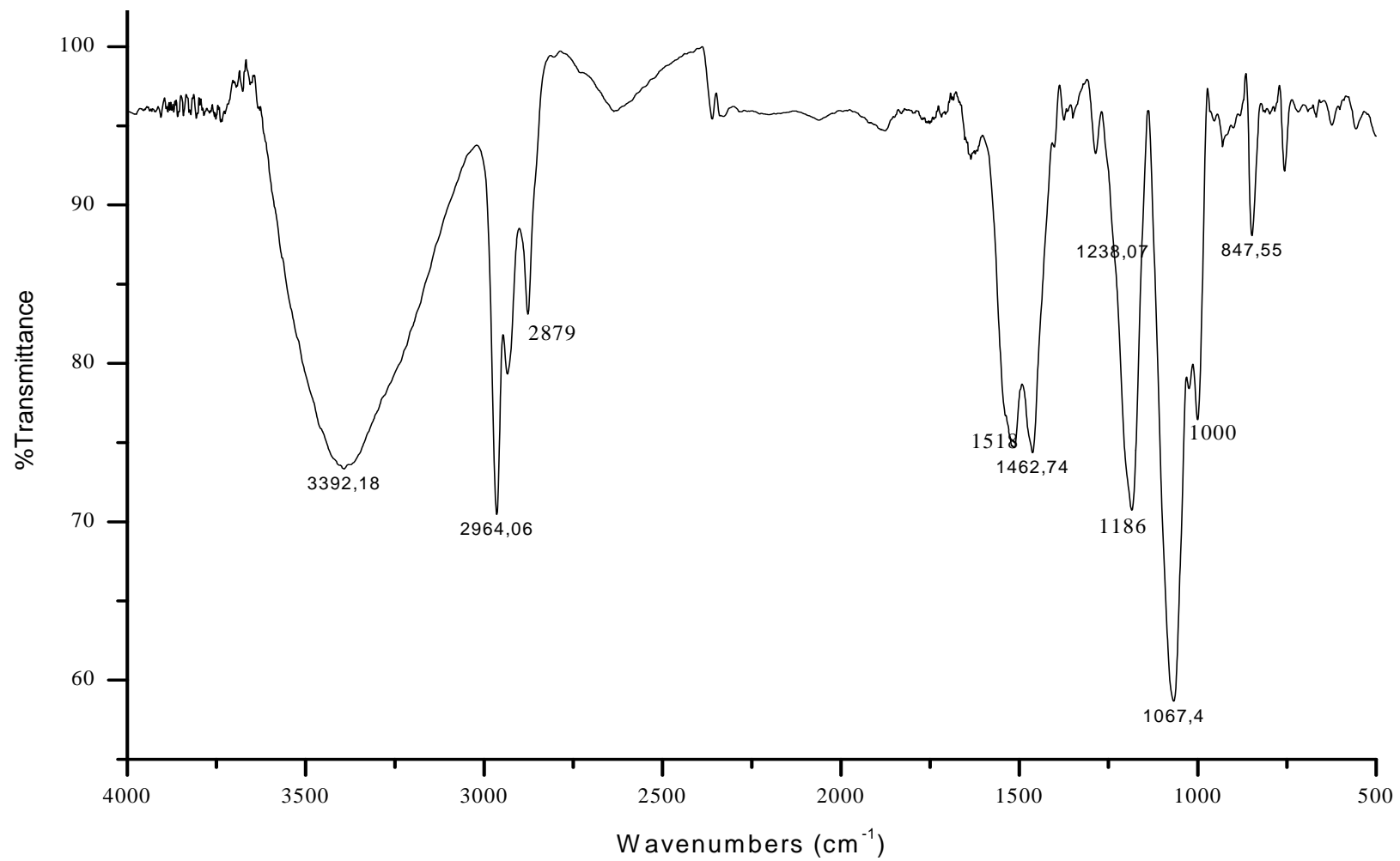
FT-IR SPECTRUM OF Ca_8MgPz

APPENDIX J

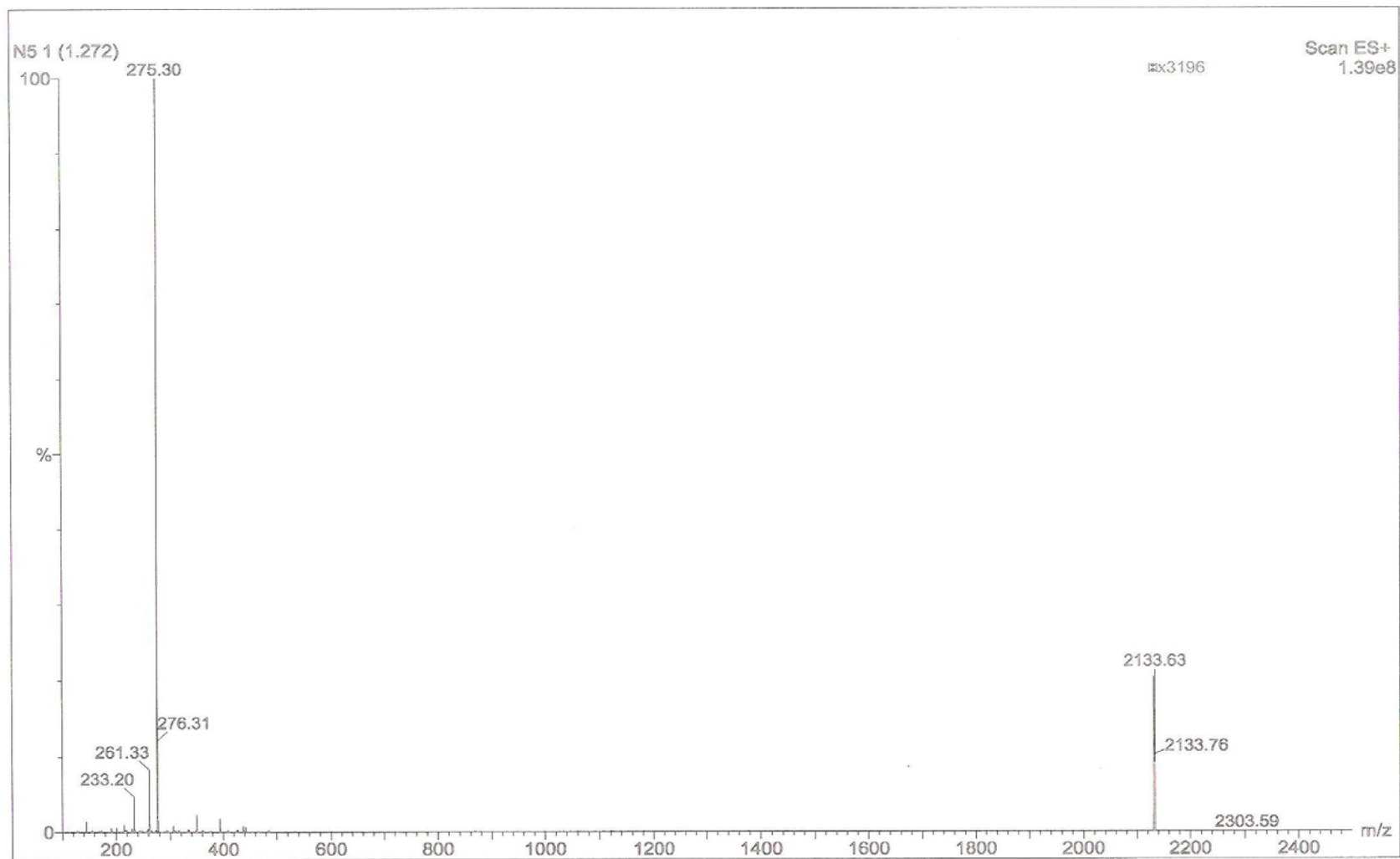
 ^{13}C NMR OF MgPz 3b ^{31}P NMR OF MgPz 3b

APPENDIX K

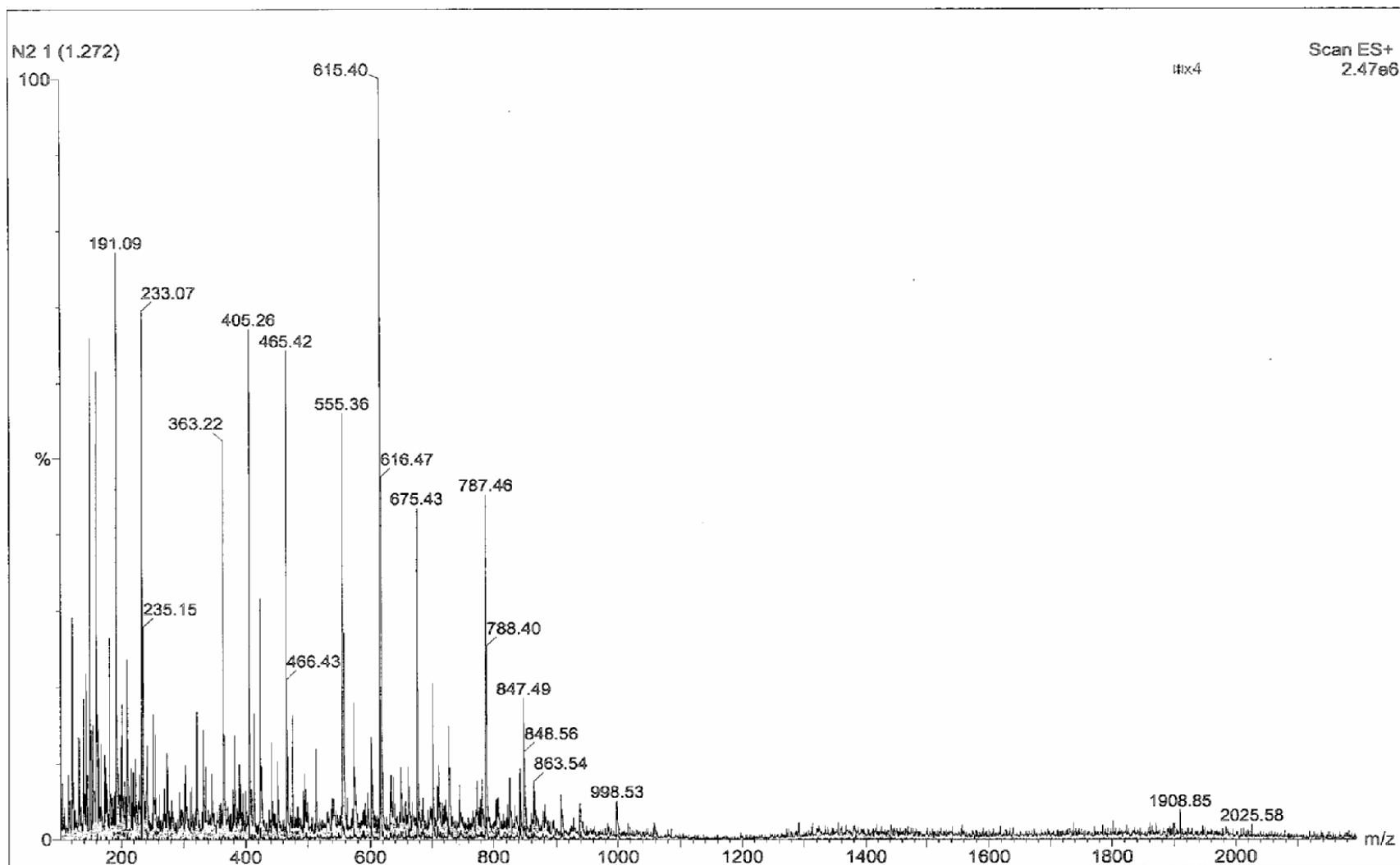




FT-IR SPECTRUM OF Pz 3a

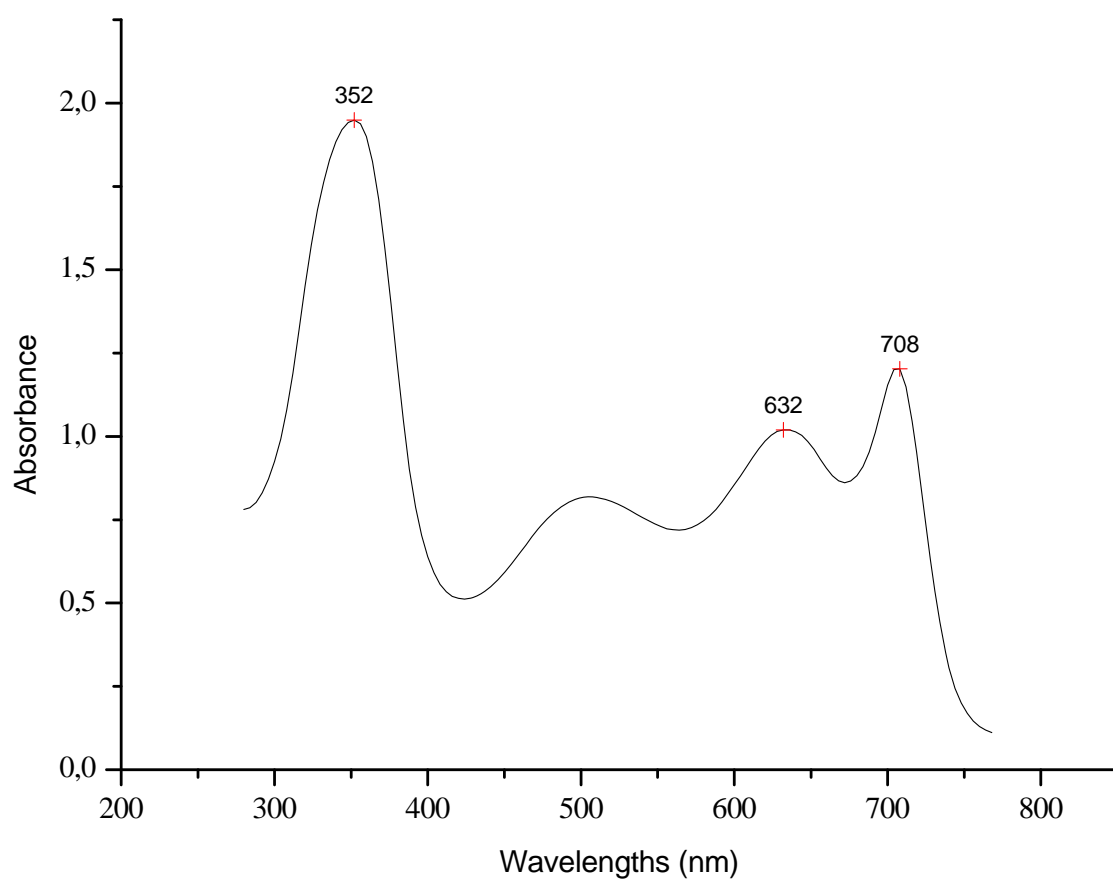


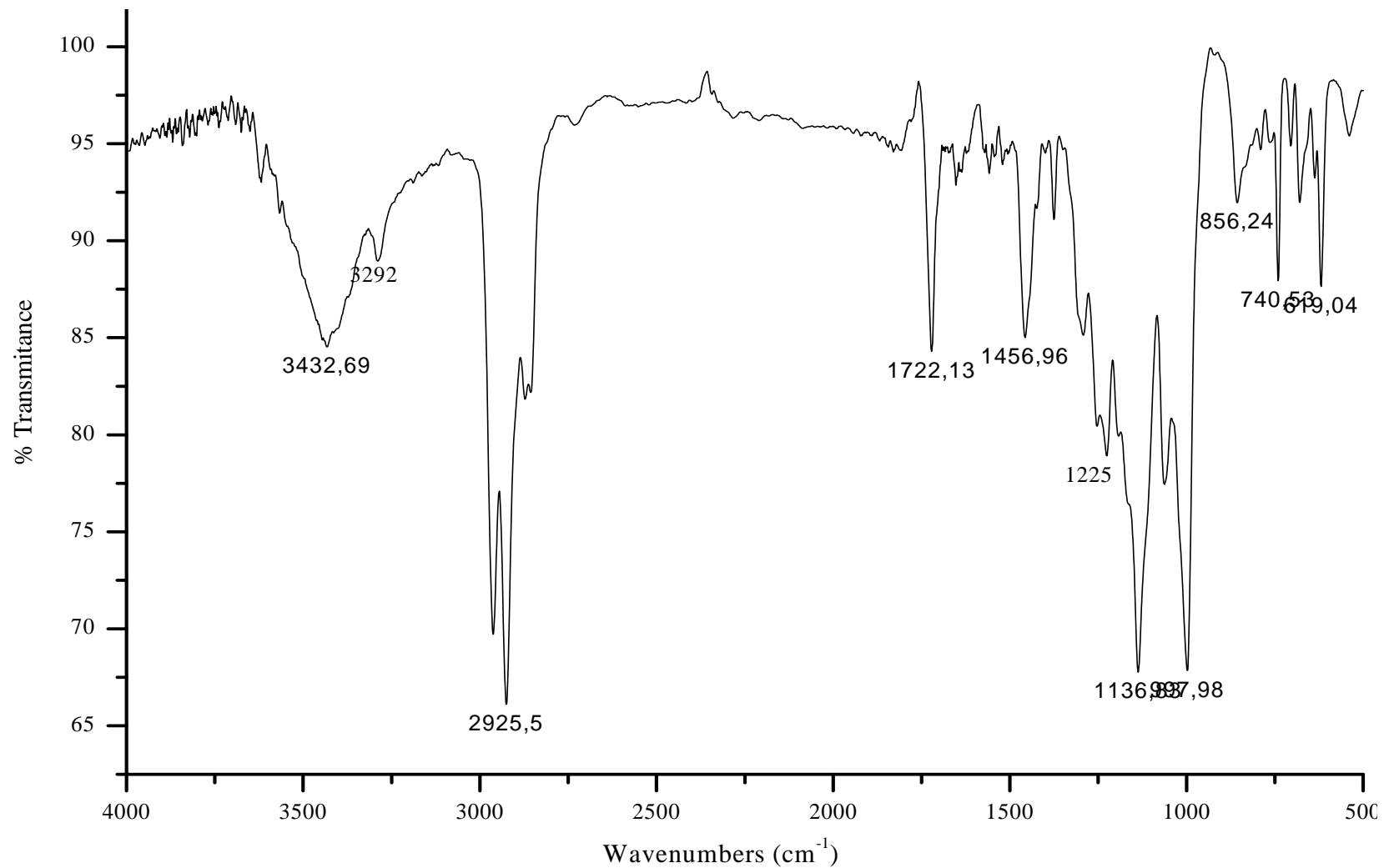
FAB-MASS SPECTRUM OF MgPz (PROPYL) 3b



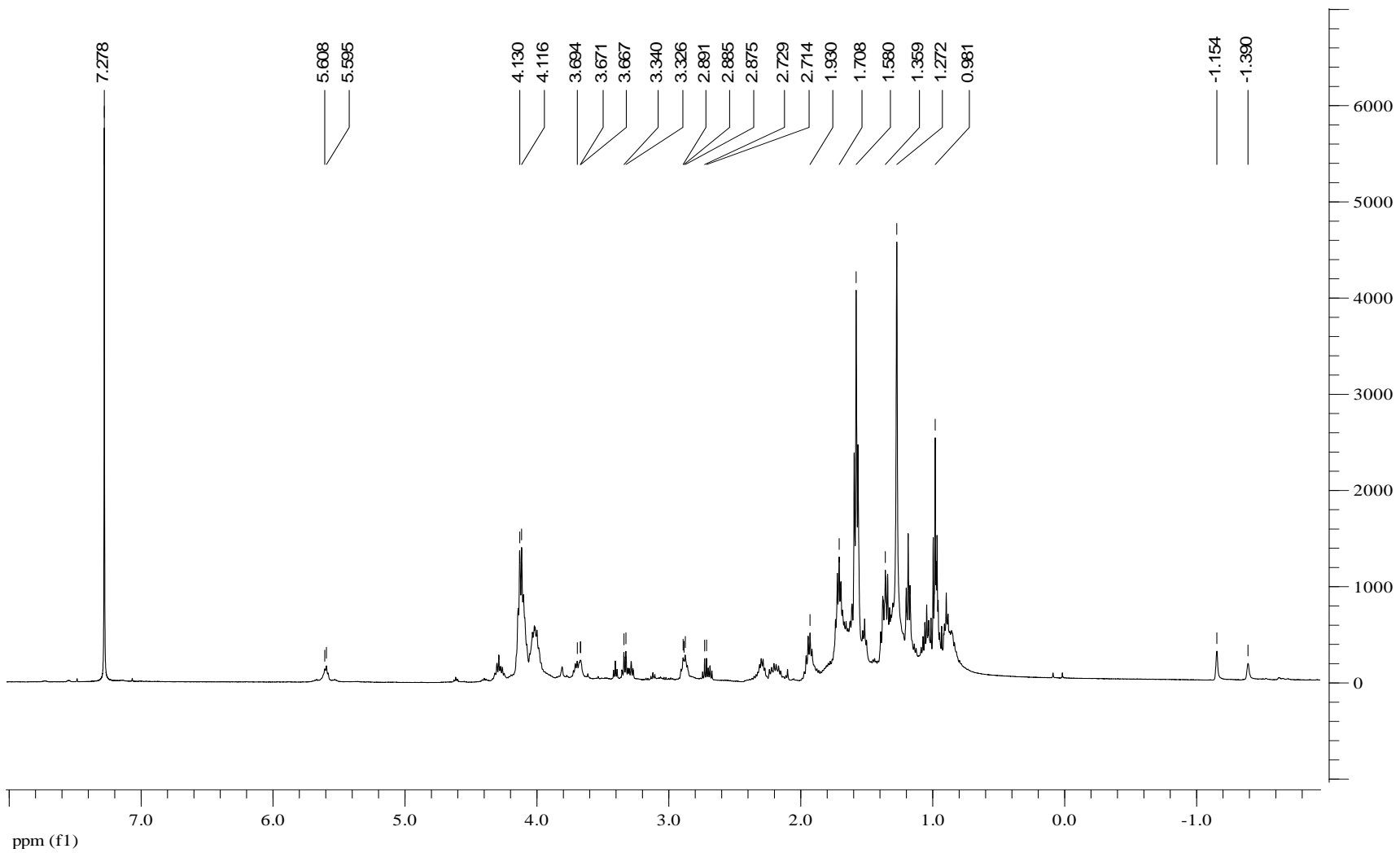
FAB-MASS SPECTRUM OF MgPz (ETHYL) 3a

APPENDIX O

UV-VISIBLE SPECTRUM OF H₂Pz

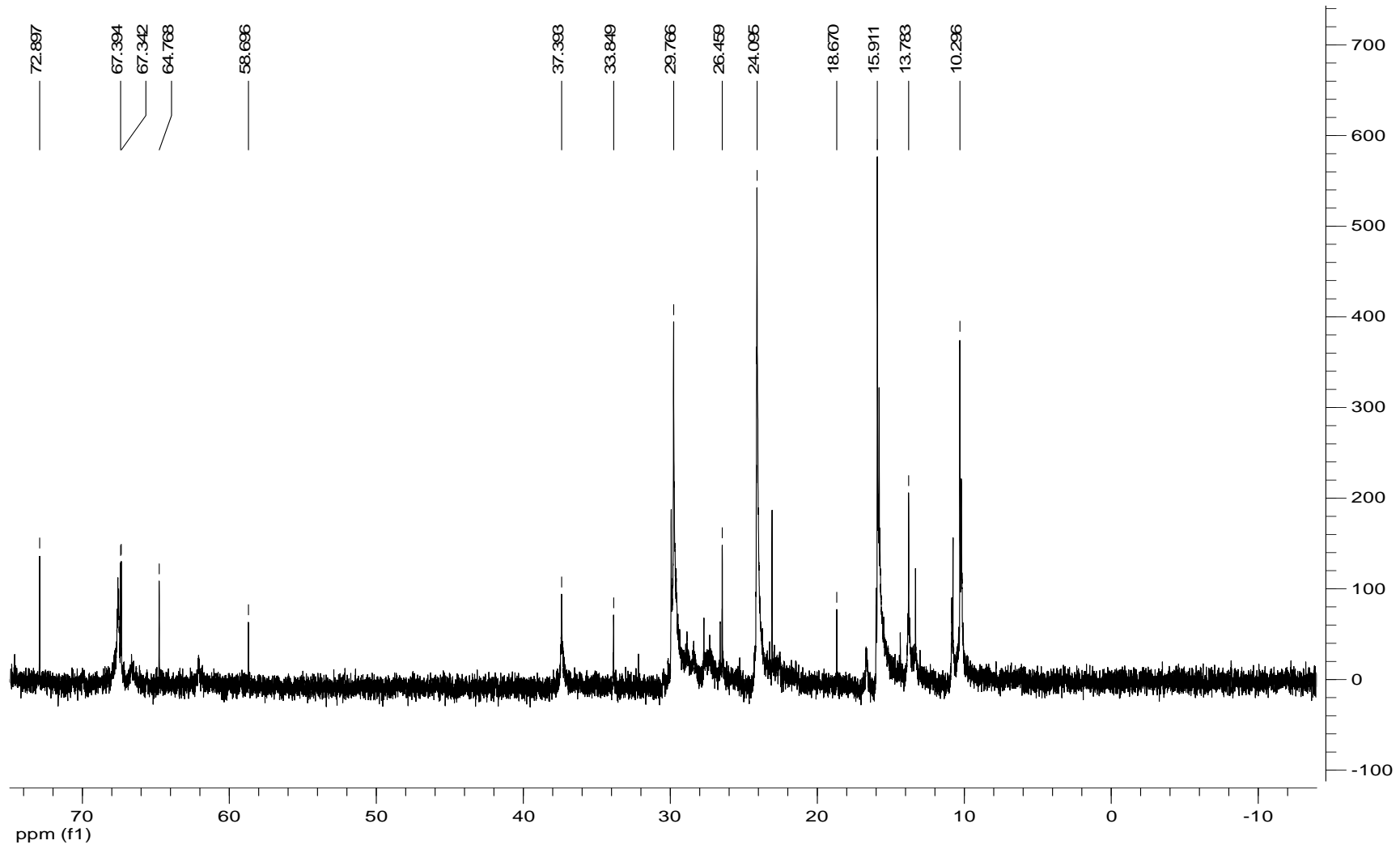


FT-IR SPECTRUM OF H₂Pz



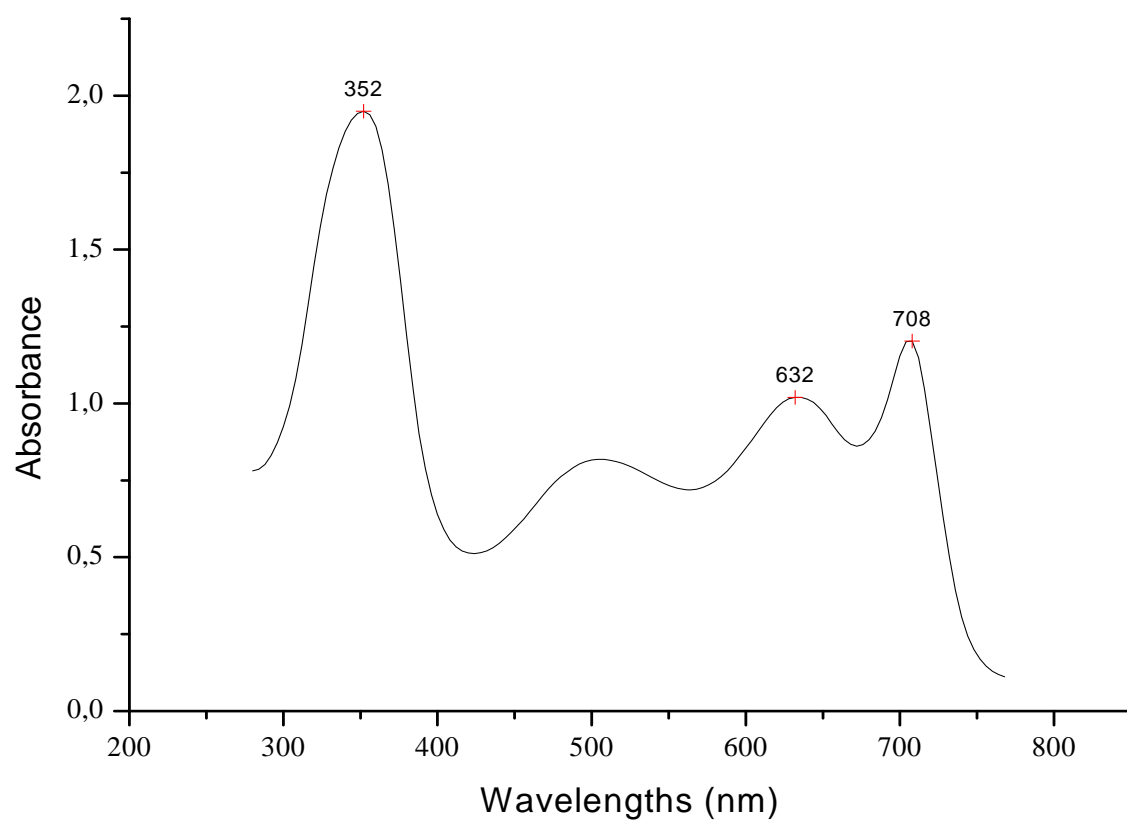
¹H NMR OF H₂Pz

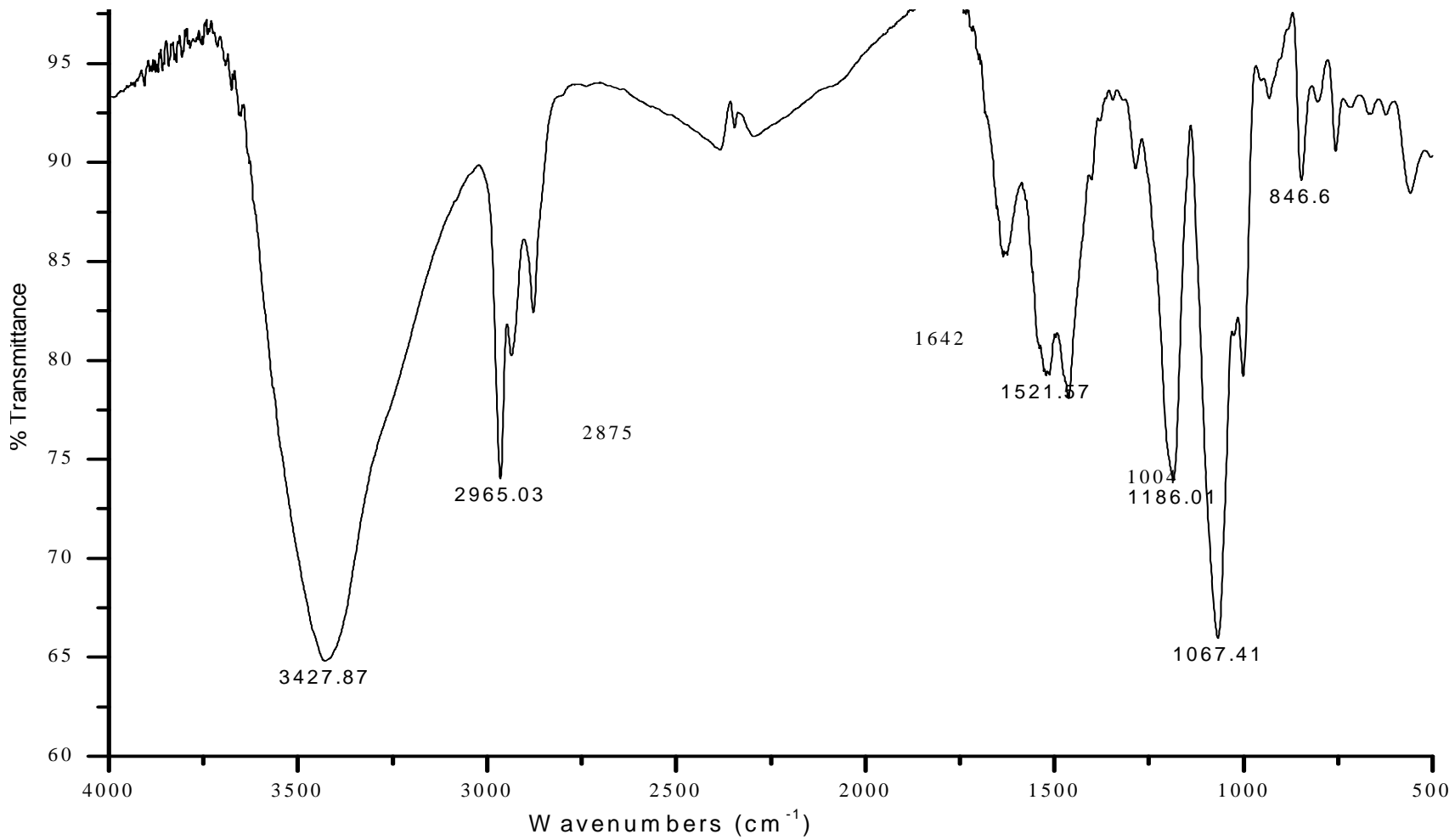
APPENDIX Q



^{13}C NMR H_2Pz

APPENDIX S

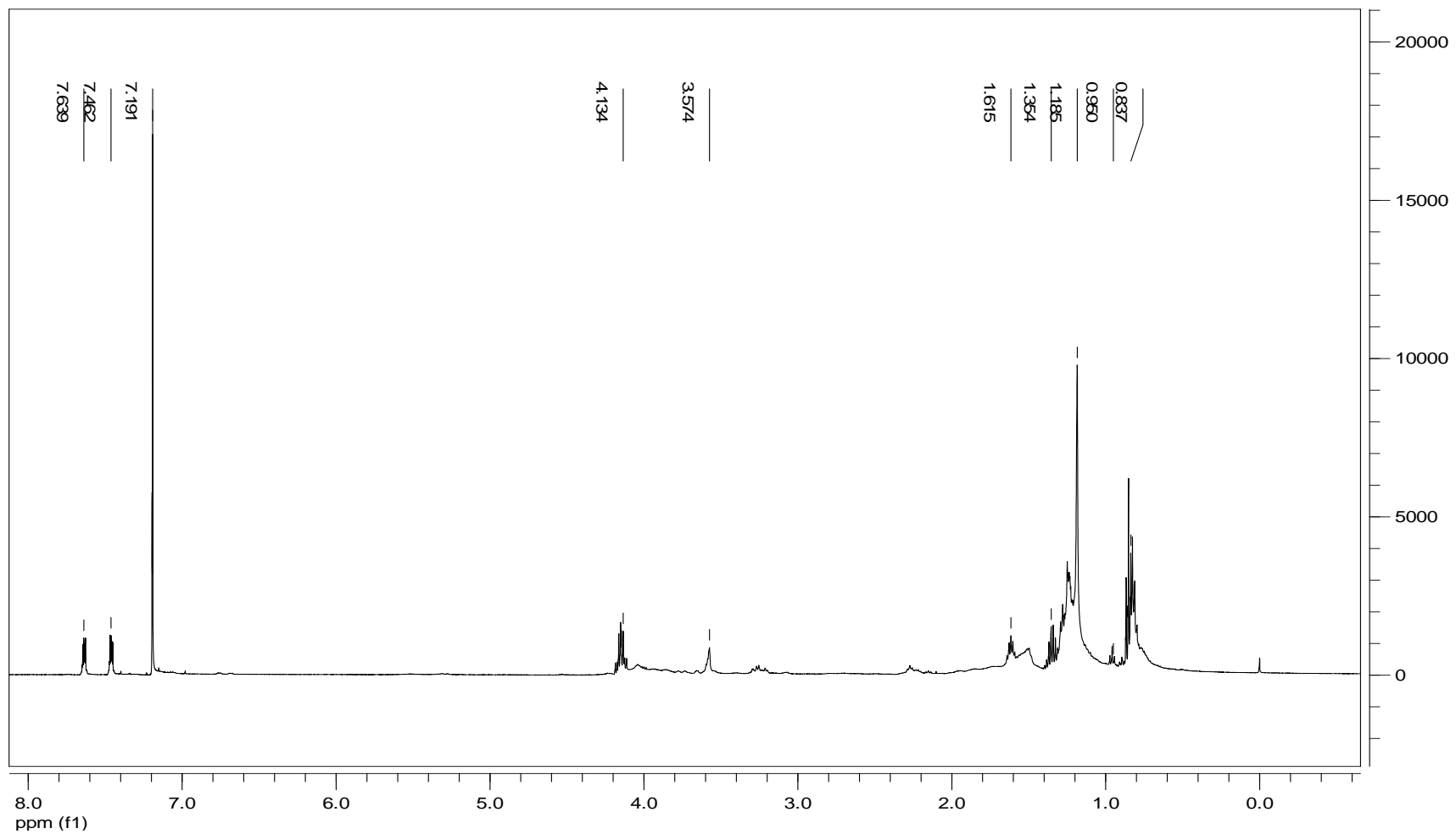
UV-VISIBLE SPECTRUM OF MgPz-P(O)(OH)₂



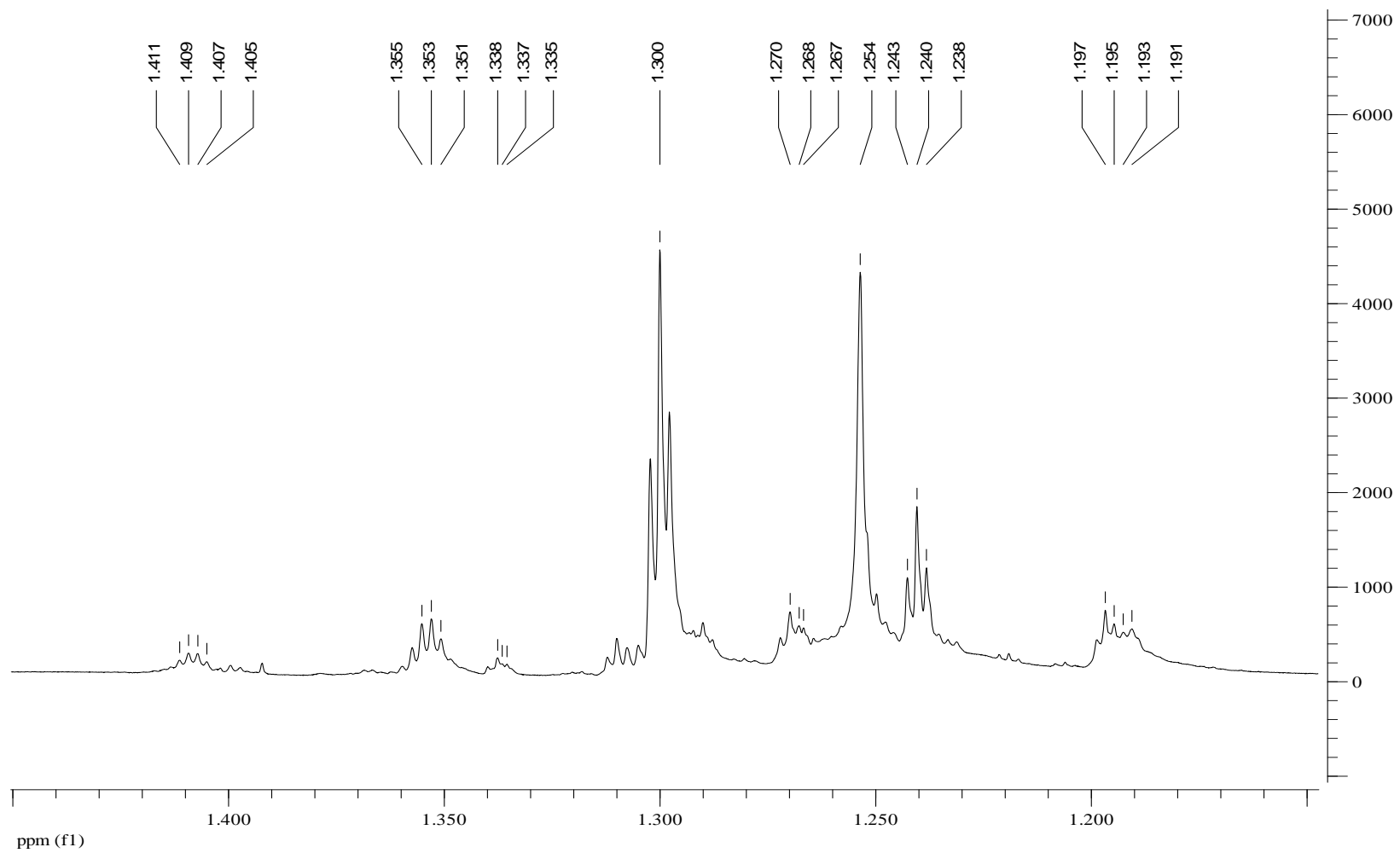
FT-IR SPECTRUM OF MgPz-P(O)(OH)₂

APPENDIX T

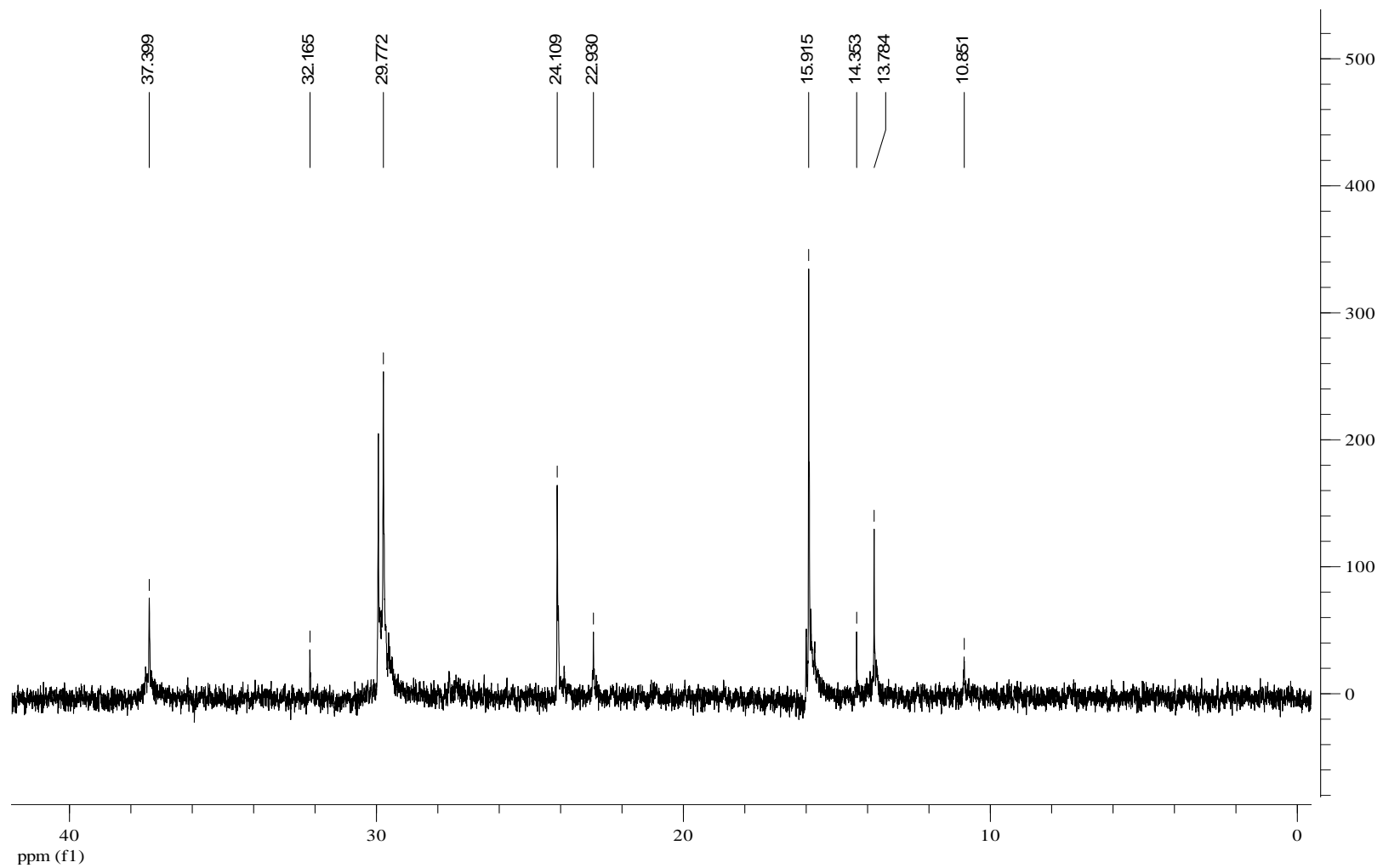
APPENDIX U



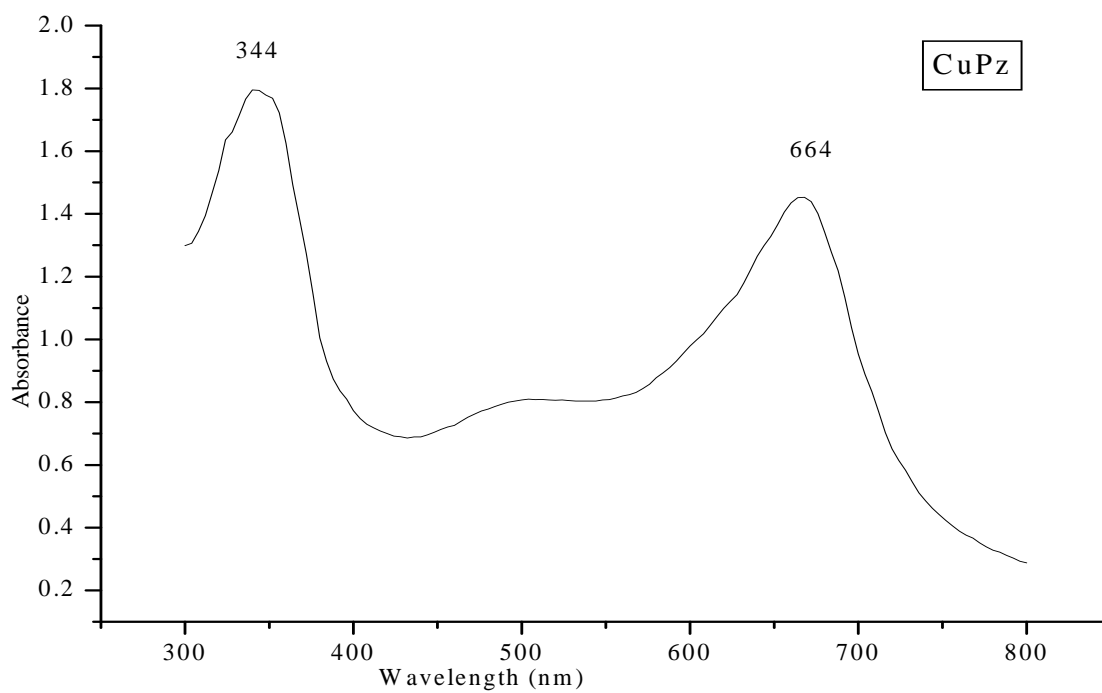
¹H NMR OF (MgPz-P(O)(OH)₂)



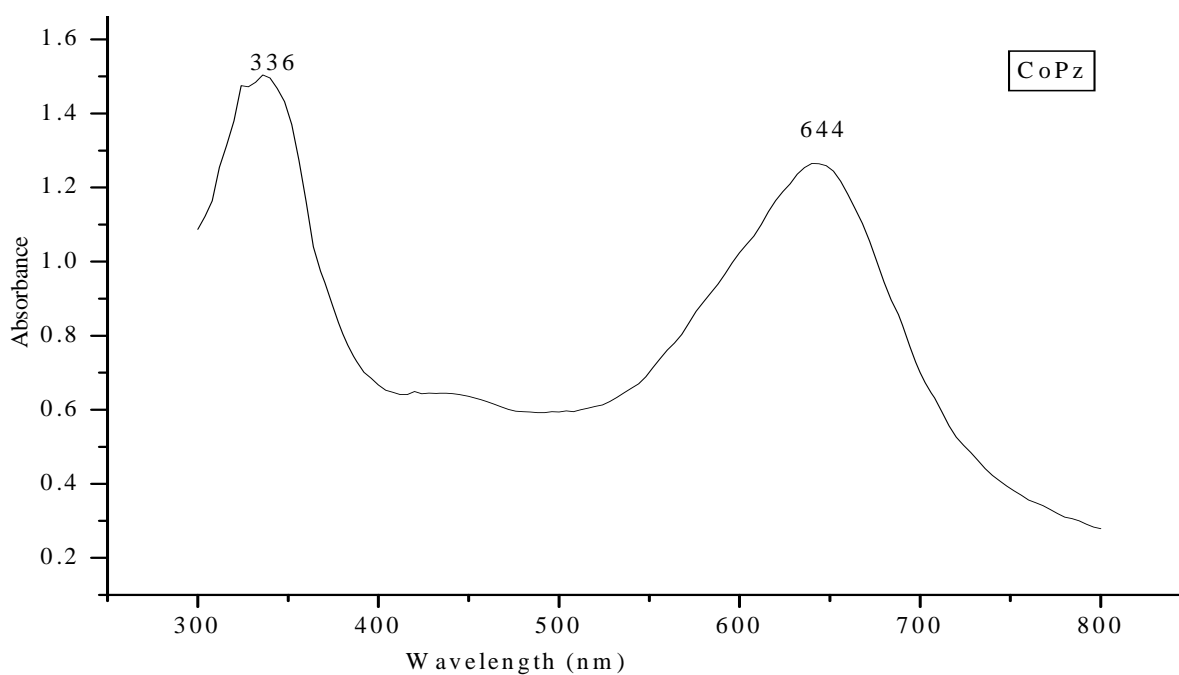
EXPANDED ¹H NMR OF (MgPz-P(O)(OH)₂)



^{13}C NMR OF (MgPz-P(O)(OH)_2)

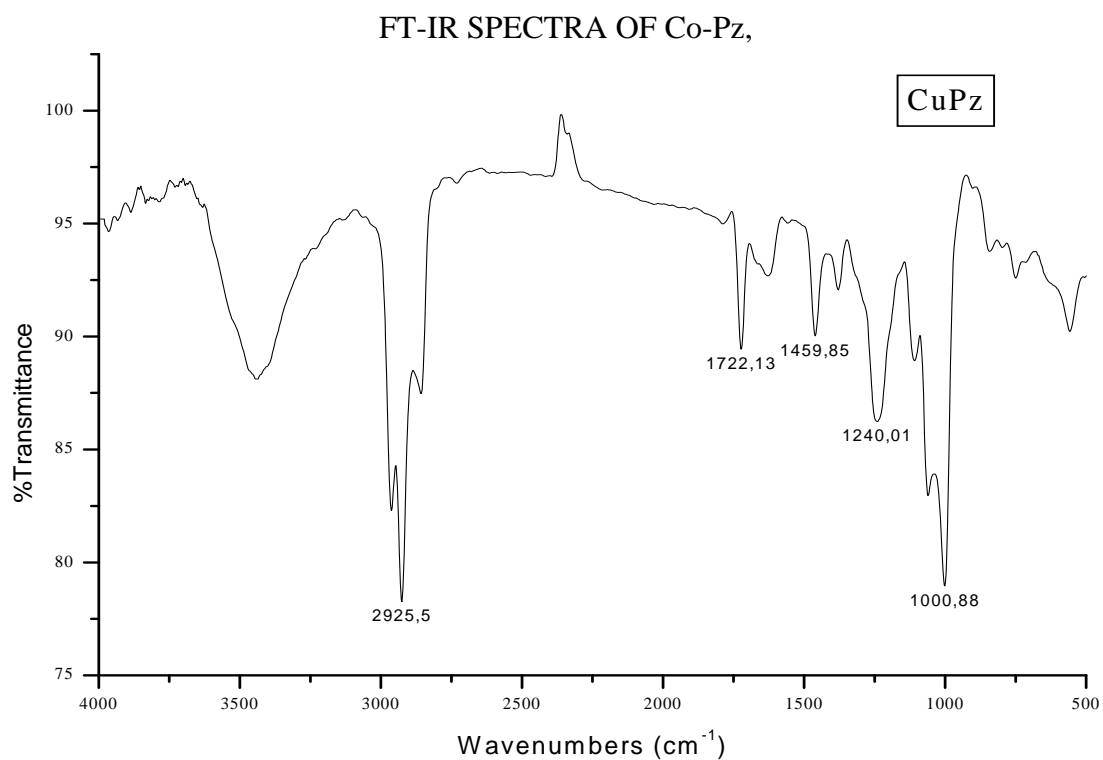
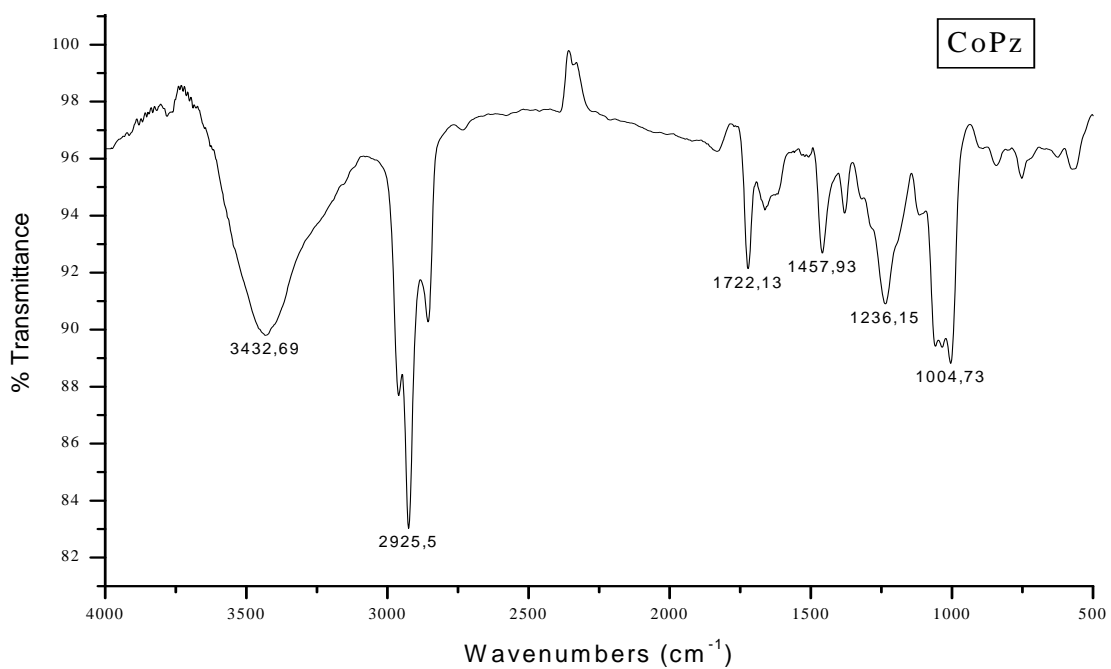
APPENDIX X

UV-VISIBLE SPECTRUM OF Cu-Pz



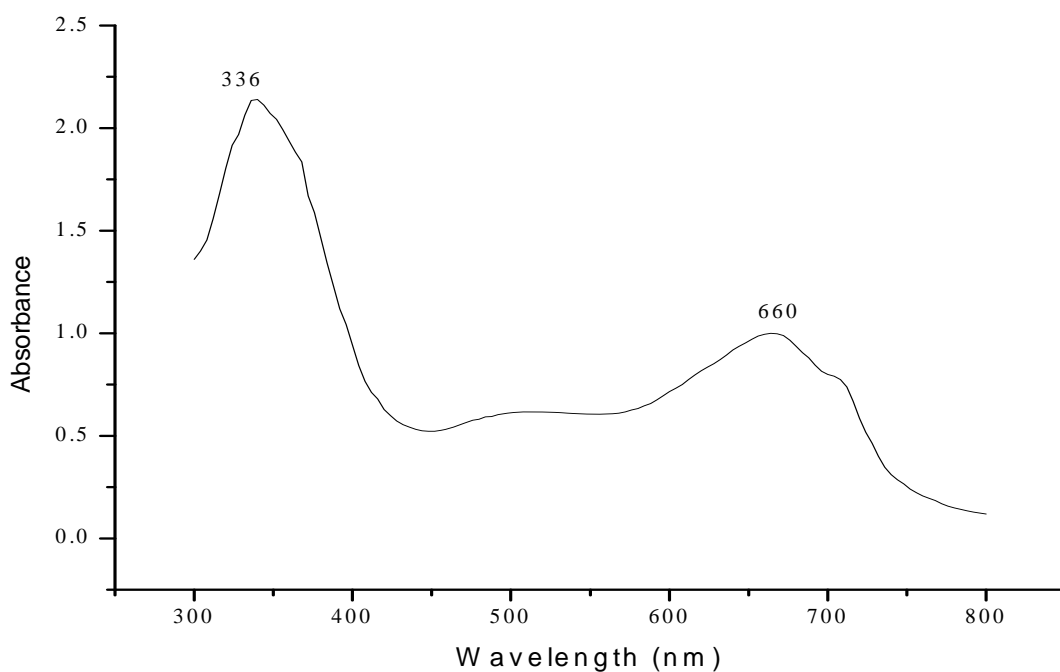
UV-VISIBLE SPECTRUM OF Co-Pz

APPENDIX Y

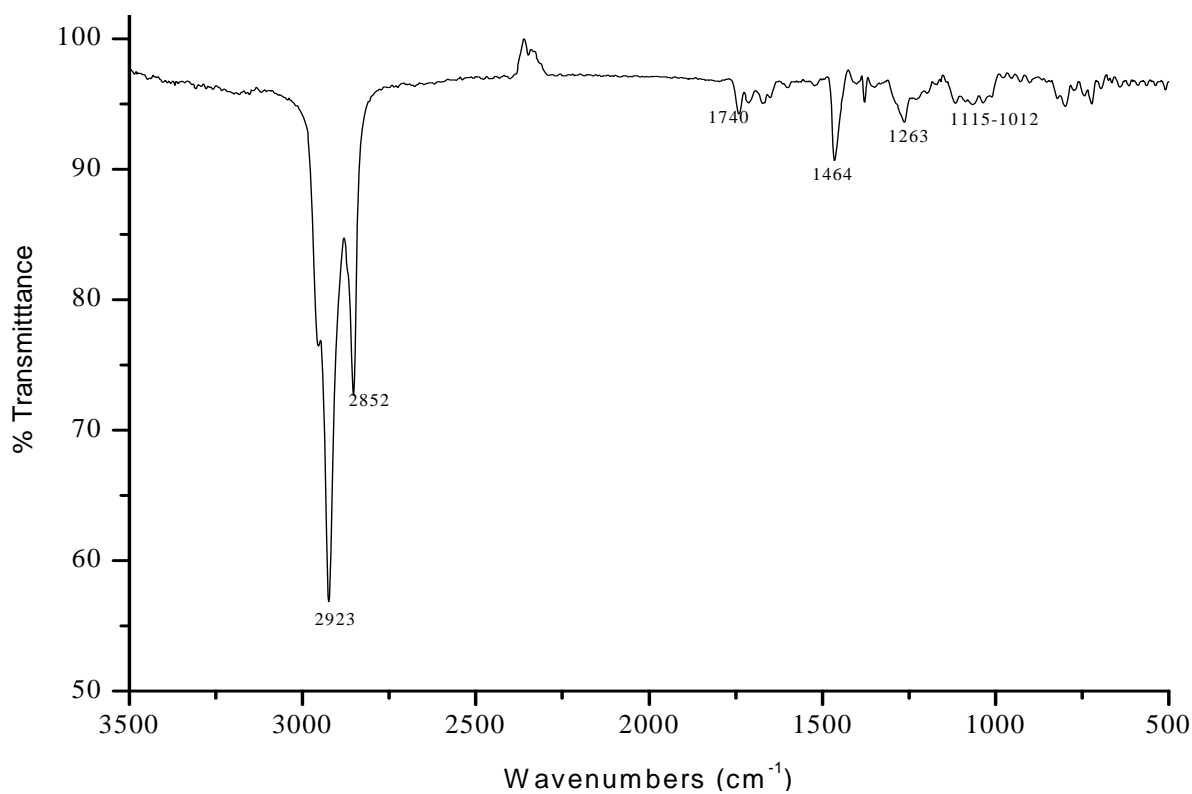


FT-IR SPECTRA OF Cu-Pz

APPENDIX Z

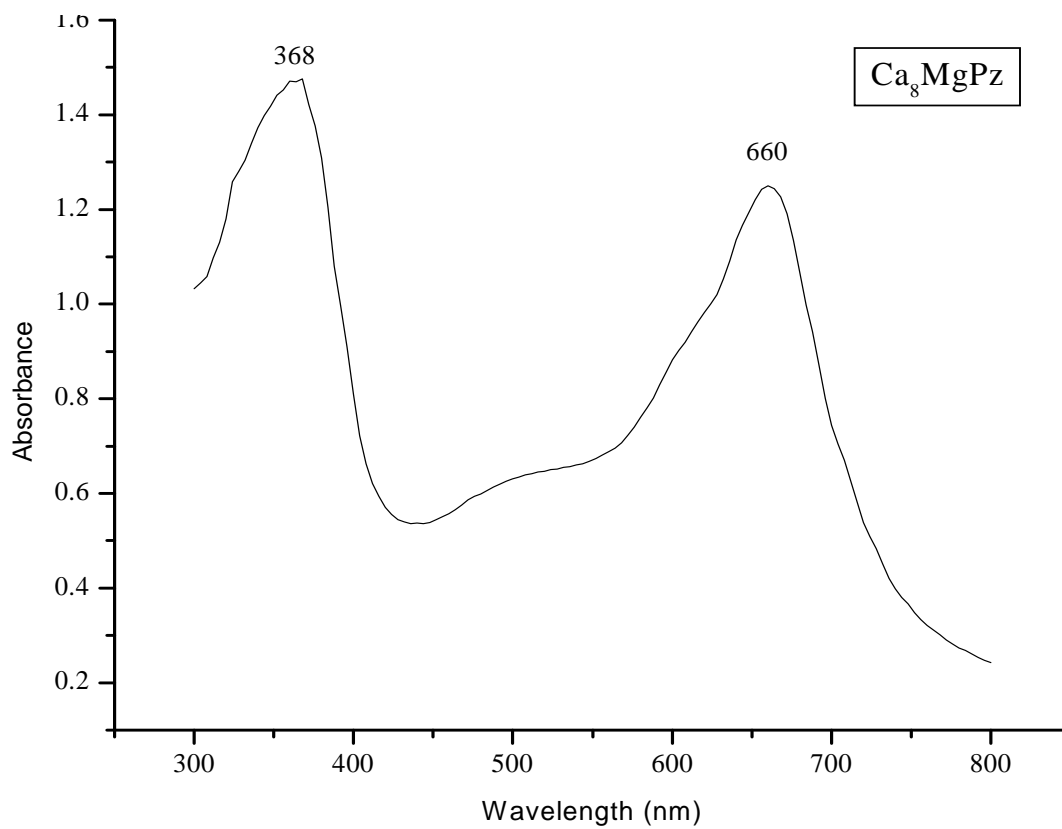


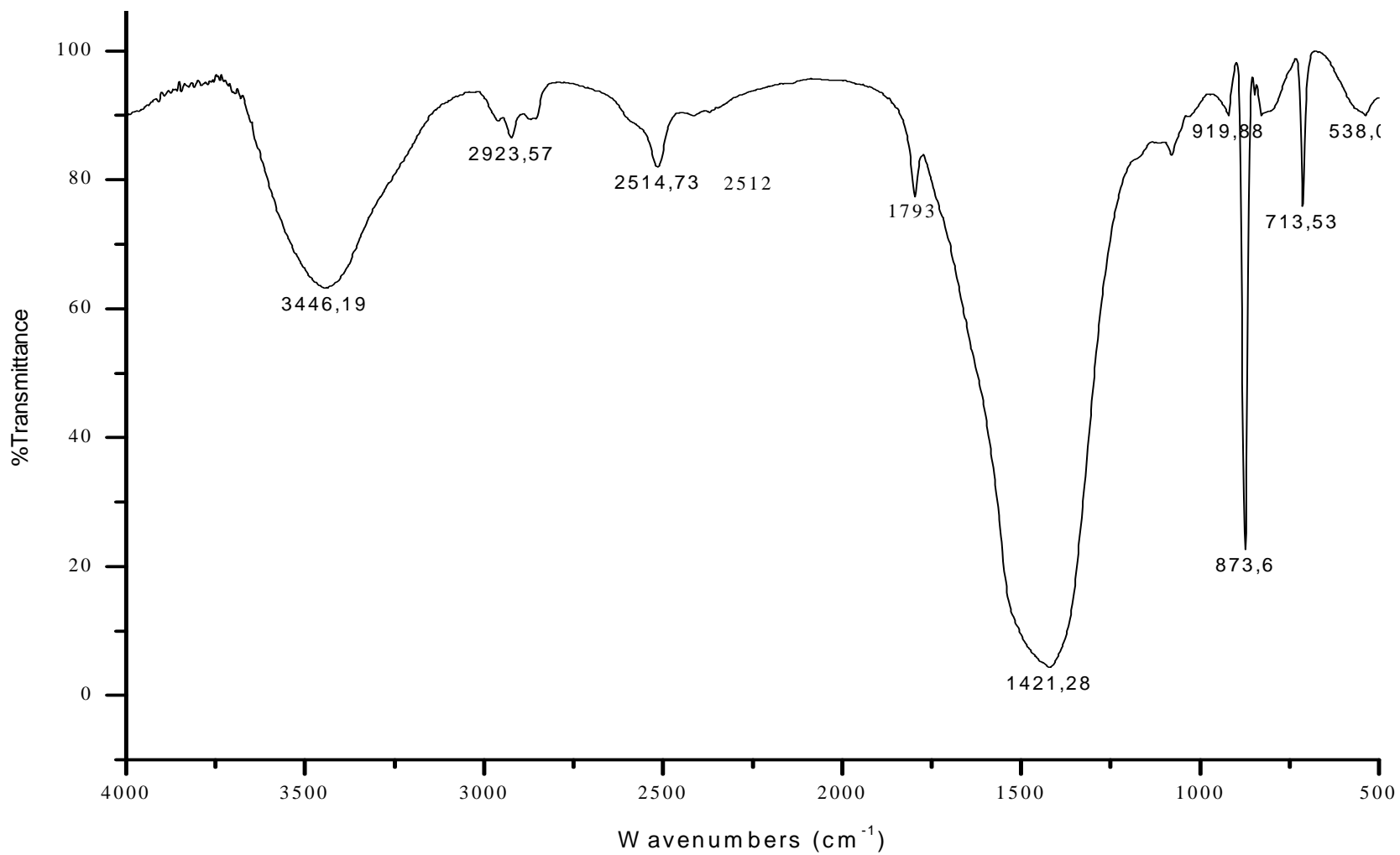
UV-VISIBLE SPECTRUM OF VO-Pz.



FT-IR SPECTRUM OF VO-Pz.

APPENDIX A1

UV-VISIBLE SPECTRUM OF Ca_8MgPz



FT-IR SPECTRUM OF Ca₈MgPz

APPENDIX B1